NONLINEAR INTERACTIONS IN MIXING LAYERS AND COMPRESSIBLE HEATED ROUND JETS

by

Yousef Mohd Jarrah

A Dissertation Submitted to the Faculty of the

DEPARTMENT OF AEROSPACE AND MECHANICAL ENGINEERING

In Partial Fulfillment of the Requirements
For the Degree of

DOCTOR OF PHILOSOPHY
WITH A MAJOR IN MECHANICAL ENGINEERING

In the Graduate College

THE UNIVERSITY OF ARIZONA

1 9 8 9

THE UNIVERSITY OF ARIZONA
GRADUATE COLLEGE

As members of the Final Examination Committee, we certify that we have read the dissertation prepared by Yousef M. Jarrah

entitled NONLINEAR INTERACTIONS IN MIXING LAYERS AND COMPRESSIBLE HEATED ROUND JETS

and recommend that it be accepted as fulfilling the dissertation requirement for the Degree of Doctor of Philosophy.

Dr. Thomas F. Balsa	Oct 26/88 Date
Dr. Chuan F. Chen	November 4, 1988 Date
Dr. Arne J. Pearlstein	March 27, 1989 Date
Dr. Henry C. Perkins	Nov 4, 1988 Date
Dr. Robert A. Petersen	Nov 4, 1988 Date

Final approval and acceptance of this dissertation is contingent upon the candidate's submission of the final copy of the dissertation to the Graduate College.

I hereby certify that I have read this dissertation prepared under my direction and recommend that it be accepted as fulfilling the dissertation requirement.

Dissertation Director	Oct 26/88 Date

STATEMENT BY AUTHOR

This dissertation has been submitted in partial fulfillment of requirements for an advanced degree at The University of Arizona and is deposited in the University Library to be made available to borrowers under rules of the Library.

Brief quotations from this dissertation are allowable without special permission, provided that accurate acknowledgment of source is made. Requests for permission for extended quotation from or reproduction of this manuscript in whole or in part may be granted by the head of the major department or the Dean of the Graduate College when in his or her judgment the proposed use of the material is in the interests of scholarship. In all other instances, however, permission must be obtained from the author.

SIGNED: 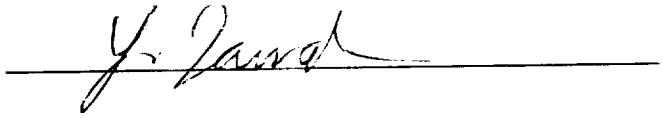

DEDICATION

To my mother Noura, wife Helen and sisters Asma, Kawla and Hend.

ACKNOWLEDGEMENT

I am deeply grateful to many individuals whose technical or emotional support made possible the completion of this work. I am especially indebted to Dr. Thomas F. Balsa for the direction of this dissertation and for encouraging rich interaction with the available literature on the subject of this research. I am also indebted to NASA-Lewis Research Center, which sponsored this research under grant NAG 3-485. My deepest thanks and consideration are extended to my committee members, Dr. H.C. Perkins, Dr. A.J. Pearlstein, Dr. C.F. Chen and Dr. R.A. Petersen, who contributed a lot to what I have come to understand. Last, but not least, I would like to extend my appreciation and respect to Ms. Linda Harper for typing this dissertation.

TABLE OF CONTENTS

TABLE OF CONTENTS--continued

LIST OF ILLUSTRATIONS

LIST OF ILLUSTRATIONS--continued

LIST OF ILLUSTRATIONS--continued

LIST OF ILLUSTRATIONS--continued

LIST OF ILLUSTRATIONS--continued

LIST OF TABLES

ABSTRACT

The nonlinear interactions between a fundamental instability mode and both its harmonics and the changing mean flow are studied using the weakly nonlinear stability theory of Stuart and Watson, and numerical solutions of coupled nonlinear partial differential equations. The first part of this work focuses on incompressible cold (or isothermal; constant temperature throughout) mixing layers, and for these, the first and second Landau constants are calculated as functions of wavenumber and Reynolds number. It is found that the dominant contribution to the Landau constants arises from the mean flow changes and not from the higher harmonics. In order to establish the range of validity of the weakly nonlinear theory, the weakly nonlinear and numerical solutions are compared and the limitation of each is discussed. At small amplitudes and at low-to-moderate Reynolds numbers, the two results compare well in describing the saturation of the fundamental, the distortion of the mean flow, and the initial stages of vorticity roll-up. At larger amplitudes, the interaction between the fundamental, second harmonic, and the mean flow is strongly nonlinear and the numerical solution predicts flow oscillations, whereas the weakly nonlinear theory yields saturation. Beyond the region of exponential growth, the instability waves evolve into a periodic array of vortices.

In the second part of this work, the weakly nonlinear theory is extended to heated (or nonisothermal; mean temperature distribution) subsonic round jets where quadratic and cubic nonlinear interactions are present, and the Landau constants also depend on jet temperature ratio, Mach number and azimuthal mode number. Under exponential growth and nonlinear saturation, it is found that heating and compressibility suppress the growth of instability waves, that the first azimuthal mode is the dominant instability mode, and

that the weakly nonlinear solution describes the early stages of the roll-up of an axisymmetric shear layer.

The receptivity of a typical jet flow to pulse type input disturbances is also studied by solving the initial value problem and then examining the behavior of the long-time solution. The excitation produces a wave packet which consists of a few oscillations and is convected downstream by the mean flow. The magnitude of the disturbance in the jet depends on the location of the excitation and there is an optimum position at which little energy input will produce large perturbations. It is found that in order to generate the largest perturbations at any point in the jet, the disturbance should be deposited into the flow at a point where the phase velocity of the most amplified wave equals the fluid velocity (of the base flow).

CHAPTER 1

INTRODUCTION

1.1 Historical Background

Mixing layers, wakes and jets belong to a class of flows characterized by inflectional profiles in the mean streamwise velocity. These flows are inviscidly unstable; when excited by an oscillatory disturbance of suitable frequency (or wavenumber), the amplitude of the disturbance in the fluid increases exponentially with downstream distance (or time) according to linear stability theory (Drazin and Reid, 1981; Betchov and Criminale, 1967). The disturbance extracts energy from the mean flow, while at the same time it is convected with it. The instability mechanism is a Kelvin-Helmholtz type with viscosity being slightly stabilizing.

The exponential growth of the disturbance restricts the domain of validity of linear theory to short distances and times. Further downstream, the growth rate of the instability wave generally decreases and a "nonlinear region" appears, in which higher harmonics are present and the growth of the fundamental deviates from the exponential behavior. In this region, the "self-interactions" of the finite-amplitude disturbance become important and generate a wave Reynolds stress, which has an appreciable effect on the mean flow. This distortion of the mean flow modifies the rate of energy transfer from the mean flow to the disturbance and, since this energy transfer is the cause of the growth of the disturbance, there is a modification of the growth rate of the latter.

It is now generally accepted that large scale coherent structures, in addition to fine-scale chaotic motions, exist within turbulent free shear flows. Evidence of the wave-like coherent structures in fully turbulent subsonic (unheated) round jets is convincingly

displayed in the Schlieren photographs by Ahuja, Lepicovsky, Tam, Morris and Burrin (1982). These large-scale structures, whose dimension is on the order of the shear layer thickness, play an important role in controlling the dynamics of turbulent flows. The sequential mergings of these coherent structures in the downstream direction is a possible mechanism for the mixing and spreading of a shear layer (Winant and Browand, 1974). Ffowcs Williams and Kempton (1978) found that a large part of jet noise is a direct consequence of the large-scale structures, while the fine-scale chaotic turbulence plays a relatively minor role. On the other hand, Ahuja et al. (1982) argued that, although the large-scale structures are responsible for producing considerable changes in the fine-scale turbulence, the actual noise generation mechanism is a result of the latter. Irrespective of the mechanism through which this noise is produced, the large-scale structure plays an important role in the dynamics of turbulent shear flows.

Miksad (1972) has reviewed the results of many experiments on the instability of free shear layers, and also reported on his own work. He classified the instability into six successive flow regions: (1) the instability is initiated in a region close to the origin of the shear layer. A disturbance of small amplitude has exponential growth rate; the speed and wavelength are well predicted by the linear theory of spatially growing modes in an inviscid fluid, (2) in a region downstream, further exponential growth leads to nonlinearity, and to the generation of subharmonics as well as harmonics, (3) the fundamental, harmonics and subharmonics then equilibrate in unison, (4) a second region of subharmonic generation follows next, in accord with the theory of Kelly (1967). The fundamental remains little changed, but the harmonics begin to decay, (5) three-dimensional distortion of the fundamental begins, and (6) finally there is a region of breakdown into turbulence.

There is now considerable experimental evidence that the large-scale structures, and hence, the global features of turbulent flows can be organized by artificial excitations such as oscillating flaps, vibrating ribbons and acoustic devices (Wygnanski and Petersen, 1987). Ahuja et al. (1982) presented a series of measurements for subsonic jets excited at different frequencies. They have concluded that higher Mach number heated jets require higher excitation levels to produce noticeable changes in both large-scale structures and small-scale turbulence intensities. Control of flows by intentional excitation of natural flow instabilities involves new and largely unexplored phenomena and offers considerable potential for improving component performance in areas where mixing is important, such as combustors, rocket engines, internal mixers and ejectors. Petersen and Samet (1988) have shown that the mean velocity profile and the spreading rate of a turbulent axisymmetric cold low speed jet can be altered by introducing a controlled acoustic excitation. Stone and McKinzie (1984) concluded that deliberate acoustic excitation of coherent structures offers a promising new means of controlling turbulent shear flows. They have also emphasized the fact that, to date, most research work has been centered around unheated jet flows, usually at low speed. Therefore, future research work should be directed towards the understanding and control of coherent structures in heated high speed jets.

A jet is unstable to axisymmetric and azimuthal modes. Michalke and Hermann (1982) calculated the spatial growth rates of axisymmetric and (first) azimuthal disturbances and found that at low frequencies the first azimuthal mode is more unstable than the axisymmetric one. They also found that the phase velocity of the first azimuthal disturbance (β=1) is always smaller than the axisymmetric one (β=0). The phase velocity measured in jet turbulence, excited artificially by a loudspeaker (Chan, 1974), showed the

dominance of the axisymmetric disturbance. Thus, a jet forced by a loudspeaker in the plenum chamber is presumably dominated by axisymmetric modes. On the other hand, for an unexcited jet, the measured phase velocity follows more closely that of the first azimuthal disturbance at low frequencies, as can be seen from Ko and Davies (1975). The basic dynamical difference between axisymmetric and azimuthal modes is the presence of vortex-stretching in the latter.

In the study by Crow and Champagne (1971), a disturbance with a certain frequency and amplitude was introduced into the jet and the development of the disturbance was then followed downstream. By measuring the velocity fluctuations along the centerline of the jet, they found a distinct wave system, the wavelength being dependent on the forcing frequency and the jet velocity. The amplitude of the wave reached a peak and then gradually decayed downstream. The observed wave-like structures attained their greatest amplification at a Strouhal number (St; based on the jet diameter) of 0.3; waves of higher frequencies peaked (in the amplitude of the velocity fluctuations) closer to the nozzle exit but those of lower frequencies persisted further downstream. Excitation modified the mean flow along the centerline of the jet. Crow and Champagne also introduced the concept of a "preferred mode" of jet instability to denote that wave-like structure which attains the largest peak amplitude as the excitation Strouhal number is varied; the preferred mode was found to occur around St = 0.3.

The preferred mode of instability was investigated in an axisymmetric air jet of moderate Reynolds number by Petersen and Samet (1988). They examined the spatial evolution of the preferred mode by exciting the flow acoustically and then mapping the phase-locked velocity fluctuations. They found that throughout the potential core region, the phase-locked profiles agreed with the eigensolutions of the Orr-Sommerfeld stability equations provided the calculations were based on the measured, mean velocity profiles.

The excitation intensity was varied from low levels where the flow was merely tagged, to high levels where the mean flow was substantially distorted, and over that range of excitation there was no apparent deterioration in the agreement with stability predictions.

The effects of excitation are clearly shown in the excellent Schlieren photographs of Ahuja et al. (1982) in which concentrated vortex rings have formed in the shear layer downstream of the nozzle exit. By measuring the centerline variation of instability-wave pressure amplitude at various excitation levels as a function of axial distance, they found that the centerline mean velocity decays faster with downstream distance at lower Mach numbers when the jet is unheated (than at higher Mach numbers when the jet is heated). They also found that increasing the excitation level causes the jet to spread more rapidly; at a fixed downstream location, the mean velocity at the centerline decreased when the excitation level was increased. This work of Ahuja et al. was also extended to supersonic speeds (Lepicovsky et al., 1988). These investigators found that the threshhold of excitation level increases with increasing jet temperature (i.e., the sensitivity of heated jets to upstream acoustic excitation strongly varies with the jet operating conditions) and that no vortex pairings could be discerned from the Schlieren photographs (at high speeds; for an earlier report on this work, see Ahuja, Lepicovsky, and Brown, 1986).

The roll-up of the vorticity in a free shear layer is definitely a nonlinear phenomenon. In order to describe the early stages of this phenomenon and to provide some understanding of how it is affected by the various parameters in our problem (i.e., Mach number, heating, etc.), we use the weakly nonlinear theory of Stuart (1960) and Watson (1960).

This theory is extended to compressible and heated jets. We use a "temporal theory" in order to deal with a well-posed problem, although our results may not be as applicable

as those of a "spatial theory" to actual laboratory experiments. For a certain range of parameters, the issue here centers around the concepts of convective and absolute instabilities; an issue that was not resolved (for jets) until the work of Sohn (1986) (see also Monkewitz and Sohn, 1986, 1988). Sohn found that when the heating of the jet exceeds a certain amount, the axisymmetric and first azimuthal modes become absolutely unstable at some axial location. For an absolutely unstable flow, spatial theory is meaningless. Finally, Sohn speculated that whenever a jet is absolutely unstable, it is likely to be less sensitive to external excitation, and therefore, no longer controllable by low level forcing.

The Stuart-Watson approach has been applied to shear layers with the hyperbolic tangent velocity profile. Schade (1964) calculated the value of the first Landau constant at exactly the neutral point at infinite Reynolds number. He neglected the effect of the mean flow distortion (as we shall see from this study, this is the most important effect) and found that the first Landau constant is negative. This suggests that, at large amplitudes, the fundamental will saturate into an equilibrium amplitude. Maslowe (1977) carried this analysis further by establishing the dependence of the first Landau constant on the Reynolds number.

This was essentially the status of affairs at the beginning of the present study. Actually, the picture was even further confused by the work of Huerre (1980) in which a rather elaborate asymptotic analysis was carried out to study the effect of the mean flow distortion (which was neglected by Schade and Maslowe) on the nonlinear stability of a mixing layer. He found, through an incorrect analysis, that the mean flow distortion was destabilizing. This finding has since been revised by Huerre (1987).

In the work of Stuart and Watson, as well as in the references just cited, the weakly nonlinear stability theory was applied to the neutral waves. In an interesting paper,

Herbert (1983) has introduced an idea which removed this restriction; Herbert has shown how all the Landau constants may be defined systematically at all wavenumbers by a suitable "normalization" of the amplitude. All definitions of the Landau constants agree at the neutral wavenumber so that Herbert's work is consistent with the classical works on this subject.

The hydrodynamic instability of shear flows has been the subject of numerical investigation as well. Zabusky and Deem (1971) analyzed the nonlinear evolution of an unstable two-dimensional wake. They found that even in the nonlinear stage the disturbance amplitude does not reach a steady state, but instead exhibits a low frequency nonlinear oscillation. By examining the evolution of each Fourier component of the disturbance, they concluded that the interaction between the mean flow and the most unstable mode of the disturbance is responsible for the observed amplitude oscillation. Miura and Sato (1978) studied the nonlinear development of the most unstable mode for a bounded shear layer. By considering only the fundamental mode and a mean flow correction, and disregarding higher harmonics, they found that the amplitude oscillation is due to a temporal variation of the mean velocity profile.

In the classical, normal-mode, analysis of shear flows, nothing is said about the amplitude of the growing mode in relation to the input disturbance. Such a relationship is called the receptivity of the flow. Receptivity analysis gives the response of the flow to an impulsive or periodic-type source by solving the initial value problem. The long-time asymptotic solution to a pulse is a wave packet (Gaster, 1975), which may be defined as an amplitude modulated wavetrain of finite extent or as a group of waves of different amplitudes and wavenumbers. The long-time asymptotic solution to a periodic excitation

is a spatial instability mode whose characteristics (i.e., amplitude) depend on the location of the source.

The response of the flow to a pulse gives us information on the absolute/convective instabilities of the flow. A study along these lines was carried out by Huerre and Monkewitz (1985) for free shear flows with the tanh family of basic velocity profiles. By studying the branch point singularities of the complex dispersion relation, they found that spatial instability modes cannot evolve when there is a significant amount of reverse flow. In this case, the instability is termed absolute. On the other hand, when the external streams are co-flowing, the instability is convective, and the large (x,t) behavior of the solution is identical with that of the spatial instability mode at the excitation frequency. Balsa (1988) studied the receptivity of a typical free shear layer to pulse-type and periodic excitation. By solving the initial value problem completely, and studying its long-time behavior, Balsa found that the shear layer is very receptive to high-frequency disturbances that are generated near the centerline of the layer. While the work of Gaster (1965, 1975) and Huerre and Monkewitz (1985) describes the general structure of wave packets and spatial instability modes without explicitly addressing the receptivity issue or solving the initial value problem, the work of Balsa (1988) was mainly concerned with establishing the explicit connection between the perturbations in the flow and the external disturbances which generate them. This connection, which can be derived only by solving the initial value problem, contains what might be termed the "receptivity" of the flow.

Understanding the physics of large-scale structures or instability waves in free shear flows is important in engineering. Experimental evidence indicates that artificial excitation alters the mixing process. Arbey and Ffowcs Williams (1984) conducted experiments on a circular jet simultaneously excited by two different acoustic tones. By varying the phase

between two signals at harmonically related frequencies, they found that control can be exercised on the process of harmonic generation. The efficiency of many engineering devices which rely on fluid mixing such as combustors, diffusers and turbine blades can be improved by controlling the mixing process. In jets there is a close link between the flow characteristics and the noise radiated to the far-field. Based on classical aeroacoustics, an excited jet with significantly modified mean flow and large scale structures will generate different noise levels compared with those of an unexcited jet.

Techniques have long been sought for the controlled modification of various flow fields, such as jets, wakes, boundary layers, and separated flows. Recent published results of laboratory experiments (Brown and Roshko, 1974) have established that coherent structures exist even within apparently chaotic turbulent flow fields. Even more recent published results (Stone and McKinzie, 1984; Ahuja, et al., 1982) show that deliberate excitation of these coherent structures has a significant effect on the mixing characteristics of shear layers. Control of flows by intentional excitation of natural flow instabilities involves new and largely unexplored (especially in the presence of heating and Mach number effects) phenomena and offers considerable potential for improving component performance. Ejector performance can be improved by enhanced mixing leading to size and weight savings. Internal mixer nozzles are used to increase thrust, improve fuel economy, and reduce noise for turbofan engines. Enhanced mixing due to excitation has the potential to achieve better mixing with simpler (lower cost) mixer designs or to reduce mixing length to allow a shorter cowl, resulting in weight savings. Enhanced mixing may be applied to combustors to improve fuel/air mixing, leading to shorter combustors along with the possibility of improved pollution control; and to improve mixing of products and coolant to lower peak metal temperature. Excitation can provide the means to control

separation to improve the performance of wings, flaps, turbomachinery blades and diffusers. Stall due to flow separation is a concern for flow over airfoils and rotating machinery blades because it can lead to catastrophic failures. Increased mixing and spreading rates may be useful in reducing ground effects for vertical and short takeoff and landing aircraft. Since the exhaust is directed toward the ground, enhanced mixing might reduce ground heating and erosion. High-frequency excitation may also prove useful in preventing exhaust impingement on the fuselage. Finally, mechanical and aeroacoustic excitation may permit more efficient propulsion systems.

1.2 Scope of the Present Investigation

The main goals of the present investigation are: (1) to understand the nonlinear evolution of disturbances in mixing layers and in heated subsonic jets. The fundamental disturbance grows exponentially until forced to make some adjustment due to the combined effects of higher harmonics and mean flow changes. These nonlinear adjustments depend on the disturbance axial and azimuthal wavenumbers, on the mean velocity and temperature profiles, and on the Reynolds number, the Mach number and the jet temperature ratio; (2) to clarify certain issues related to the weakly nonlinear stability theory of Stuart and Watson. In particular, the relative contribution to the first Landau constant arising from the second harmonic and from the mean flow distortion; the dependence of the first Landau constant on the disturbance wavenumber; and the applicability of the theory to heated compressible jets; and (3) to study the receptivity problem in order to find out how to excite the flow in such a way as to produce large perturbations everywhere in the jet. For a typical jet flow, there is an optimum position to place a disturbance in such a way as to produce maximum perturbation velocities.

Instability waves in a base flow will be convected downstream by the flow, while at the same time they will grow in amplitude. In the course of time, a finite amplitude disturbance will evolve as the balance between the unsteady linear, nonlinear and viscous terms in the governing equations changes. Soon after the disturbance is introduced into the flow, self-interactions generate higher harmonics and a wave Reynolds stress, which will distort the mean flow and alter its stability characteristics. One objective of this investigation is to clarify the effect of the mean flow distortion on the growth of the nonlinear disturbance.

The Landau constants, which measure the importance of nonlinearity, are obtained for neutral and amplified waves in order to establish the range of validity of the weakly nonlinear theory and to see how the importance of the nonlinearity changes as the neutral wave is approached. The relative contributions of the harmonics and the mean flow distortion to the Landau constants are investigated.

In addition, the weakly nonlinear theory is extended to heated (i.e., nonisothermal) and compressible (i.e., with nonzero Mach number) jets which are subject to axisymmetric or azimuthal forcing. Cubic nonlinearities, which arise due to heating and are absent in incompressible flows, have significant effects on the Landau constants.

The weakly nonlinear theory is an asymptotic theory valid for (small) finite amplitudes. But available experimental data indicate that the amplitude of the perturbations can reach as much as 10 to 20% of the characteristic mean quantities. Furthermore, the weakly nonlinear theory cannot predict any nonlinear oscillations observed in experiments beyond the initial saturation of the fundamental wave. The numerical calculations of Miura and Sato (1978) for the inviscid bounded shear layer, which are based on the fundamental and the mean flow distortion component, show flow oscillations due to an energy exchange

between the mean flow and the fundamental. Therefore, in order to understand the behavior of strongly nonlinear waves and to test the applicability of the weakly nonlinear theory when nonlinearity is moderate, a numerical study is presented for the shear layer. The disturbance streamfunction is expanded in a Fourier series in the axial variable which, on substitution into the Navier-Stokes equations, leads to a system of coupled nonlinear partial differential equations in the coefficient functions. In this work, only the fundamental wave, the second harmonic and the mean flow distortion are present; these equations are solved numerically.

Finally, the receptivity of an ideal jet to a pulse type disturbance is studied by solving the initial value problem completely, and then studying the behavior of the long time solution. This solution depends on the strength and the location of the disturbance. The most receptive place is obtained by varying the location of the source along the radial direction and examining the magnitude of the subsequent perturbations.

In summary, the sensitivity of the flow to excitation is established via receptivity analysis and the way nonlinearity sets in is established via a combination of the weakly nonlinear theory and numerical solutions of nonlinear partial differential equations governing the fundamental, mean flow distortion and second harmonic modes. The applicability of the weakly nonlinear theory in describing the evolution of amplified disturbances is established by making a comparison with the numerical calculations. The weakly nonlinear theory of Stuart and Watson is extended to heated subsonic jets and the behavior of the first Landau constant is studied as a function of wavenumbers, Reynolds number, Mach number and temperature ratio.

CHAPTER 2

NONLINEAR ANALYSIS

2.1 The Compressible Heated Jet

The main purposes of this section are to provide the basic equations which will be used in the weakly nonlinear theory of a nonisothermal (heated and/or subsonic) jet and to discuss the validity of the simplifying assumptions. We begin with the equations of motion (Bird, Stewart and Lightfoot, 1960; the equations of state and continuity of an ideal gas with constant specific heats are used to reduce the energy equation (10.1-19(I) on page 322) of this reference into the form below, after neglecting viscous dissipation):

Continuity: $$\frac{\partial \rho}{\partial t} + \nabla\cdot(\rho \underset{\sim}{v}) = 0 \qquad (2.1\text{-}1)$$

Momentum: $$\frac{\partial}{\partial t}(\rho \underset{\sim}{v}) + \nabla\cdot(\rho \underset{\sim}{\underset{\sim}{v}}\underset{\sim}{v}) = -\nabla p + \nabla\cdot\underset{\sim}{\tau} \qquad (2.1\text{-}2)$$

Energy: $$\frac{\partial p}{\partial t} + \underset{\sim}{v}\cdot\nabla p + \kappa p \nabla\cdot\underset{\sim}{v} = (1-\kappa)\,\nabla\cdot\underset{\sim}{Q} \qquad (2.1\text{-}3)$$

where ρ, $\underset{\sim}{v}$, p, $\underset{\sim}{\tau}$ and $\underset{\sim}{Q}$ denote the fluid density, velocity, pressure, shear stress (tensor) and heat flux, respectively, and κ = const stands for the ratio of the specific heat capacities (c_p/c_v).

In the momentum equation, Eq. (2.1-2), we have neglected the effects of gravity because of the dominance of forced convection. Our primary interest in this study focuses on the "shear flow instability" of a gas jet in which convection dominates so that gravity and buoyance (the Richardson number is small) effects may be neglected. Buoyancy effects can be eliminated almost completely by orienting the jet column vertically,

if needed. The energy equation, Eq. (2.1-3), is valid for an ideal gas with constant specific heats, under the assumption that viscous dissipation is negligible. In addition to the above equations, we also have the familiar equation of state for an ideal gas as well as the usual constitutive relations, which express the shear stress in terms of the velocity gradients.

Our physical variables are decomposed into two parts; one corresponding to the base (also called the mean) flow (i.e., $\underset{\sim}{U}$ for velocity, P for pressure, R for density, etc.) and the other corresponding to the disturbances (i.e., $\underset{\sim}{u}$, p, ρ, etc.). We shall also assume that viscous and heat conduction effects are "unimportant" (the Reynolds number and hence the Peclet number Pe = RePr is assumed to be large, where Pr = O(1); we are interested in the "shear flow instability" in which convection dominates over viscous and conduction effects; free shear flows are especially unstable when they are nondissipative; actually, we shall neglect heat conduction altogether but retain viscous diffusion in order to treat neutral waves) so that the base flow may be considered (at least locally) parallel. This implies that $\underset{\sim}{U} \simeq U(y,z)\ \underset{\sim}{i}$, P $\simeq$ const, R $\simeq$ R(y,z) where $\underset{\sim}{x}$ = (x,y,z) is a Cartesian coordinate system, in which x points along the axis of the jet (y and z are transverse coordinates) and $\underset{\sim}{i}$ is the corresponding unit vector. When we get to the details of the analysis, the transverse coordinates will be replaced by polar coordinates (r,θ), but first it is convenient to write down the disturbance equations in vectorial form. After substituting our decomposition into Eqs. (2.1-1) through (2.1-3), we arrive at

$$\frac{\partial \rho}{\partial t} + \nabla\cdot(R\underset{\sim}{u} + \rho\underset{\sim}{U}) = -\nabla\cdot\rho\underset{\sim}{u} \tag{2.1-4}$$

$$\begin{aligned}\frac{\partial}{\partial t}(R\underset{\sim}{u} + \rho\underset{\sim}{U}) + \nabla\cdot(R\underset{\sim}{U}\underset{\sim}{u} + R\underset{\sim}{u}\underset{\sim}{U} + \rho\underset{\sim}{U}\underset{\sim}{U}) + \nabla p \\ - \frac{1}{Re}\nabla^2\underset{\sim}{u} = -\frac{\partial}{\partial t}(\rho\underset{\sim}{u}) \\ - \nabla\cdot(R\underset{\sim}{u}\underset{\sim}{u} + \rho\underset{\sim}{U}\underset{\sim}{u} + \rho\underset{\sim}{u}\underset{\sim}{U} + \rho\underset{\sim}{u}\underset{\sim}{u})\end{aligned} \tag{2.1-5}$$

$$\frac{\partial p}{\partial t} + \underset{\sim}{U}\cdot\nabla p + \kappa P \nabla\cdot\underset{\sim}{u} = -\underset{\sim}{u}\cdot\nabla p - \kappa p \nabla\cdot\underset{\sim}{u} \qquad (2.1\text{-}6)$$

The significance of the locally parallel approximation, within the context of shear flow instability, is well understood and will not be discussed further. On the other hand, in deriving Eqs. (2.1-4) through (2.1-6), we have made some additional assumptions that need further clarification. First, the equations are written in a nondimensional form in which distances have been normalized by the jet radius, velocities by U_c (where the subscript c denotes the value of the quantity on the jet centerline), density by R_c, pressures by $R_c\ U_c^2$ and time by the characteristic transit time (jet radius)/U_c. As a result of this nondimensionalization, viscosity in Eq. (2.1-5) is replaced by an inverse Reynolds number, Re = (jet radius) $U_c\ \rho_c/\mu_{crit} \simeq$ const, where μ_{crit} is the viscosity of the fluid in the so-called critical layer. We next explain how this replacement comes about.

One of the main objectives of this research is to study the nonlinear evolution of an instability mode in a subsonic heated jet at high Reynolds number. As is well-known, these instabilities are inviscid (they arise from the inflectional character of the base velocity profile), and for all practical purposes, the viscous term in Eq. (2.1-5) is unimportant, except for a neutral (or a very near-neutral) wave, and even for this wave the effects of viscosity are important only in a thin layer in the jet whose (nondimensional) thickness is on the order of $Re^{-1/3}$. This thin layer, centered on the inflection point, is called the critical layer. The key observation is that within this thin layer, the viscosity is a constant to a good degree of approximation, so that $\mu \simeq \mu_{crit}$. To be sure, outside the critical layer, we have the incorrect value of the viscosity, but because of the inviscid character of the instability, this is immaterial as long as the Reynolds number is large.

Furthermore, because of the very small thickness of the critical layer, derivatives normal to this layer are very much larger than those tangential to the layer, and the

component of the velocity tangential to the layer is much larger than those normal (these remarks are very reminiscent of the classical boundary layer approximation). Thus, the shear force in the critical layer is given by $\mu_{crit}\ \nabla_t^2\ \underset{\sim}{u}$, where ∇_t is the gradient operator in the transverse, (y,z), space. In Eq. (2.1-5), we replace ∇_t by ∇ (i.e., we keep an unimportant term) in order to simply effect comparisons between published results (for constant property flows) and our results in this special case. This approximation for the shear stress, together with scaling arguments, is also discussed by Shen (1964, p. 761).

In this study, we set the thermal conductivity to zero in the disturbance energy equation, Eq. (2.1-6). This approximation brings about considerable simplification in the weakly nonlinear theory, as well as in the numerical solution of the relevant equations, because the entire disturbance problem can be formulated in terms of ρ, $\underset{\sim}{u}$ and p, without any reference to the temperature field. The main limitation of this assumption is that we cannot accurately compute the density (or temperature) field associated with a neutral instability wave. In a separate study (Ng, 1989), this limitation is studied more carefully and quantitatively. Our assumption of neglecting thermal conductivity is summarized rather succinctly by Lees and Lin (1946): "The influence of the conductivity on the viscous solutions of the velocity components is only secondary for Reynolds numbers of the order of magnitude of those encountered in most aerodynamic problems."

In the analysis, a cylindrical coordinate system (x, r, θ) with velocity components(u, v, w) is used and the mean profiles are given in Appendix A. The chosen base velocity profile agrees reasonably well with both experimental data and the similarity solution. The mean density profile is an approximate solution of the Navier-Stokes equations when the Reynolds number is large and the Prandtl number is unity. The latter profile is obtained (Schlichting, 1979, pp. 330) by solving the boundary layer-type momentum and energy

equations after assuming that the temperature T depends solely on the velocity component U and that the viscosity and the thermal conductivity are constants. The resulting density distribution depends on the jet temperature ratio, $T^* = T_C/T_\infty$; the jet Mach number, M, and the ratio of the specific heats, κ (see Appendix A). The ambient temperature is denoted by T_∞ (in appropriate units). The numerical calculations will be carried out for these base flow profiles although the general theory is valid for arbitrary profiles. Typical velocity and temperature profiles are shown in Figure 1.

In linear stability theory, the right-hand sides of (2.1-4), (2.1-5), and (2.1-6) are ignored because they are (at least) quadratically small in the perturbations, and a modal solution is studied in the form

$$v(x,r,\theta,t) = A_0\, e^{a_0 t}\, v_{10}(r)\, e^{i(\alpha x+\beta\theta-\omega_0 t)} + \text{c.c.} \qquad A_0 = \text{const} \qquad (2.1\text{-}7a)$$

with some arbitrary normalization, say $v_{10}(r_0) = 1$; r_0 is the location of the inflection point in the mean velocity profile and c.c. denotes the complex conjugate. We may think of A_0 $\exp(a_0 t)$ as the amplitude of this mode. The complex growth rate is $\lambda_0 = a_0 - i\omega_0$; ω_0 is the (real) frequency, the axial and azimuthal wavenumbers, α, β are real, and $v_{10}(r)$ is the radial distribution of the mode. Similar forms hold for u, w, p and ρ, although only one of these quantities may be normalized.

We shall also refer to the complex growth rate λ_0 as the (linear) eigenvalue, although in classical (linear) stability theory it would be more conventional to call $i\lambda_0/\alpha$ the eigenvalue (which is usually denoted by c). The objective of <u>linear</u> stability theory is the determination of the complex mode shape, v_{10}, and the corresponding eigenvalue λ_0. In general (subsonic flows), v_{10} vanishes at $r = \infty$ and is finite on the jet axis, $r = 0$. The objectives of <u>nonlinear</u> stability theory are quite similar, more specifically we wish to find

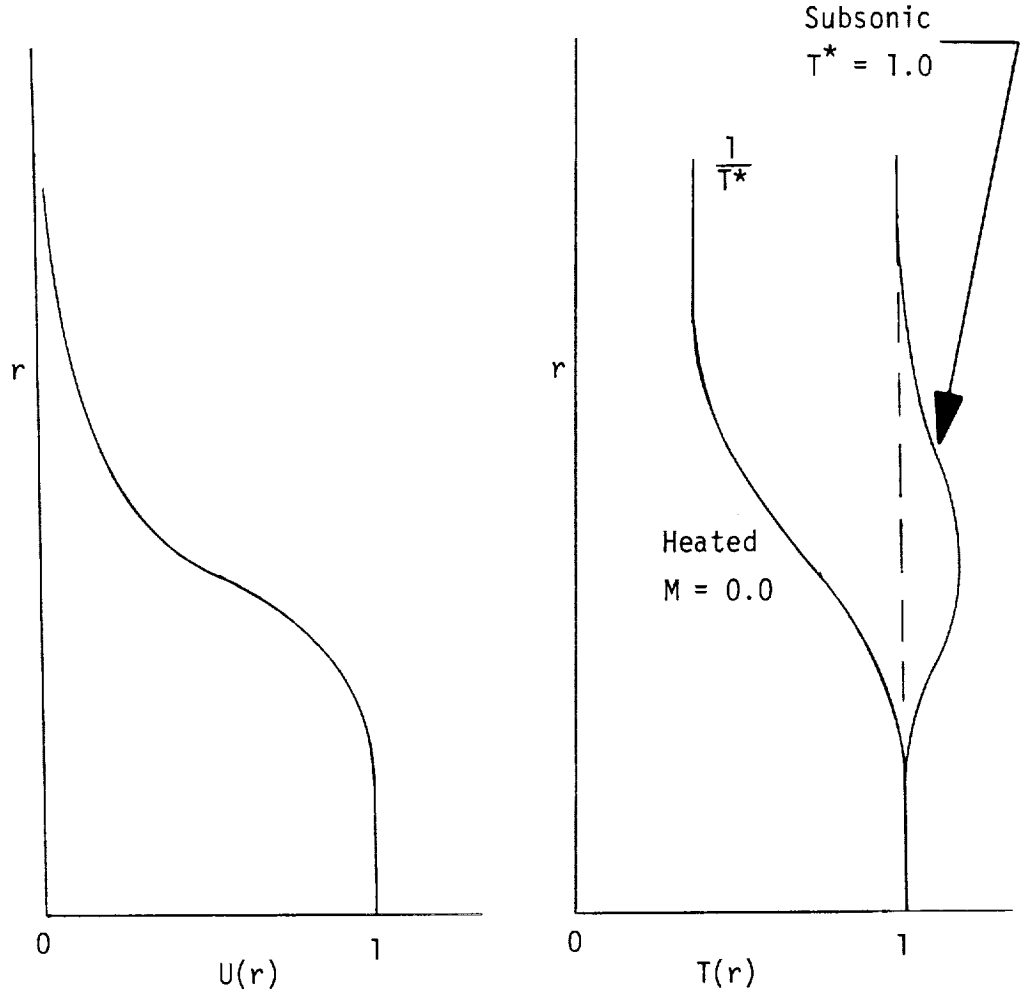

Figure 1. General mean velocity and temperature profiles. The mean temperature distribution depends on jet temperature ratio ($T^* = T_c/T_\infty$) and Mach number (M). The dashed line is that of a cold ($T^* = 1$) incompressible (M = 0) jet.

out how the growth rate and frequency, and the mode shape are altered by finite amplitude effects.

There are several types of nonlinear stability theory, usually characterized by the phrases "viscous critical layer," "nonlinear critical layer" (or some combination of them), "equilibrium" and "non-equilibrium critical layers." Examples of these may be found in (Stuart, 1960; Benney and Bergeron, 1969; and Stewartson, 1978). The present work is a direct extension of Stuart's seminal work to subsonic and heated jets, and may be characterized as a "viscous and equilibrium critical layer theory." It is essentially the temporal theory in which the flow is spatially periodic in the streamwise direction.

When the nonlinear terms are taken into account, the disturbance interacts with itself in addition to the mean flow. These interactions result in the generation of harmonics, a mean-flow distortion and a distortion of the fundamental. Moreover, the amplification rate (a_0) and frequency (ω_0) of the disturbance will change with amplitude due to nonlinear effects. Therefore, we expand the disturbance in its Fourier series

$$\underset{\sim}{u}(\underset{\sim}{x},t) = \sum_{n=-\infty}^{\infty} \underset{\sim}{u}_n(r,t)\, e^{in\phi} \qquad (2.1\text{-}7b)$$

where the phase ϕ is $\phi = \alpha x + \beta\theta - \gamma(t)$, n is the order of the harmonic, and $\gamma(t)$ is real. After comparing Eq. (2.1-7b) for n = 1 with Eq. (2.1-7a), we see that $d\gamma/dt$ is essentially a frequency. The disturbance is taken to be periodic in x and θ but its time dependence is still arbitrary since $\underset{\sim}{u}_n$ also is allowed to depend on time. By using the series (2.1-7b), we restrict the class of solutions to those that are periodic in x and θ with wavenumbers α and β. The series (2.1-7b) contains all the harmonics but only the first few will be calculated, namely, the fundamental (n = 1), the second harmonic (n = 2), the mean flow

distortion (n = 0) and the third harmonic (n = 3). Similar equations hold for p and ρ. For a real solution,

$$\underset{\sim}{u}_{-n}(r,t) = \underset{\sim}{u}_n^*(r,t) \tag{2.1-8}$$

must be satisfied where * denotes the complex conjugate.

Attention is focused on finite but sufficiently small disturbance amplitudes, which may be reached at some finite time; therefore, each of the harmonics $\underset{\sim}{u}_n(r,t)$ is expanded in a "Taylor series" of the real amplitude A = A(t) of the fundamental mode (n = 1). We write

$$\underset{\sim}{u}_n(r,t) = A^n(t) \sum_{m=0}^{\infty} \underset{\sim}{u}_{nm}(r)\, A^{2m}(t)\ ;\quad n \geq 0 \tag{2.1-9}$$

with

$$\underset{\sim}{u}_{00} = p_{00} = \rho_{00} = 0 \tag{2.1-10}$$

The validity of Eq. (2.1-9) may be seen heuristically as follows. Consider the n = 2 term (the second harmonic) as an example; when the amplitudes are very small, this second harmonic is generated by the square of the fundamental, therefore, its dominant amplitude should scale as AA = A^2 (or more generally as A^n). This is the leading coefficient on the right-hand side of Eq. (2.1-9). However, a second harmonic can also be generated by a quadratic interaction between the third harmonic (whose leading amplitude scales a as A^3) and the fundamental; the result is that this latter interaction should scale as $A^3A = A^4$. This type of an interaction is represented by the second term of the infinite sum (i.e., n = 2, m = 1) in Eq. (2.1-9). Clearly, there is an infinite set of interactions that will regenerate the second harmonic, and this observation explains the presence of the infinite sum.

Note that for $n < 0$, we use (Eq. (2.1-8); we cannot have negative values of n in Eq. (2.1-9). In order to ensure that the disturbance is always small, we require Eq. (2.1-10). Otherwise, the fundamental disturbance would begin with $\underset{\sim}{u}_0 = \underset{\sim}{u}_{00}(r) + \cdots$ which has already been accounted for as the base flow. Finally, note that for compressible flows, we also have cubic interactions [e.g., $\rho\underset{\sim\sim}{uu}$ in the momentum equation, Eq. (2.1-5)] in addition to the more familiar quadratic interactions which also occur in constant density flows. It is consistent with the above expansions Eqs. (2.1-7b) and (2.1-9) to seek an amplitude equation of the form (Stuart, 1960; Watson, 1960; Herbert, 1983)

$$\frac{1}{A}\frac{dA}{dt} - i\frac{d\gamma}{dt} = \sum_{m=0}^{\infty} \lambda_m A^{2m} \qquad (2.1\text{-}11)$$

where

$$\lambda_m = a_m - i\omega_m = \text{complex Landau constants, } m \geq 1$$

Indeed, the seminal contribution of Stuart and Watson lies in the demonstration that Eqs. (2.1-7b), (2.1-9) and (2.1-11) will solve the incompressible Navier-Stokes equations exactly, provided that the Landau constants, λ_1, λ_2, $\cdots$, are chosen in a certain way (we shall come back to this issue momentarily). Recall that λ_0 is the linear eigenvalue. It is, of course, important to recognize that this solution is a formal solution (essentially a Taylor series in the amplitude) whose radius of convergence is unknown. There is some evidence (Sen and Venkateswarlu, 1983) for plane Poiseuille flow, which suggests that this radius of convergence is nonzero; the present study also suggests that this is indeed the case when the Reynolds number is low to moderate (see Chapter 5). We will truncate the right-hand side of Eq. (2.1-11) after the quadratic term and use this nonlinear amplitude equation to study the evolution of small amplitude (but nonlinear) disturbances.

Apart from the convergence issue, which was very briefly alluded to previously, the success of amplitude equation, Eq. (2.1-11), depends on the rational and systematic determination of the Landau constants. In the classical theories, where the linear mode - whose nonlinear characteristics are sought - is exactly neutral, the so-called solvability condition (or Fredholm alternative) allows such a determination (Stuart, 1960). Herbert (1983) suggested an alternative approach to the definition of the Landau constants. This latter approach may be applied to unstable linear modes as well, and appears to be easier to enforce than the classical solvability condition. In the present work, we shall follow Herbert's ideas because we are very much interested in the calculation of the Landau constants of (slightly) unstable waves, and their attendant variation with wavenumbers α, β. Indeed, we find that the Landau constants vary extremely rapidly with the wavenumbers. This is a completely new result that was not anticipated at all at the beginning of this research.

The key idea of Herbert is that the amplitude A = A(t) must be that of the fundamental (n = 1) mode at an arbitrary point (say, $r = r_0$), that is, $v_1(r_0,t) = A(t)$. In view of Eq. (2.1-9), the last remark implies

$$\sum_{m=0}^{\infty} v_{1m}(r)\, A^{2m} = 1 \quad \text{at} \quad r = r_0 \tag{2.1-12a}$$

or

$$v_{10}(r_0) = 1$$

$$v_{11}(r_0) = v_{12}(r_0) = \cdots = 0 \tag{2.1-12b}$$

Equations (2.1-12b) serve as the normalization conditions for the linear and the nonlinear contributions to the fundamental.

It can be shown that Herbert's and the classical definitions of the Landau constants are identical when the linear mode is precisely neutral (Herbert, 1983). It should also be noted that different choices for r_0 (we usually set r_0 to the position of the inflection point of the base velocity profile) imply different normalizations, hence different amplitudes. Finally, we choose to normalize the cross-section component v because in this way our results are easily compared with published (incompressible) results that usually employ a streamfunction.

After substituting Eqs. (2.1-7b), (2.1-9) and (2.1-11) into the governing equations, Eqs. (2.1-4), (2.1-5), and (2.1-6), and collecting terms, the following ordinary differential equations are obtained for the mode shapes $\underset{\sim}{u}_{nm}(r)$, $p_{nm}(r)$ and $\rho_{nm}(r)$

$$\Lambda\rho_{nm} + R\nabla\cdot\underset{\sim}{u}_{nm} + R'v_{nm} = F_{nm}^{(1)} - nm\lambda_1\,\rho_{10} \tag{2.1-13}$$

$$\left[R\Lambda - \frac{1}{Re}\nabla^2\right] u_{nm} + RU'v_{nm} + in\alpha p_{nm} = F_{nm}^{(2)} - nm\lambda_1 R u_{10} \tag{2.1-14}$$

$$\left[R\Lambda - \frac{1}{Re}\left(\nabla^2 - \frac{1}{r^2}\right)\right] v_{nm} + p'_{nm} + \frac{1}{Re}\frac{2in\beta}{r^2} w_{nm} = F_{nm}^{(3)} - nm\lambda_1 R v_{10} \tag{2.1-15}$$

$$\left[R\Lambda - \frac{1}{Re}\left(\nabla^2 - \frac{1}{r^2}\right)\right] w_{nm} + \frac{in\beta}{r} p_{nm} - \frac{1}{Re}\frac{2in\beta}{r^2} v_{nm} = F_{nm}^{(4)} - nm\lambda_0 R w_{10} \tag{2.1-16}$$

$$M^2 \Lambda p_{nm} + \nabla \cdot \underset{\sim}{u}_{nm} = M^2 \left[F_{nm}^{(5)} - nm\lambda_1 p_{10} \right] \tag{2.1-17}$$

where

$$\Lambda(r) = 2ma_0 + in\alpha(U - c_0)$$

$$\nabla \cdot \underset{\sim}{u}_{nm} = in\alpha u_{nm} + v'_{nm} + \frac{1}{r} v_{nm} + \frac{in\beta}{r} w_{nm}$$

$$\nabla^2 = \frac{d^2}{dr^2} + \frac{1}{r}\frac{d}{dr} - n^2\left[\alpha^2 + \frac{\beta^2}{r^2}\right]$$

$$\lambda_0 = -i\alpha c_0 = a_0 - i\omega_0 = \text{linear eigenvalue}$$

where the prime represents differentiation with respect to r and n = 0,1,2,3, m = 0,1. Recall that R = R(r) and U = U(r) denote the (nondimensional) density and velocity profiles of the base flow respectively, and Re and M are the characteristic Reynolds and Mach numbers of the flow (see Appendix A). The nonlinear interactions are contained in the terms $F_{nm}^{(j)}$, j = 1,⋯,5. They vanish for the linear mode, and every nonlinear mode is forced by modes of lower order in the amplitude. They are given in detail in Appendix B. The following first few modes are of interest: the O(A) linear mode n = 1 and m = 0; the second harmonic mode n = 2 and m = 0; the third harmonic mode n = 3 and m = 0; the mean flow distortion mode n = 0 and m = 1; and the distortion of the fundamental mode n = 1 and m = 1. The mode n = 0 and m = 0 is set to zero per (2.1-10). The first Landau constant is denoted by λ_1.

Our governing equations, Eqs. (2.1-13) to (2.1-17), are solved numerically using finite difference methods. For n = 1, m = 0, the relevant equations contain the unknown eigenvalue λ_0. The only other set of equations which poses some difficulty arises from n = m = 1 and contains the first Landau constant, λ_1. Before solving these equations, we

first observe that the operators on the left-hand sides of these equations are almost the same as those in the case of the fundamental (n = 1, m = 0). Therefore, the homogeneous system will admit a nontrivial solution and the corresponding inhomogeneous system will have a solution if and only if the right-hand sides of Eqs. (2.1-13) to (2.1-17) satisfy a certain condition. This condition determines the first Landau constant, λ_1.

In fact, when the growth rate, a_0, vanishes, this condition is given by the Fredholm alternative. In the present work, where $a_0 \neq 0$, we follow Herbert (1983) and decompose our dependent variables as

$$(\cdot)_{11} = - \frac{\lambda_1}{2a_0} (\cdot)_{10} + (\hat{\cdot})_{11} \tag{2.1-18}$$

where the quantities $(\hat{\cdot})_{11}$ satisfy a system of inhomogeneous equations which are independent of λ_1. More importantly, when $a_0 \neq 0$, the equations for $(\hat{\cdot})_{11}$ may be solved uniquely and λ_1 is determined by enforcing $( )_{11} = 0$ at $r = r_0$ for one of the dependent variables (see Eq. (2.1-12b)). This procedure of Herbert is the one that we follow in the present study.

For each nm-mode, the above equations are solved as follows. First, an inhomogeneous Orr-Sommerfeld type equation is obtained in terms of the pressure, p_{nm}. The forcing terms on the right-hand side of this equation include the known nonlinear interactions from the previous modes and some velocity terms associated with the nm-mode, which are set to zero in the first iteration. Second, once the pressure (not yet the exact solution) is calculated, equations (2.1-14), (2.1-15) and (2.1-16) are then solved for u_{nm}, v_{nm} and w_{nm} respectively. Third, the pressure and velocities are updated by a second iteration and the process is repeated until the solutions no longer change. Usually three to six iterations are enough to bring the final two successive solutions to within a

fraction of a percent of each other. Finally, equation (2.1-13) is used to solve explicitly for ρ_{nm} using the last calculated values of the velocities and the pressure.

The Orr-Sommerfeld-like equations are solved by finite difference matrix methods where the governing ordinary differential equations are replaced by difference equations using central difference approximations to the derivatives to yield a system of algebraic equations (Paragiri, 1985). A fourth-order scheme (truncation error is $O(\Delta r)^4$) is employed, which translates the ordinary differential equations into a pentadiagonal system of equations which is solved by standard L-U decomposition. In order to ensure the convergence of the numerical results, we require that the calculated eigenvalues and modes be independent of the input parameters such as the number of mesh points N. We ran numerical experiments for different values of N (between 100 and 600) and r_{max} (i.e., the radial location of the outer boundary condition; between 3.0 and 6.0) and decided that N = 200, r_{max} = 4.0 and Δr = 0.02 give accurate results. For example, the relative errors in the calculations made with these values (N = 200, r_{max} = 4.0) and those with (200, 6.0) and (400, 4.0) were 0.002% and 0.001%, respectively (incompressible and cold jet, Re = ∞, α = 1.25, β = 0). Since the theoretical approach is based on a perturbation about the linear solution, the linear problem is solved first, and the higher modes are then found in succession. The solution is obtained to $O(A^3)$. The eigenvalues are found by the Newton-Raphson method, which is a local not a global method, where iterations (usually three to six) are performed until Eq. (2.1-12) is satisfied. Our (most unstable) eigenvalues agree with those of Batchelor and Gill (1962), Michalke (1964), Morris (1976) and Michalke and Hermann (1982).

The boundary conditions satisfied by the disturbance pressure are:

$$p_{nm}(0) = \text{finite}, \qquad p_{nm}(\infty) = 0 \tag{2.1-19}$$

Since the base flow derivatives, U′ and R′, vanish as $r \to 0$ and as $r \to \infty$, the pressure, p_{nm}, satisfies a modified Bessel-type equation, and therefore, the asymptotic solutions of p_{nm} which satisfy boundary conditions (2.1-19) are

$$p_{nm}(r\to 0) \sim I_{n\beta}\left[(n^2\alpha^2 + M^2\, R(r\to 0)\, A^2(r\to 0))^{1/2}\, r\right] \qquad (2.1\text{-}20a)$$

$$p_{nm}(r\to \infty) \sim K_{n\beta}\left[(n^2\alpha^2 + M^2\, R(r\to \infty)\, A^2(r\to \infty))^{1/2}\, r\right] \qquad (2.1\text{-}20b)$$

where $I_{n\beta}$ and $K_{n\beta}$ are the modified Bessel functions of order $n\beta$. Recall that β is the azimuthal mode number. Physically, the boundary conditions mean that the flow is inviscid near the centerline of the jet and at large r. In the numerical calculations, the outer boundary condition ($r \to \infty$) is implemented at r = 4.0.

2.2 The Incompressible Shear Layer

We briefly digress to derive the weakly nonlinear characteristics of a mixing layer in the viscous critical layer limit. In Chapter 5, we study the (strongly) nonlinear behavior of a mixing layer numerically and it is desirable to compare the latter with the former. These weakly nonlinear results for the mixing layer could be obtained from those for the jet in the limit of (momentum thickness)/(jet radius) $\to$ 0, but it is simpler to start anew. We shall provide only the essential results as this derivation was also given by Herbert (1983).

The streamfunction $\psi(x,y,t)$ of an instability wave riding on top of a parallel flow, with velocity $\underset{\sim}{U} = [U(y),0]$, obeys

$$\left[\frac{1}{Re}\nabla^4 - \left(U\frac{\partial}{\partial x}\nabla^2 - U''\frac{\partial}{\partial x}\right) - \frac{\partial}{\partial t}\nabla^2\right]\psi$$

$$= \left(\frac{\partial\psi}{\partial y}\frac{\partial}{\partial x} - \frac{\partial\psi}{\partial x}\frac{\partial}{\partial y}\right)\nabla^2\psi\,. \qquad (2.2\text{-}1)$$

where all lengths have been nondimensionalized by the momentum thickness of the base flow, θ_* and all velocities by the value of the external stream at $y = +\infty$ [i.e., $U(y \to \infty)$]. Therefore, the Reynolds number is $Re = \theta_* U(y \to \infty)/\nu$, where ν is the kinematic viscosity. As usual, the disturbance is expanded in its Fourier components, $\phi_n(y,t)$,

$$\psi(x,y,t) = \sum_{n=-\infty}^{\infty} \phi_n(y,t)\, e^{in(\alpha x - \gamma(t))} \qquad (2.2\text{-}2)$$

where α is the wavenumber and $\gamma(t)$ is undefined at this point. Furthermore, each of the harmonics $\phi_n(y,t)$ is expanded in terms of the small amplitude A(t)

$$\phi_n(y,t) = A^n(t) \sum_{m=0}^{\infty} \phi_{nm}(y)\, A^{2m}(t)\,; \quad n \geq 0 \qquad (2.2\text{-}3)$$

After substituting Eqs. (2.2-2) and (2.2-3) along with an amplitude expansion (2.1-11) into Eq. (2.2-1) and separating out the various Fourier components and powers of the amplitude, the following hierarchy of equations is obtained for the mode shapes $\phi_{nm}(y)$,

$$\left[\frac{1}{Re}\nabla_n^4 - A\,\nabla_n^2 + in\alpha\,U''\right]\phi_{nm}$$

$$= \sum_{k=1}^{m}\left[2(m-k)\,a_k + n\lambda_k\right]\nabla_n^2\,\phi_{n\;m-k}$$

$$+ \sum_{L=0}^{n}\sum_{k=0}^{m} N[\phi_{Lk},\phi_{n-L\;m-k}]$$

$$+ \sum_{L=1}^{m}\sum_{k=0}^{m-L}\Big\{N[\phi_{-Lk},\phi_{n+L\;m-L-k}]$$

$$+ N[\phi_{n+L\;m-L-k},\phi_{-Lk}]\Big\} \qquad (2.2\text{-}4)$$

where

$$A(y) = 2ma_0 + in\alpha(U-c_0)$$

$$\nabla_n^2 = \frac{d^2}{dy^2} - n^2\alpha^2\,; \qquad \nabla_n^4 = (\nabla_n^2)^2$$

and

$$N[\phi_{kn},\phi_{Lm}] = i\alpha\left(L\,\frac{d\phi_{kn}}{dy} - k\,\phi_{kn}\,\frac{d}{dy}\right)\nabla_L^2\,\phi_{Lm}$$

The operator N expresses all the nonlinear interactions that are relevant to a particular $(\,)_{nm}$ mode. These are, of course, known from the lower levels of the hierarchy. Recall that λ_k ($k = 1,2,\cdots$) are the Landau constants

$$\lambda_k = a_k - i\omega_k$$

and $\lambda_0 = a_0 - i\omega_0$ is the linear eigenvalue; a_0 is the growth rate and ω_0 is the frequency. Note from Eq. (2.1-11) that

$$\frac{d\gamma}{dt} = \sum_{m=0}^{\infty} \omega_m A^{2m}$$

so that the above quantity is essentially a frequency (which in a nonlinear theory depends on the amplitude). Therefore, $\gamma(t)$ is a measure of the phase of the disturbance. The boundary conditions satisfied by the disturbance are

$$\phi_{nm}(y) \sim e^{\pm n\alpha y} \quad \text{as} \quad y \to \mp \infty \tag{2.2-5}$$

The mode shapes are arbitrarily normalized according to

$$\sum_{m=0}^{\infty} \phi_{1m}(y)\, A^{2m} = 1 \quad \text{at} \quad y = 0. \tag{2.2-6a}$$

so that

$$\phi_{10}(0) = 1$$

$$\phi_{1m}(0) = 0 \qquad m = 1,2,\cdots \tag{2.2-6b}$$

It is precisely this normalization which defines the complex Landau constants λ_k ($k = 1,2,\cdots$).

We shall solve (2.2-4) for the following modes: $O(A)$ linear mode $(n,m) = (1,0)$; $O(A^2)$ second harmonic mode $(n,m) = (2,0)$; $O(A^3)$ third harmonic mode $(n,m) = (3,0)$; $O(A^2)$ mean flow distortion mode $(n,m) = (0,1)$; $O(A^3)$ distortion of the fundamental mode $(n,m) = (1,1)$; $O(A^4)$ distortion of the second harmonic mode $(n,m) = (2,1)$; $O(A^4)$ mean flow distortion mode $(n,m) = (0,2)$; and $O(A^5)$ distortion of the fundamental mode

(n,m) = (1,2). The mode (n,m) = (0,0) is set to be equal to zero to ensure that nonlinearities first enter at $O(A^2)$.

The linear eigenvalue λ_0 and the corresponding mode shape ϕ_{10} are obtained by the method of Paragiri (1985). The higher order modes are obtained by solving (2.2-4) in succession and the Landau constants are determined from the normalization condition (2.2-6b) and a decomposition of the type (2.1-18) [see Herbert (1983)]. The differential equations are converted into a pentadiagonal system (fourth-order accuracy in grid size so that the truncation error is $O(\Delta y)^4$) of linear algebraic equations and these are solved by L-U decomposition. The method is very robust and efficient and we did not encounter any serious numerical problems. Numerical experiments were carried out (the number of mesh points was varied from 201 to 601) to ensure convergence via the insensitivity of the eigenvalues and modes to assigned input parameters to arrive at: N = number of mesh points or the number of algebraic equations = 401, domain from y = -4 to y = 4 (the boundary conditions are enforced at these values of y) and $\Delta y = 0.02$ (see our remarks on page 41).

2.3 Strong Nonlinearities

In the temporal nonlinear stability theory (Stuart, 1960; Watson, 1960; Herbert, 1983) of unstable flows, a small single disturbance of linear growth rate a_0, amplitude A(t) and axial wavenumber α will, due to nonlinear interactions, generate higher harmonics with wavenumbers $n\alpha$ ($n = 2,3,\cdots$) and distort the mean flow (via the zeroth harmonic; n = 0) during the evolution of the flow. Once the flow is perturbed by an unstable fundamental wave, $e^{i\alpha x}$, its amplitude increases exponentially with time until it interacts with itself to generate the second harmonic $e^{2i\alpha x}$ (the sum mode) and with its complex conjugate to generate the zeroth harmonic $e^{0i\alpha x}$ (the difference mode). Once the second

harmonic is in the flow, it interacts with the fundamental to generate the third harmonic $e^{3i\alpha x}$. This is how the third harmonic appears initially. Further interactions between these harmonics will generate other harmonics, products of which will also produce new harmonics or reinforce others that already exist in the flow. The flow will then be made up of all the harmonics of the fundamental.

Any numerical solution of the Navier-Stokes equations can only account for a finite number (but moderately large) of these product interactions. In our analytical work, we can formally calculate all the interactions via the hierarchy of equations expressed by (2.2-4). In order to examine the accuracy of truncating this hierarchy at a low level, we perform some numerical studies on an incompressible mixing layer.

The central idea of classical weakly nonlinear theory is that the second harmonic interacting with the fundamental reproduces the fundamental. In essence, the fundamental exists for two reasons: first, it is the principal disturbance which is placed in the base flow and, secondly, it is also generated by the mechanism just described above. This mechanism can either increase or decrease the total amount of the fundamental - in other words, nonlinearities may destabilize or stabilize the flow.

In the following numerical work, we wish to adhere to this central idea of classical weakly nonlinear theory and consider the first few harmonic interactions. The principal difference between the numerical and analytical work is the treatment of the critical layer. In the analysis, which is an asymptotic solution of the truncated equations for small amplitudes, the critical layer is linear (to first order) and viscous, whereas in the numerical work, it is nonlinear and viscous. A comparison of these results will show (at least qualitatively) the amplitude of the instability wave at which the critical layer becomes strongly nonlinear. The nonlinear evolution of a two-dimensional shear layer is described

by Equation (2.2-1). The disturbance streamfunction is once more expanded in a Fourier series in the axial variable x,

$$\psi(x,y,t) = \sum_{n=-\infty}^{\infty} \phi_n(y,t)\, e^{in\alpha(x-ct)} \tag{2.3-1}$$

where c is the disturbance phase velocity. The disturbance is considered to be periodic in x but its time dependence is arbitrary since ϕ_n also depends on time, and the exponential time factor associated with the phase speed is extracted for convenience only.

Substitution of (2.3-1) into (2.2-1) yields a set of equations for each Fourier component. The equations for the fundamental mode ϕ_1, the first harmonic ϕ_2 and the mean flow distortion ϕ_0 are (Stuart, 1960)

$$\left[\frac{\partial}{\partial t} + i\alpha(U-c)\right] \nabla_1^2 \phi_1 - i\alpha\, U''\, \phi_1 - \frac{1}{Re} \nabla_1^4 \phi_1$$
$$= i\alpha\, \phi_{2y}\, \nabla_1^2 \phi^*_1 + 2i\alpha\, \phi_2\, \nabla_1^2 \phi^*_{1y} - 2i\alpha\, \phi^*_{1y}\, \nabla_2^2 \phi_2$$
$$- i\alpha\, \phi^*_1\, \nabla_2^2 \phi_{2y} + i\alpha\, \phi_1\, \phi_{0yyy} - i\alpha\, \phi_{0y}\, \nabla_1^2 \phi_1$$
$$+ O(\phi_2 \phi_3) \tag{2.3-2}$$

$$\left[\frac{\partial}{\partial t} + 2i\alpha(U-c)\right] \nabla_2^2 \phi_2 - 2i\alpha\, U''\, \phi_2 - \frac{1}{Re} \nabla_2^4 \phi_2$$
$$= i\alpha\, (\phi_1\, \phi_{1yyy} - \phi_{1y}\, \phi_{1yy}) + O(\phi_0 \phi_2) \tag{2.3-3}$$

$$\phi_{0yyt} - \frac{1}{Re} \phi_{0yyyy} = i\alpha(\phi_1\, \phi^*_{1yyy} + \phi_{1y}\, \phi^*_{1yy}$$
$$- \phi^*_1\, \phi_{1yyy} - \phi^*_{1y}\, \phi_{1yy}) + O(\phi_2\, \phi_2) \tag{2.3-4}$$

where

$$\nabla_n^2 = \frac{\partial^2}{\partial y^2} - n^2\alpha^2 \qquad n = 1,2,\cdots$$

$$\phi_{ny} = \frac{\partial \phi_n}{\partial y}$$

and * denotes complex conjugation.

The phase speed c is assumed to be given from linear stability theory. In this work, only ϕ_1, ϕ_0 and ϕ_2 are kept and higher order terms are neglected because they are of higher order in amplitude. The basic idea of this temporal analysis is to solve numerically the above coupled nonlinear partial differential equations and then compare the solution with that obtained from the weakly nonlinear theory (Section 2.2). The same interactions are contained in both.

One might note, for historical reasons, that (2.3-2) to (2.3-4) are also the starting point for the Stuart-Watson weakly nonlinear theory - in their theory, these equations are solved by amplitude expansion (2.1-9) for small amplitudes. This automatically forces the critical layer to be viscous, since it assumes that there is a uniformly valid (in y) solution (which is ϕ_{10}) about which the small nonlinear perturbations may be carried out. When these equations are solved numerically, the only assumption is that the third harmonic is unimportant - the critical layer may be nonlinear.

In order to simplify the equations, the vorticity is introduced

$$\Omega_n(y,t) = -\nabla_n^2 \phi_n \; ; \quad n = 0,1,2. \tag{2.3-5}$$

and Equations (2.3-2), (2.3-3) and (2.3-4) reduce to

$$\Omega_{nt} - \frac{1}{Re}\Omega_{nyy} + g_n(y)\,\Omega_n = F_n(y,t) \qquad (2.3\text{-}6)$$

where

$$g_n(y) = \frac{1}{Re} n^2\alpha^2 + in\alpha(U-c)$$

$$F_1(y,t) = i\alpha(-U''\,\phi_1 + \phi_{2y}\,\Omega^*_1 + 2\phi_2\,\Omega^*_{1y} - 2\phi^*_{1y}\,\Omega_2 - \phi^*_1\,\Omega_{2y} + \phi_1\,\Omega_{0y} - \phi_{0y}\,\Omega_1)$$

$$F_2(y,t) = i\alpha(-2U''\,\phi_2 + \phi_1\,\Omega_{1y} - \Omega_1\,\phi_{1y})$$

and

$$F_0(y,t) = i\alpha(\phi_1\,\Omega^*_{1y} + \phi_{1y}\,\Omega^*_1 - \phi^*_1\,\Omega_{1y} - \phi^*_{1y}\,\Omega_1)$$

In order to solve the system of parabolic partial differential equations (2.3-6), the following initial and boundary conditions are used

$$\Omega_1(y,0) = -A(0)\left(\frac{d^2\phi_{10}}{dy^2} - \alpha^2\,\phi_{10}\right)$$

$$\Omega_2(y,0) = \Omega_0(y,0) = 0$$

$$\Omega_1(\pm\infty,t) = \Omega_2(\pm\infty,t) = \Omega_0(\pm\infty,t) = 0$$

where

$\phi_{10}(y)$ = shape of the fundamental as obtained from linear stability theory

and

$A(0)$ = $A(t=0)$ = specified initial amplitude

Initially, only the fundamental wave is present in the flow. Its shape $\phi_{10}(y)$ and phase velocity c are obtained by solving the Orr-Sommerfeld equation for various

wavenumbers α and Reynolds numbers. As $y = \pm\infty$, the flow becomes linear and inviscid, and so the vorticities of the various modes are set to zero. This is the required boundary condition in the external flow.

Equation (2.3-6) is discretized using Crank-Nicolson (Mitchell, 1969; Peyret and Taylor, 1983) differencing in time. That is, knowing Ω_n at the k-th time step, to advance to the (k+1)-th step all terms other than the time derivative are taken to be the average of the values at the two time levels. The Crank-Nicolson approach is characterized by a small time truncation error and is known to be numerically stable in simpler (i.e., linear) problems for which the theory of numerical stability is well developed. Fourth-order space differencing is employed, so the overall truncation error is of order ($O(\Delta y)^4$ + $O(\Delta t)^2$; in this work $\Delta y = 0.04$ and $\Delta t = 0.02$). Numerical experiments (where the number of mesh points N and the sizes of Δy and Δt were varied from 201 to 601, 0.01 to 0.10 and 0.005 to 0.05, respectively) were performed to ensure the insensitivity of the solution to assigned input parameters such as N (number of mesh points; N = 201 in this work), domain of solution (in this work, the domain in y is from y = -4 to y = +4 and in t is from t = 0 to t = 20 to 100 depending on the time that it takes the disturbance to saturate) and the size of Δt. The nonlinear terms are evaluated first explicitly at the k-th time step to obtain the solution at the (k+1)-th step; then the average is used to update the solution. Changes in the nonlinear terms between two successive time steps are small and, therefore, no further iterations are employed. Once Ω_n is known, Equation (2.3-5) is used to solve for ϕ_n.

CHAPTER 3

JET RECEPTIVITY

Hydrodynamic stability deals solely with the behavior of instability modes. The detailed mechanisms of the initial creation of these modes are not considered. In free shear flows, for example, travelling wave disturbances have been observed in the developing downstream zone, and although stability theory attempts to describe their growth, little effort has so far been made to discuss the process of their generation. Balsa (1987) studied the receptivity of a typical free shear layer to pulse-type and periodic excitation by solving the initial value problem and studying its long-time behavior, and found that the shear layer is very receptive to high-frequency disturbances that are generated near the centerline of the layer. The connection between the perturbations in the flow and the external disturbances which generate them may be termed the "receptivity" of the flow. The receptivity of the flow, or the magnitude of perturbations in the flow, depends on the magnitude, the location, and the frequency of the input excitation.

The study of receptivity is intimately connected with the initial value problem and the excitation of the various instability modes by the initial disturbance. Fourier and Laplace transforms are used to solve the linear equations governing the perturbations in the jet and the long-time behavior of the solution is extracted using the saddle point method (Carrier, Krook and Pearson, 1966). For example, a pulse input in the jet generates a wave packet (a group of waves) which moves with the flow at its group velocity and spreads while it grows.

3.1 Basic Equations

Consider the linear evolution of an incompressible inviscid forced jet subject to an axisymmetric disturbance. The mean axial velocity is U(r) and the perturbation equations are

Continuity: $$\frac{\partial u}{\partial x} + \frac{\partial v}{\partial r} + \frac{v}{r} = 0 \qquad (3.1\text{-}1)$$

x-Momentum: $$\frac{\partial u}{\partial t} + U\,\frac{\partial u}{\partial x} + U'v + \frac{\partial p}{\partial x} = 0 \qquad (3.1\text{-}2)$$

r-Momentum: $$\frac{\partial v}{\partial t} + U\,\frac{\partial v}{\partial x} + \frac{\partial p}{\partial r} = \epsilon\,\delta(x)\,\delta(r-r_0)\,\delta(t) \qquad (3.1\text{-}3)$$

where

ϵ = source strength

r_0 = transverse source coordinate

$\delta(x)$ = delta function

prime denotes $\frac{d}{dr}$

and (u, v, 0) and p are the perturbation velocity and pressure.

The perturbations in the flow are produced by a force which acts on the base flow at $x = 0$, $r = r_0$ and $t = 0$. Since the problem is linear, the source strength ϵ is taken to be unity with the understanding that all perturbation quantities are proportional to ϵ. The force is represented by the right-hand side of (3.1-3) and the transverse coordinate r_0 is arbitrary. There is no loss in generality by taking the x-coordinate of the force to be zero.

The assumption of linearity carries with it the usual restrictions to small initial perturbations and implies that the disturbance does not significantly modify the base flow in the course of time. The assumption of incompressibility carries with it the usual restrictions to low Mach number flows. The assumption of zero viscosity is justified on

the basis that typical inflectional jet base velocity profiles are unstable to inviscid perturbations.

The topic of normal modes (Drazin and Reid, 1981), which forms the basis of linear hydrodynamic stability, is concerned with the determination of stability boundaries, complex growth rates and mode shapes. While studies of normal modes can shed light on the stability of the flow, such studies say nothing about when and how the modes actually evolve and how their amplitudes are related to the strength and the location of the input disturbance. Furthermore; in practice one would expect to see not only one normal mode, but some superposition of many normal modes which is determined by the nature of the initial disturbance. Alternatively, this work is concerned with the subsequent development of the solutions u(x,r,t), v(x,r,t) and p(x,r,t) of the linearized equations for $t > 0$ provided the flow is subject to an initial disturbance that is impulsive in time and localized in space. The result of this excitation is a wave packet type disturbance which travels with the flow at its group velocity and which grows exponentially as it travels.

The governing equations (3.1-1, 3.1-2, and 3.1-3) are solved by using Fourier transforms in x and Laplace transforms in t. Let the Fourier transform pairs be

$$\hat{(\cdot)}\,(\alpha,r,t) = \int_{-\infty}^{\infty} (\cdot)\,(x,r,t)\, e^{-i\alpha x}\, dx$$

$$(\cdot)\,(x,r,t) = \frac{1}{2\pi} \int_{-\infty}^{\infty} \hat{(\cdot)}\,(\alpha,r,t)\, e^{i\alpha x}\, d\alpha$$

and the Laplace transform pairs be

$$\tilde{(\cdot)}\,(\alpha,r,\Omega) = \int_0^{\infty} \hat{(\cdot)}\,(\alpha,r,t)\, e^{-\Omega t}\, dt$$

$$\hat{(\cdot)}\,(\alpha,r,t) = \frac{1}{2\pi i} \int_{Br} \tilde{(\cdot)}\,(\alpha,r,\Omega)\, e^{\Omega t}\, d\Omega$$

where α is the complex axial wavenumber and Br is the Bromwich contour in the complex Ω-plane.

After performing the Fourier and Laplace transforms on our governing equations, and assuming that no perturbations exist anywhere in the flow prior to time t = 0, the following equations are obtained

$$i\alpha\tilde{u} + \frac{d\tilde{v}}{dr} + \frac{\tilde{v}}{r} = 0 \qquad (3.1\text{-}4)$$

$$(\Omega + i\alpha U)\,\tilde{u} + U'\tilde{v} + i\alpha\tilde{p} = 0 \qquad (3.1\text{-}5)$$

$$(\Omega + i\alpha U)\,\tilde{v} + \frac{d\tilde{p}}{dr} = \delta(r-r_0) \qquad (3.1\text{-}6)$$

The base velocity profile used and a typical wave packet like solution, v(x,r,t), are shown in Figure 2. The mean flow consists of two straight line segments joined by a smooth curve satisfying $U'/r - U'' = 0$. This profile is chosen for simplicity so that a closed form solution can be obtained. The velocity profile is not differentiable at $r = r_1$ and at $r = r_2$, but this should not alter the physics of the problem, as was justified by Balsa (1987) where he found (in studying the instability of piecewise linear free shear layers) that the temporal and spatial instabilities of an infinitely differentiable velocity profile at large Reynolds numbers are virtually identical with those of the inviscid

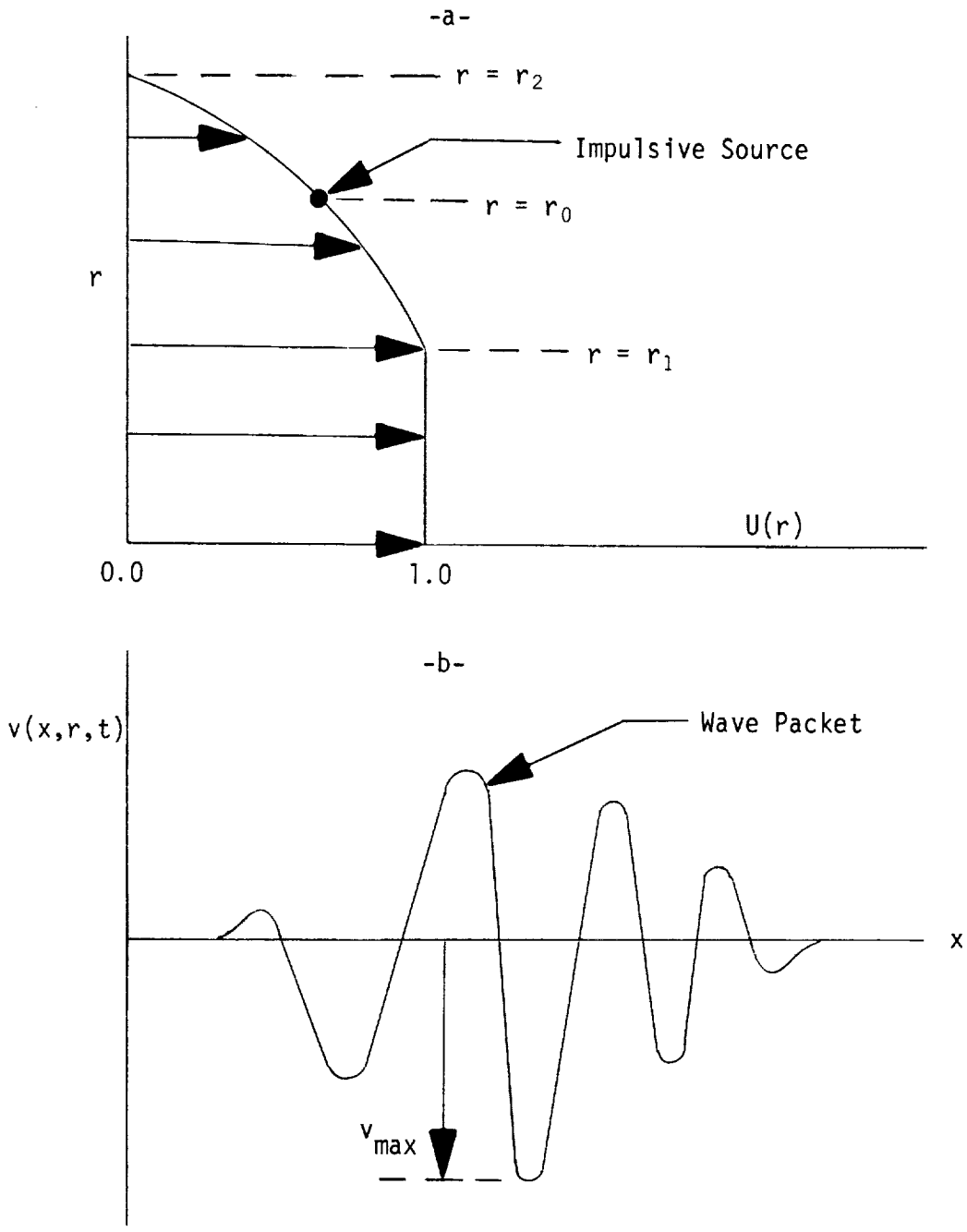

Figure 2. (a) Mean velocity profile. $U(r) = 1 - (r^2-r_1^2)/(r_2^2-r_1^2)$ for $r_1 \leq r \leq r_2$. (b) Typical behavior of the radial velocity component with x after a long time has elapsed.

instabilities of a piecewise linear profile. The source location r_0 is arbitrarily chosen to be between r_1 and r_2 and different source locations will yield receptivities.

Eliminating $\tilde{u}$ and $\tilde{p}$ in Eqs. (3.1-4, 3.1-5 and 3.1-6) in favor of $\tilde{v}(\alpha,r,\Omega)$, the following inhomogeneous Rayleigh-type ordinary differential equation in r is obtained (which is actually Bessel's equation)

$$\frac{d^2\tilde{v}}{dr^2} + \frac{1}{r}\frac{d\tilde{v}}{dr} - \left(\alpha^2 + \frac{1}{r^2}\right)\tilde{v} = \frac{-\alpha^2\,\delta(r-r_0)}{(\Omega+i\alpha U)} \tag{3.1-7}$$

The solution of (3.1-7) is

$$\tilde{v}(\alpha,r,\Omega) = \begin{cases} c_1\, I_1(\alpha r) & 0 \le r \le r_1 \\ c_2\, I_1(\alpha r) + c_3\, K_1(\alpha r) & r_1 \le r \le r_0 \\ c_4\, I_1(\alpha r) + c_5\, K_1(\alpha r) & r_0 \le r \le r_2 \\ c_6\, K_1(\alpha r) & r \ge r_2 \end{cases} \tag{3.1-8}$$

where c_1 through c_6 are constants and I_1 and K_1 are the modified Bessel functions of order 1.

Four conditions at interfaces r_1 and r_2 and two conditions at the source location r_0 are needed to obtain a unique solution for $\tilde{v}(\alpha,r,\Omega)$. The mean velocity U(r) is continuous across r_1, r_0, and r_2; therefore, $\tilde{v}$ is continuous there too, and integrating (3.1-7) across $r = r_0$ yields one jump condition for $\tilde{v}'$, where the prime denotes differentiation with respect to r. The continuity of pressure across the two interfaces further provides two more jump conditions. All three conditions are listed below:

$$(\Omega + i\alpha)\,(\tilde{v}'(r_1^+) - \tilde{v}'(r_1^-)) = i\alpha\,\tilde{v}(r_1)\,U'(r_1^+)$$

$$(\Omega + i\alpha\,U_0)\,(\tilde{v}'(r_0^+) - \tilde{v}'(r_0^-)) = -\alpha^2$$

$$\Omega\,(\tilde{v}'(r_2^+) - \tilde{v}'(r_2^-)) = -i\alpha\,\tilde{v}(r_2)\,U'(r_2^-)$$

where

$$U_0 = U(r_0)$$

Let

$$b_2 = \alpha r_1\, I_1(\alpha r_1)\, K_1(\alpha r_1)\, U'(r_1^+)$$

$$b_1 = \alpha r_1\, I_1(\alpha r_1)\, I_1(\alpha r_1)\, U'(r_1^+)$$

$$d_1 = \alpha r_2\, K_1(\alpha r_2)\, K_1(\alpha r_2)\, U'(r_2^-)$$

$$e_1 = \alpha r_2\, I_1(\alpha r_2)\, K_1(\alpha r_2)\, U'(r_2^-)$$

$$b_3 = \alpha + b_2 - e_1$$

$$b_4 = \alpha e_1 + b_2 e_1 - b_1 d_1$$

$$L_0 = \alpha^2 r_0\, I_1(\alpha r_0)$$

$$L_2 = \alpha^2 r_0\, K_1(\alpha r_0)$$

$$z_1 = i(d_1 L_0 - e_1 L_2)$$

$$z_2 = i(b_2 L_0 - b_1 L_2)$$

$$w_1 = \frac{-ib_3}{2} - \frac{1}{2}\sqrt{-b_3^2 - 4b_4}$$

$$w_2 = \frac{-ib_3}{2} + \frac{1}{2}\sqrt{-b_3^2 - 4b_4}$$

and

$$F(\Omega,\alpha) = (\Omega + i\alpha U_0)\,(\Omega - w_1)\,(\Omega - w_2)$$

The matching conditions at r_1, r_2 and r_0 are used to evaluate c_1 through c_6 which are

$$c_1 = \frac{(\Omega + i\alpha)(\Omega L_2 + z_1)}{F(\Omega,\alpha)}$$

$$c_2 = \frac{[(\Omega + i\alpha) + ib_2][\Omega L_2 + z_1]}{F(\Omega,\alpha)}$$

$$c_3 = \frac{-ib_1(\Omega L_2 + z_1)}{F(\Omega,\alpha)}$$

$$c_4 = \frac{id_1[L_0(\Omega + i\alpha) + z_2]}{F(\Omega,\alpha)}$$

$$c_5 = \frac{(\Omega - ie_1)\,[L_0(\Omega + i\alpha) + z_2]}{F(\Omega,\alpha)}$$

and

$$c_6 = \frac{\Omega\,[L_0(\Omega + ib_2) + z_2]}{F(\Omega,\alpha)}$$

3.2 Asymptotic Solution

The transverse velocity component is

$$v(x,r,t) = \frac{1}{2\pi}\int_{-\infty}^{\infty}\frac{1}{2\pi i}\int_{Br}\tilde{v}(\alpha,r,\Omega)\,e^{i\alpha x + \Omega t}\,d\Omega\,d\alpha \qquad (3.2\text{-}1)$$

where Br is the Bromwich contour of integration in the complex Ω-plane.

There are three poles in the Ω-plane, as seen from the zeroes of F. The first (at $-i\alpha U_0$) corresponds to a convected mode, the second (at w_1) corresponds to a stable mode and the third (at w_2) corresponds to an unstable mode. The integral in the Ω plane is evaluated by the method of residues at the pole $\Omega = w_2$ and the contributions from the convected and stable modes are ignored. This yields

$$v(x,r,t) = \frac{1}{2\pi} \int_{-\infty}^{\infty} e^{i\alpha x + w_2 t} f \, d\alpha + \cdots$$

where

$$f(r,\alpha) = \lim_{\Omega \to w_2} [(\Omega - w_2) \tilde{v} (\alpha,r,\Omega)]$$

On the other hand, the dominant contribution to the α-integral comes from the saddle point of this unstable mode (Balsa, 1987). Since the wave packet is convected by the flow, it is simplest to observe it in a moving coordinate system. Let the (real) group velocity G be (Gaster, 1965)

$$G = \frac{x}{t} \tag{3.2-2}$$

Then the solution can be written as

$$v(x,r,t) = v(G,r,t) = \frac{1}{2\pi} \int_{\Gamma} f(r,\alpha) \, e^{h(\alpha)t} \, d\alpha \tag{3.2-3}$$

where Γ is a deformed contour which passes through the saddle point and

$$h(\alpha) = w_2(\alpha) + i\alpha G = h(\alpha,G)$$

For any given G, the saddle point $\alpha_*(G)$ is given by

$$\frac{dh}{d\alpha} = \frac{dw_2}{d\alpha} + iG = 0 \tag{3.2-4}$$

By expanding $f(r,\alpha)$ and $h(\alpha)$ about the saddle point α_*, the following long time solution is obtained

$$v(G,r,t) = \frac{1}{2\pi} f(r,\alpha_*) \sqrt{\frac{2\pi}{\left(\frac{d^2h}{d\alpha^2}(\alpha_*)\, t\right)}}\, e^{t\, h(\alpha_*)}$$

$$+ \text{complex conjugate} \qquad (3.2\text{-}5)$$

To recap, the long-time solution, as given by Equation (3.2-5), is obtained by solving the initial value problem and then applying the saddle point method. It describes not only the general structure of wave packets, but also establishes the explicit connection between the perturbations in the flow and the external disturbances which generate them. This is contained in the function $f(r,\alpha_*)$. The general characteristics of the solution are: (1) the amplitude of the wavepacket grows like $t^{-1/2}$ exp[t Real(h_*)] where $h_* = h(\alpha_*)$. The factor $t^{-1/2}$ arises from the interference of the various oscillating components of the packet; (2) the wave packet convects with the flow and an observer moving with the packet will see the wave system growing in both space (x) and time (t); note $\alpha_* = \alpha_*(G) = \alpha_*(x/t)$; and (3) at large values of time and at any prescribed radial location, the transverse component of the velocity v(x,r,t), which looks like a modulated wave train when plotted against x ($x = Gt$; see Figure 2), depends on the location of the initial excitation, r_0.

In physical terms, the instability may be described qualitatively as follows. The initial disturbance, which is an impulsive excitation, is localized in space and time. Because of this, all wavenumbers and frequencies will be excited and the modes associated with this spectrum will grow according to the modal analysis of linear stability theory. The actual disturbance is a superposition of all these modes that continuously experience a certain amount of interference (i.e., cancellation - hence the saddle point). However, for

large values of time, the most unstable mode will win out and this mode will dominate the center of the packet. The disturbance decays rapidly upstream and downstream of its center as it travels. Thus, relative to an observer moving with the group velocity, the disturbance grows exponentially in time. But the disturbance measured at any fixed station x eventually decays rapidly with time because the localized disturbance travels away; indeed, at a distant station the disturbance may appear first to grow and then decay rapidly as its center passes by. This flow is convectively unstable.

In this work, attention is focused on the effect of the position of the source on the magnitude of the disturbance velocity. For a specified positive group velocity, the solution (3.2-5), which represents a travelling wave system downstream of the source, is obtained numerically. The solution depends strongly on the location of the source of excitation, r_0, so that different locations of the source generate different perturbations, v(x,r,t), and the "most receptive" location is the one which will result in the generation of maximum perturbations.

CHAPTER 4

THE LINEAR RESPONSE OF THE JET

The rest of this dissertation is devoted to a discussion of our numerical results. In this chapter, the linear instability of a round jet is considered. First, the linear growth rate (a_0) and phase speed of the disturbance as functions of wavenumber (α), for various Reynolds numbers, temperature ratios, and jet Mach numbers, are presented. Then the receptivity of the jet is also given as a function of source location. The linear results provide information on the initial stages of the instability and are needed for the discussion of the nonlinear results, to be presented in the next chapters.

A linear disturbance is characterized by: (1) small amplitude so that the products of the perturbations may be neglected and the flow is made up of (in addition to the mean flow) the fundamental disturbance alone. The linearization leads to an Orr-Sommerfeld type equation (Lin, 1955; Drazin and Reid, 1981) whose solution gives the shape, phase speed and growth rate of the disturbance; (2) exponential growth because energy is transferred from the mean flow to the disturbance. At later times, the nonlinear interactions of the dominant mode generate higher harmonics and distort the mean flow, thereby moderating the exponential growth. The new flow will then be made up of all the harmonics of the fundamental. Linear theory is useful not only because it can describe the early stages of instability (Michalke, 1964, 1965; Michalke and Hermann, 1982; Petersen and Samet, 1988) but also because the linear solution is the limiting one for the nonlinear problem as the amplitude tends to zero. For example, in the weakly nonlinear theory (Stuart, 1960; Watson, 1960), where an expansion in the time-dependent amplitude A(t) is

used (see Equations 2.1-9 and 2.1-11), the first order approximation is given by the solution of the linear instability problem, and the other terms represent a hierarchy of nonlinearities.

For a given base flow [U(r), R(r)], where U(r) is the mean axial velocity at some downstream location and R(r) is the mean density there, for a given real wavenumber vector (α, β), where α is the axial wavenumber and β is the azimuthal wavenumber, and for a given jet Reynolds number (Re), Mach number (M) and temperature ratio (T^*), the linear problem is solved to obtain the growth rate, phase speed and shape of the disturbance. The eigenvalues depend on α, β, Re, M and T^*. The instability, therefore, depends not only on the mean flow profiles and the length scales of the disturbance but also on viscosity, compressibility and heating.

An obvious effect of viscosity is to dissipate the energy of any disturbance and thereby stabilize a flow. The molecular diffusion of momentum tends to smooth out the velocity differences of a disturbance. Linear stability calculations based on the Orr-Sommerfeld equation (Betchov and Szewczyk, 1963) have indicated that shear layers are stabilized by viscosity and that the amplification rates are very insensitive to variations in Reynolds number, provided Re > 100. In most experiments (Miksad, 1972), the Reynolds number (based on the initial momentum thickness) is equal to 100 or more, and vortex roll-up is not significantly affected by viscosity. In the isothermal subsonic jet where $T_c = T_\infty$ and $M \neq 0$, the jet Mach number M appears explicitly in the disturbance equations and influences the instability via the basic density distribution which is no longer constant because the base flow is compressible. Spatial instability calculations (Michalke, 1971) show that with increasing Mach number M, the growth rate is reduced, hence the

flow becomes less unstable, and that the phase velocity is sensitive to the Mach number only at lower frequencies where, in contrast, the growth rates become nearly independent of M. Furthermore, Michalke (1971) found that the stabilization occurring as the Mach number increases is stronger for the axisymmetric ($\beta = 0$) disturbance than for $\beta = 1$. Michalke (1971) found that the nonisothermal jet has a slightly lower phase velocity, but a larger growth rate which, however, peaks at a slightly lower frequency as compared with the isothermal jet. Furthermore, the range of unstable frequencies is reduced by the heating.

Heating may be stabilizing or destabilizing depending on the wavelength of the disturbance. In order to isolate the effect of heating, a simple inviscid analysis (similar to that of Batchelor and Gill for the isothermal incompressible jet, 1962) is carried out for a cylindrical vortex sheet type model when the Mach number is zero and the temperature jump across the sheet is $1 - T^*$. For these particular choices of the mean velocity and density profiles [$U(r) = 1$ for $r < 1$, and 0 for $r > 1$; $R(r) = 1$ for $r < 1$ and T^* for $r > 1$] and for a normal mode solution proportional to $\exp(i\alpha x + i\beta\theta - i\alpha c_0 t)$, the perturbation pressure mode is governed by the modified Bessel equation and the eigenvalue problem is completely determined by requiring that the solution is finite at $r = 0$, decays as $r \rightarrow \infty$, that the pressure is continuous across the vortex sheet, and that the interface $r = 1$ (i.e., the vortex sheet) is a material surface. In the limit as $\alpha \rightarrow 0$ (i.e., for long waves), the eigenvalue $c_0 = c_r + ic_i$, is given by

$$c_0 = \begin{cases} 1/(1+T^*) + i\sqrt{T^*}/(1+T^*)\,, & \beta \neq 0,\ \alpha \to 0 \\ 1\,, & \beta = 0,\ \alpha \to 0 \end{cases}$$

where c_r is the phase speed and $a_0 = \alpha c_i$ is the growth rate.

This simple result, which is consistent with the numerical calculations of this investigation, and which agrees with the inviscid calculations of Ng (1989), is applicable for long waves and provides two interesting results. First, while heating ($T^* > 1$) does not alter the speed of long axisymmetric waves, it reduces the speed of long azimuthal waves. When the jet is isothermal ($T^* = 1$), long waves with axial symmetry travel with the speed of the center of the jet, whereas all those not having axial symmetry travel with half that speed (Batchelor and Gill, 1962); and second, the growth rate, a_0, of long axisymmetric waves is nearly insensitive to heating, whereas that of nonaxisymmetric waves is reduced by heating. This means that long axisymmetric waves are more stable than long azimuthal waves.

4.1 Linear Stability Results

Temporal linear stability theory predicts that a continuous band of waves, corresponding to a band of wavenumbers, is exponentially amplified in time. The theory is good as long as the amplitude of the unstable wave is small so that the nonlinear terms in the equations of motion can be neglected.

The parameters affecting jet instability are the wavenumbers (α,β), the Reynolds number (Re), the jet Mach number (M), the temperature ratio ($T^* = T_c/T_\infty$) and the jet momentum thickness (θ_*). In this work, the momentum thickness is taken to be 0.2

(except in Section 4.1.5, where the effect of θ_* on the instability is presented). The main assumptions made in the analysis are: (1) the base flow is parallel. A parallel flow is not an exact solution of the Navier-Stokes equations, but only an approximate one for large Reynolds numbers; (2) the fluid is a perfect gas with constant specific heats ($\kappa = c_p/c_v = 1.4$), constant thermal conductivity and constant viscosity; (3) the Prandtl number associated with the base flow is unity. This assumption, which is used in deriving the mean density distribution (Schlichting, 1979; see Appendix A) means that (as far as the base flow is concerned) the molecular diffusions of momentum and heat are of the same order. As far as the perturbation flow is concerned, we assume that both viscous and conduction effects are unimportant but we retain the former in order to treat neutral waves when the flow is isothermal; (4) the base pressure is constant and is equal to the ambient pressure; (5) the disturbance motion is not influenced significantly by the diffusive process of heat conduction; (6) the base density profile is related to the base velocity profile by means of the Crocco equation; and (7) the disturbance is taken to be periodic in x and θ and is evolving in time. The axial wavenumber α is real and both the linear growth rate a_0 and the phase speed c of the disturbance depend on α. Temporal waves on a jet column are dispersive, whereas they are not in a mixing layer. Physically, the jet instability is caused by the induction of the vorticity contained in the jet shear layer (Batchelor, 1967; Drazin and Reid, 1981).

4.1.1 Mode Number Effects

The jet instability for inviscid, incompressible (M = 0) and cold ($T^* = 1.0$) flow is shown in Figure 3. The linear growth rate and the phase speed of the axisymmetric ($\beta = 0$), the first azimuthal ($\beta = 1$) and the second azimuthal ($\beta = 2$) disturbances versus axial wavenumber are shown and it can be seen that the first azimuthal disturbance is

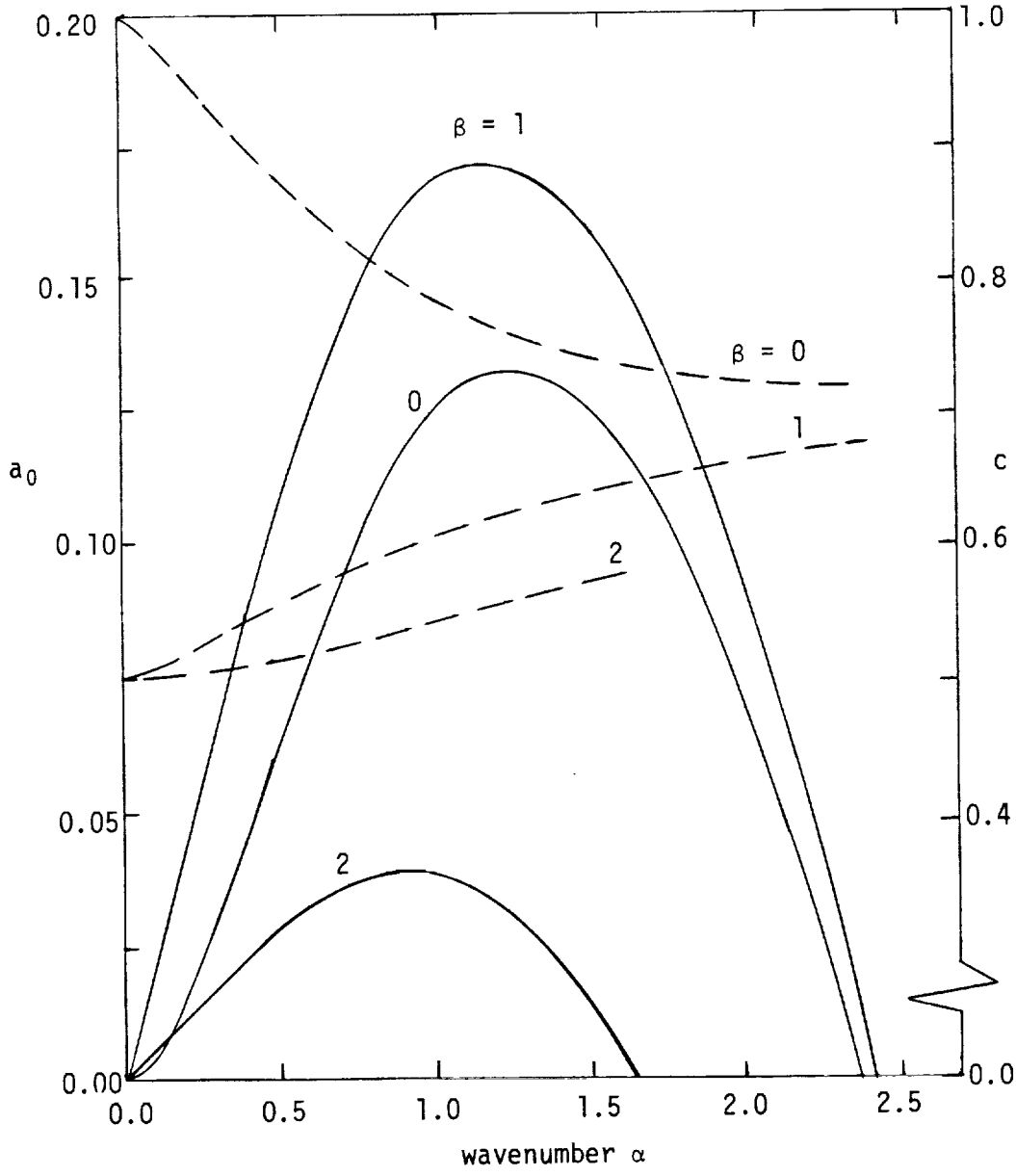

Figure 3. Inviscid instability characteristics of a round jet for various azimuthal mode numbers: Linear growth rate a_0 (solid lines) and phase speed c (dashed lines) as functions of axial wavenumber. M = 0.0; $T^* = 1.0$; $\theta_* = 0.2$.

more unstable than the other two, with the second azimuthal disturbance being the least unstable. For example, the maximum growth rates of the disturbances with $\beta = 1$, $\beta = 0$ and $\beta = 2$ are 0.174, 0.133 and 0.039 respectively. The range of unstable wavenumbers depends on the azimuthal mode number and the neutral wave numbers of the disturbances with $\beta = 1$, $\beta = 0$ and $\beta = 2$ are 2.42, 2.38 and 1.66, respectively. The convection velocity or the phase speed of the disturbance depends on the wavenumber which means that the waves are dispersive (i.e., different waves travel at different speeds). Axisymmetric disturbances travel faster than first and second azimuthal ones and second azimuthal waves travel at slightly above the average jet velocity (which is equal to 0.5). Long waves with axial symmetry ($\beta = 0$) travel with the speed of the center of the jet, whereas those not having axial symmetry ($\beta = 1,2$) travel with half that speed. The phase speeds of the most amplified disturbances with $\beta = 0$, $\beta = 1$ and $\beta = 2$ are 0.76, 0.62 and 0.53, respectively.

4.1.2 Viscosity Effects

It is known (Betchov and Szewczyk, 1963) that for an incompressible shear layer, viscosity is always stabilizing and that the stability characteristics of the viscous flow become asymptotic to those of the inviscid flow at a Reynolds number of, approximately, 100. In a jet, viscosity may be stabilizing or destabilizing, depending on the wavenumber and the mean velocity profile. For example, for the algebraic profile $U(r) = 1/(1+r^2)^2$, the growth rates at a wavenumber of 0.38 (cold and incompressible jet, azimuthal mode $\beta = 1$) are 0.02436 and 0.02142 for the viscous (Re = 150) and inviscid cases respectively. This is in perfect agreement with the work of Lessen and Singh (1973). However, for the tanh family of profiles (see Appendix A and Figure 1), the effects of viscosity are usually stabilizing, and the instability characteristics of the viscous flow become asymptotic to those

of the inviscid flow at a Reynolds number of approximately 2000, indicating that viscosity is more important in jets than in mixing layers.

The inviscid and viscous instability for an incompressible (M = 0) and isothermal ($T^* = 1$) jet is shown in Figure 4 where the linear growth rates of the axisymmetric and the first azimuthal disturbances are plotted as functions of wavenumber. Viscosity stabilizes the flow and reduces the range of unstable waves; for example, the inviscid and viscous (Re = 500) maximum growth rates of the axisymmetric disturbance are 0.133 and 0.104, respectively. The inviscid and viscous (Re = 500) maximum growth rates of the first azimuthal disturbance are 0.174 and 0.149 respectively. The neutral wavenumbers of the axisymmetric and the first azimuthal disturbances at Reynolds number of 500 are 2.17 and 2.30 respectively. It can be seen that viscosity is slightly more efficient in suppressing the growth of short (near-neutral) waves than long ones.

4.1.3 Mach Number Effects

In Figure 5, the influence of the jet Mach number M on the jet instability is shown. The linear growth rate of the axisymmetric and the first azimuthal disturbances versus wavenumber is shown for an isothermal ($T^* = 1.0$) flow. With increasing Mach number, the growth rate is reduced, hence the flow becomes less unstable. For example, the maximum growth rates of the first azimuthal disturbance (at Re = 500) are 0.149 and 0.125 for the incompressible (M = 0.0) and compressible (M = 0.9) flows, respectively. The growth rates of the disturbances with $\beta = 0$ and $\beta = 1$ are independent of the Mach number at lower wavenumbers (say for $\alpha < 0.5$; i.e., long waves are insensitive to the value of M). This result is consistent with the results of Ng (1989).

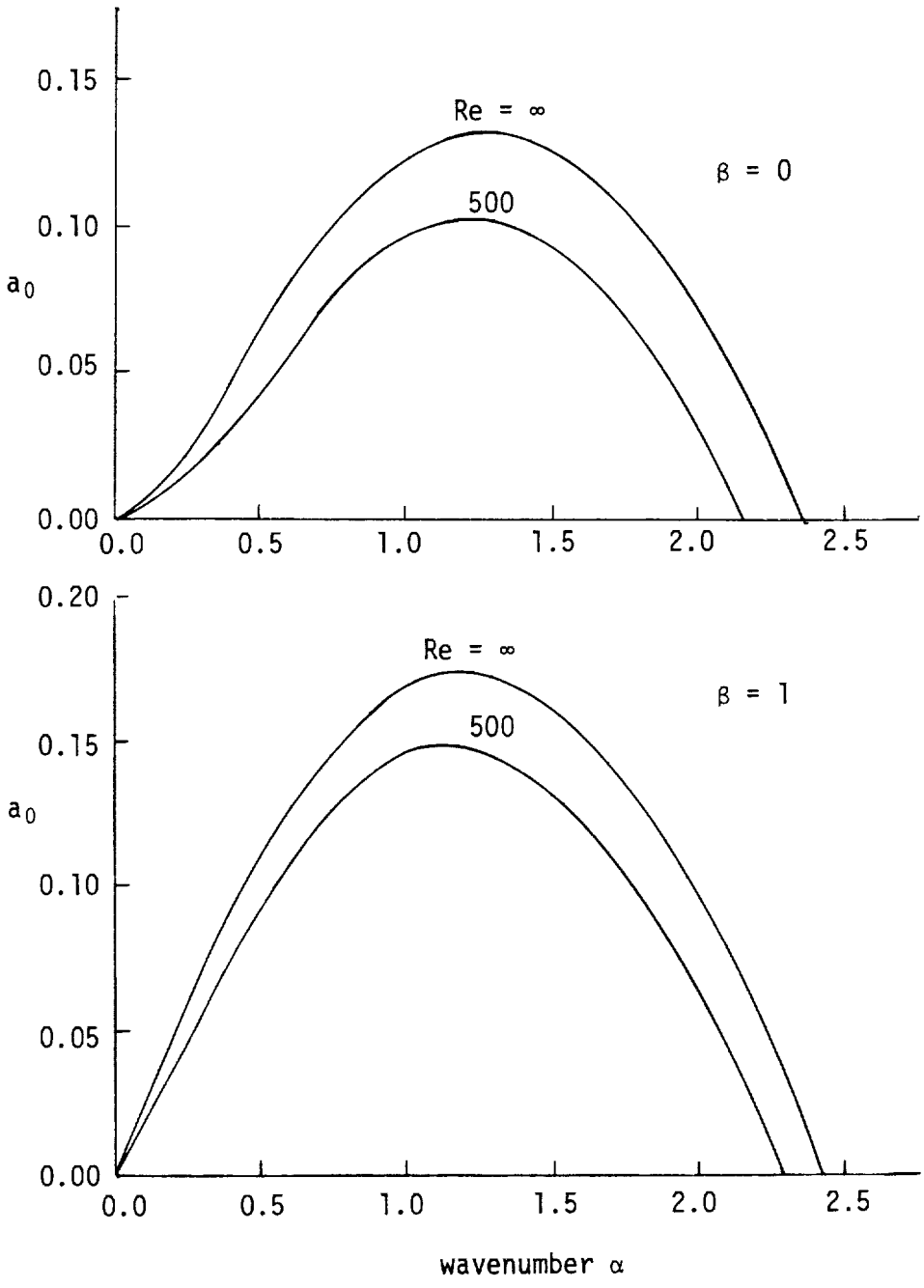

Figure 4. Inviscid and viscous instability of the round jet for the axisymmetric and the first azimuthal modes: Linear growth rate a_0 as a function of wavenumber for parametric values of jet Reynolds number. M = 0.0; $T^* = 1.0$; $\theta_* = 0.2$.

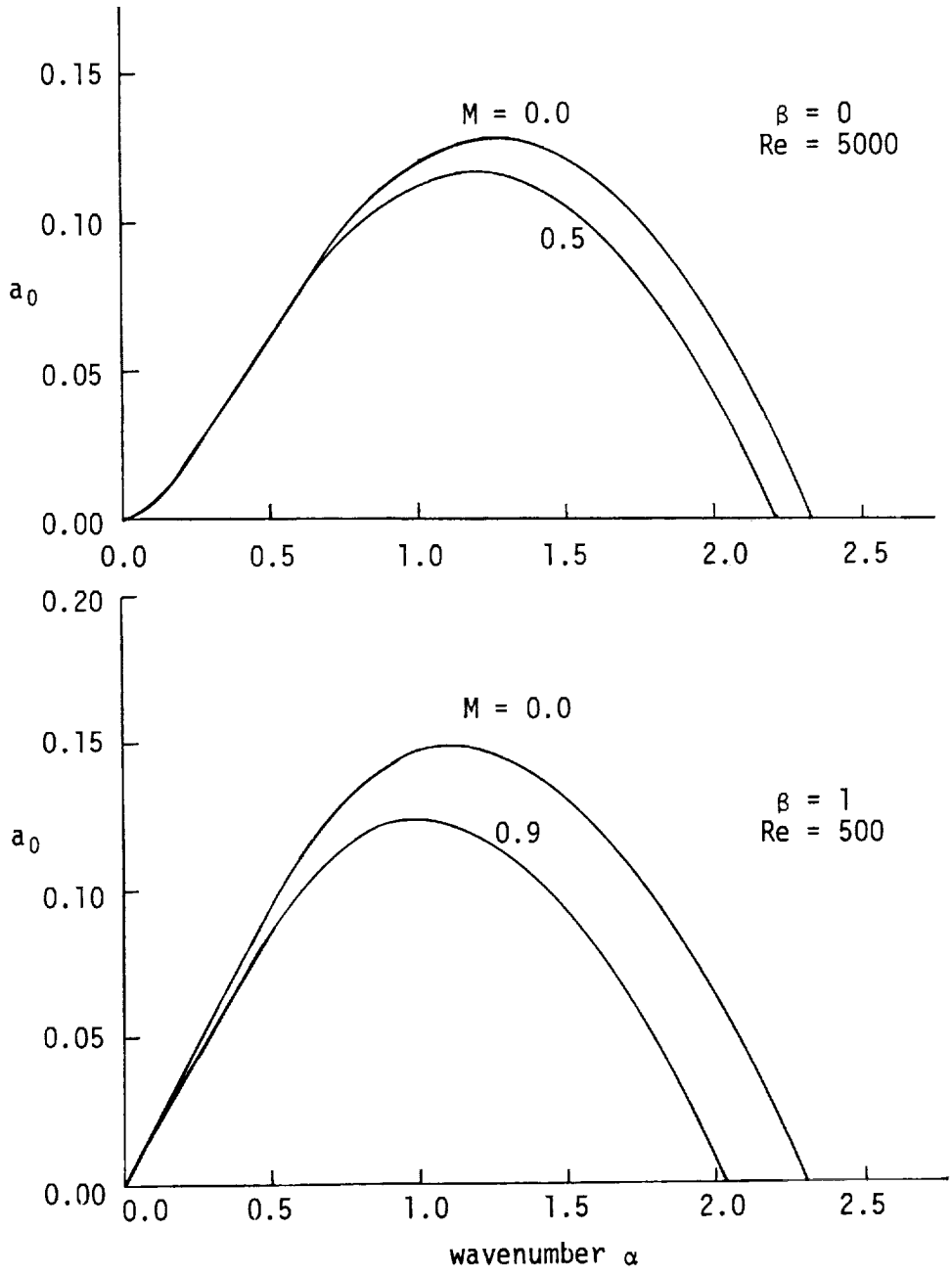

Figure 5. Incompressible and compressible instability of the round jet for the axisymmetric and the first azimuthal modes: Linear growth rate a_0 as a function of wavenumber for parametric values of jet Mach number. $T^* = 1.0$; $\theta_* = 0.2$.

The phase speed of the axisymmetric and the first azimuthal disturbances as functions of wavenumber is shown in Figure 6 for an isothermal ($T^* = 1$) flow at two Mach numbers. With increasing Mach number, the phase speed is reduced, but only slightly. In other words, the phase velocities of both disturbances ($\beta = 0$ and $\beta = 1$) are weakly dependent on the Mach number. For example, the phase speeds of the axisymmetric disturbance (Re = 1000) at $\alpha = 1.5$ are 0.74 and 0.73 for the nearly incompressible (M = 0.1) and compressible (M = 0.9) flows, respectively.

4.1.4 Temperature Effects

The jet instability for incompressible flow is shown in Figure 7 for two temperature ratios. The linear growth rate of the axisymmetric and the first azimuthal disturbances versus wavenumber is shown and it can be seen that heating reduces the range of unstable waves; for example, the neutral waves of the axisymmetric disturbance are 2.28 and 2.10 (at Re = 1000) for the cold ($T^* = 1$) and hot ($T^* = 2$) flows, respectively. For the first azimuthal disturbance heating makes the flow less unstable and the growth rate at lower wavenumbers ($\alpha < 0.6$, say) is nearly independent of heating. The maximum growth rates of the first azimuthal disturbance (Re = ∞) are 0.173 and 0.163 for the cold and hot ($T^* = 2$) flows, respectively. When the disturbance is axisymmetric, the hot jet has a slightly larger maximum growth rate which, however, occurs at a slightly lower wavenumber as compared with the cold jet. While heating destabilizes axisymmetric disturbances, it stabilizes first azimuthal disturbances and near neutral waves (with $\beta = 0$ or $\beta = 1$) are always stabilized by heating.

The phase speeds of the axisymmetric and the first azimuthal disturbances as functions of wavenumber are shown in Figure 8 for an incompressible (M = 0) flow at two temperature ratios. Heating reduces the phase speed of all waves; for example, the phase

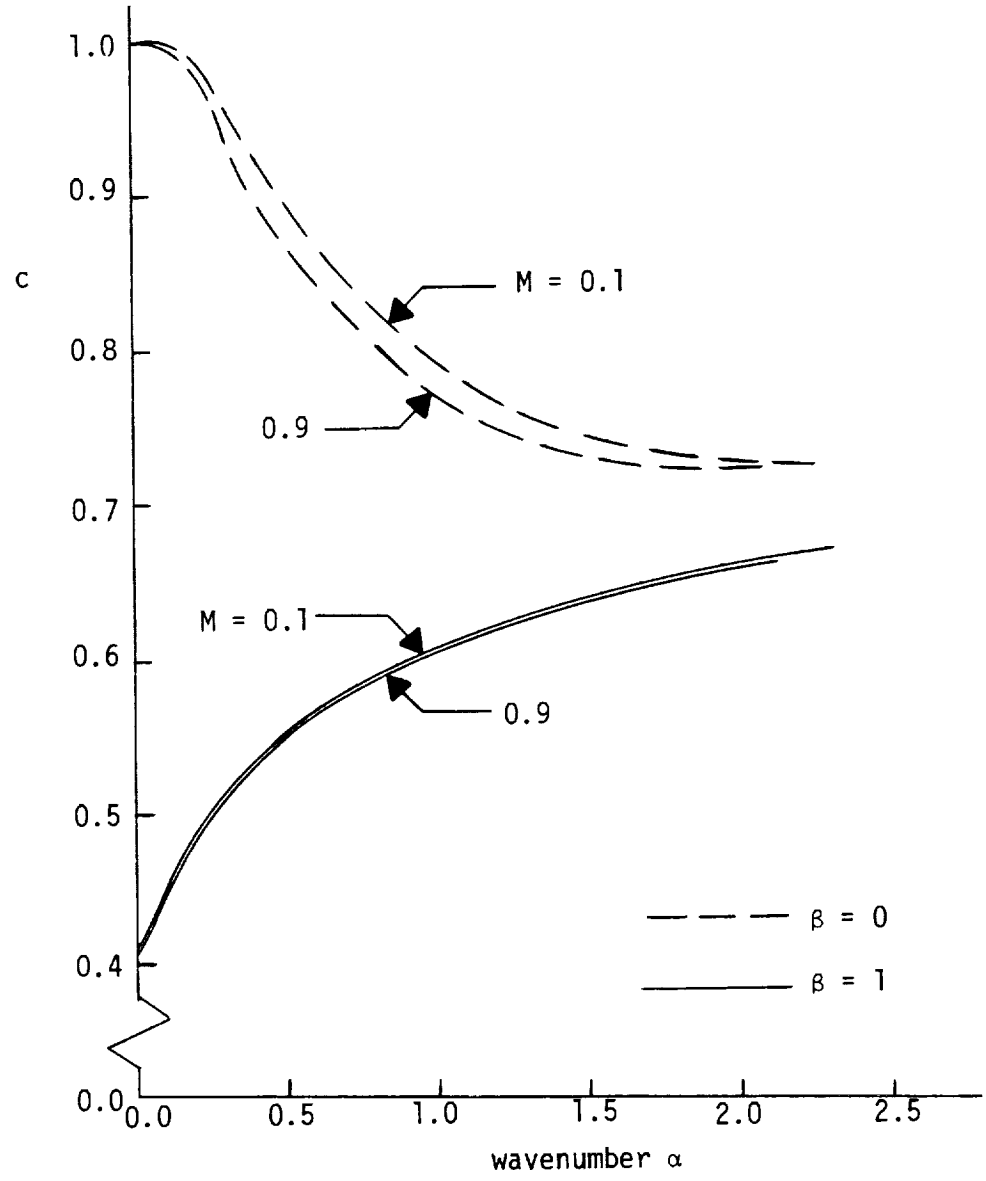

Figure 6. Phase speed c as a function of wavenumber for parametric values of jet Mach number. Re = 1000; $T^* = 1.0$; $\theta_* = 0.2$.

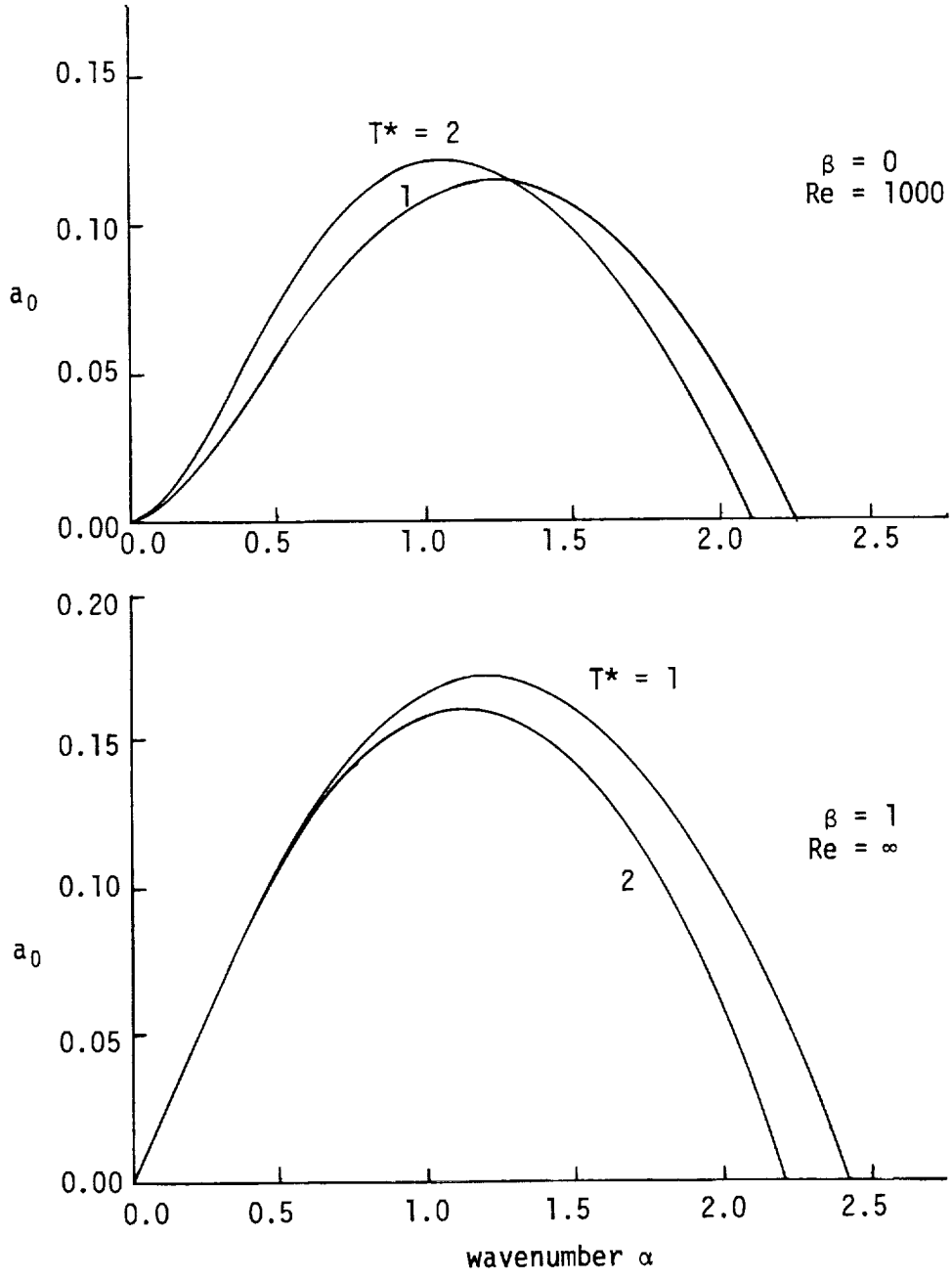

Figure 7. Instability of the cold and the hot round jet for the axisymmetric and the first azimuthal modes: Linear growth rate a_0 as a function of wavenumber for parametric values of jet temperature ratio. M = 0.0; $\theta_* = 0.2$.

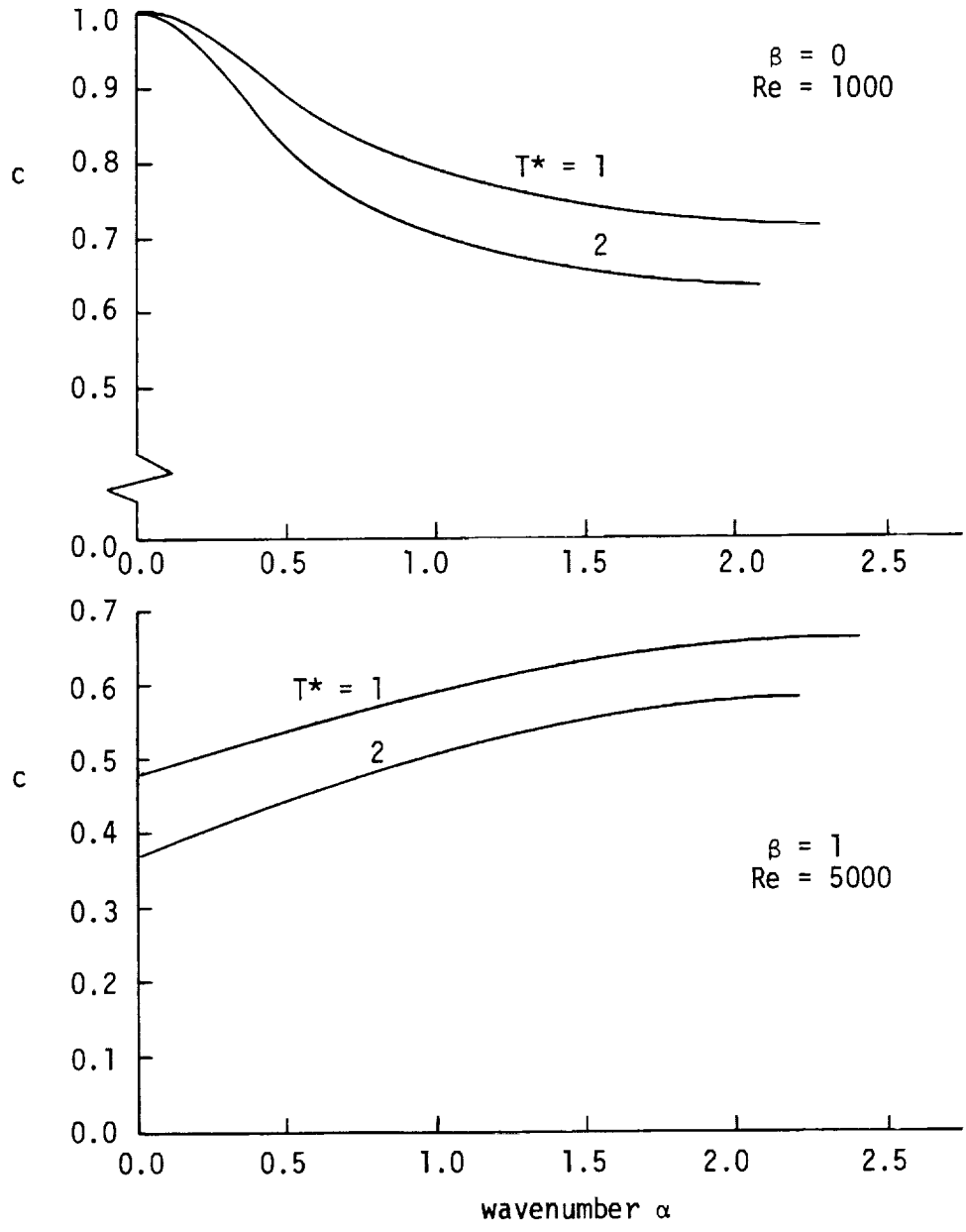

Figure 8. Phase speed c as a function of wavenumber for parametric values of jet temperature ratio. M = 0.0; $\theta_* = 0.2$.

speeds of the axisymmetric disturbance at a wavenumber of 1.0 are 0.79 and 0.70 for the cold and hot ($T^* = 2$) flows, respectively. While increasing the Mach number reduces the phase velocity only slightly (see Figure 6), heating results in moderate reduction in the phase speed, except for long axisymmetric waves.

4.1.5 Momentum Thickness Effects

The linear results presented so far in this section were obtained when the momentum thickness (θ_*) is 0.2. Obviously, increasing the momentum thickness is stabilizing (the base jet flow, which is evolving in the downstream distance, becomes less unstable with increasing θ_*) because the vorticity contained in the jet shear layer (near the inflexion point) is proportional to $1/\theta_*$ (i.e., maximum vorticity ~ $1/\theta_*$). The linear growth rates of the axisymmetric and the first azimuthal disturbances as a function of wavenumber are shown in Figure 9 for a cold incompressible flow at two values of θ_*. Increasing the momentum thickness makes the flow less unstable; for example, the maximum growth rate of the first azimuthal disturbance (Re = 5000) is reduced from 0.253 to 0.172 as θ_* is increased from 0.15 to 0.20. With decreasing θ_*, the range of unstable wavenumbers increases and as $\theta_* \rightarrow 0$ (vortex sheet), the jet becomes unstable to all waves (Batchelor and Gill, 1962). In general, the phase speed increases slightly with increasing θ_* except for small wavenumbers (as $\alpha \rightarrow 0$) where c is nearly independent of θ_*. For example, the phase speed of the axisymmetric disturbance at a wavenumber of 1.5 (Re = 5000; M = 0; $T^* = 1.0$) increases from 0.71 to 0.74 as θ_* increased from 0.15 to 0.20.

The above (numerically obtained) temporal instability results, which agree well with the inviscid results of Ng (1989) and which are consistent with the spatial results of Michalke (1971), Morris (1976) and Michalke and Hermann (1982), show that: (1) instability waves riding on a jet flow are dispersive and those with axial symmetry ($\beta = 0$)

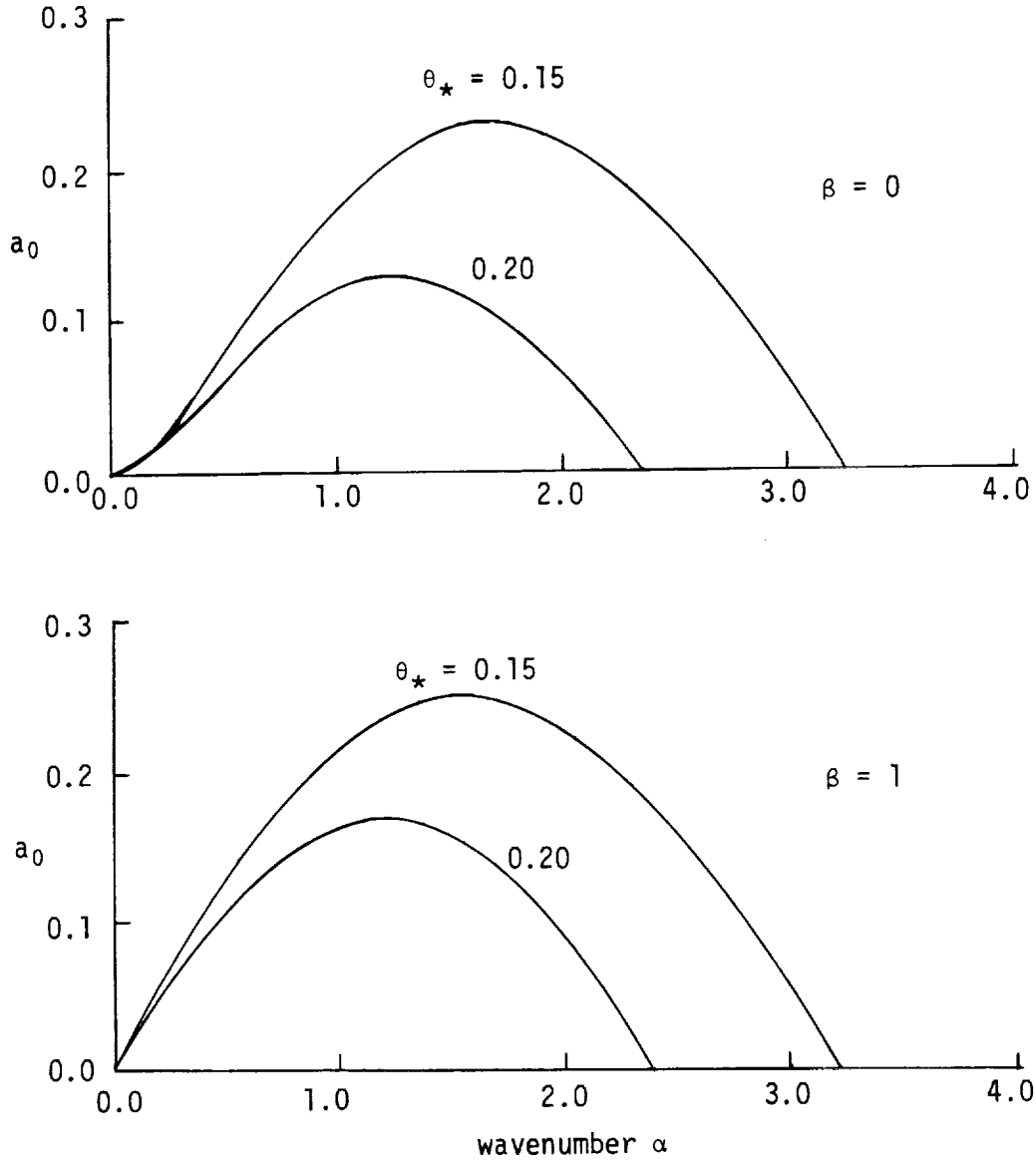

Figure 9. Effect of momentum thickness on jet instability: Linear growth rate a_0 as a function of wavenumber for two values of jet momentum thickness. Re = 5000; M = 0.0; $T^* = 1.0$.

travel relatively faster than those not having axial symmetry (β = 1 and β = 2). The phase speed decreases with increasing jet temperature (i.e., with heating); (2) the instability of a round jet is dominated by the axisymmetric and first azimuthal modes and (with everything else being the same) the latter is more unstable; (3) viscosity stabilizes the flow and the stability of a viscous jet flow becomes asymptotic to that of an inviscid flow at a Reynolds number (based on jet radius and centerline velocity) of approximately 2000; (4) compressible jets are less unstable than incompressible jets. The maximum growth rate decreases with increasing jet Mach increasing jet Mach number M; and (5) heating stabilizes first azimuthal disturbances. But when the disturbance is axisymmetric, long waves (lower wavenumbers) are destabilized and short waves (near-neutral wavenumbers) are stabilized by heating and the maximum growth rate is slightly higher for the hot jet.

4.2 Receptivity

The receptivity analysis gives the relationship between the position of the source, r_0, and the magnitude of the resulting disturbance velocity v(x,r,t). Since the disturbance extracts its energy from the mean velocity shear, it is expected that the largest perturbations are generated when the source is placed in regions of high relative mean shear. The study of receptivity is intimately connected with the initial value problem and the excitation of the various instability modes by the initial disturbance. The long time solution (see Eq. 3.2-5) of the initial value problem is a wave packet (Gaster, 1965, 1975; Balsa, 1988) which moves with the flow at its group velocity and spreads while it grows.

In this work, the excitation is impulsive in time and localized in space and different source locations result in different perturbations in the jet. In other words, the subsequent perturbations u(x,r,t), v(x,r,t) and p(x,r,t) in the jet depend on r_0 and there is an optimum position $r_{0,max}$ which will result in maximum perturbations. The most efficient way of

perturbing the flow is to place the excitation (i.e., the input disturbance) at $r_{0,max}$ because little input energy will then be needed to excite the flow. If the input disturbance is placed in the flow away from $r_{0,max}$; say, in a region of uniform base flow velocity where the mean shear is small, then very large amplitudes of the driver will be required to generate comparable perturbations in the flow.

The perturbation radial velocity v(x,r,t) depends on the positions x and r and on the time t and the long time solution is valid at all large times when all the transients have decayed; say, t = 30, 40, 50, etc. In this work, the results (wave-like shape and amplitude of the packet) at a typical instant of time (say, t = 40) will be presented with the understanding that the wave packet grows exponentially in time. At larger values of time, the general wave-like character of the packet is unaltered, although its amplitude is greater. For fixed t and radial position r, the solution v(x, r-fixed, t-fixed) as functions of x or of G (since x = Gt and t is fixed) looks like a wave packet or a concentrated wave-like disturbance that decays rapidly upstream and downstream of its center as it travels. An observer moving with the packet at some average jet velocity will see a wave system that is growing in both space and time. The amplitude of the wave system depends on the location of the source.

In order to see if there is any connection between the optimum location of the source $r_{0,max}$ and the transverse location in the jet at which the speed of the base flow and the phase speed of the most amplified wave (in the linear stability sense) are equal, the linear inviscid instability of our model jet with $r_1 = 1$ and $r_2 = 2$ (see Figure 2) is studied. In the mixing layer with either a tanh or a piecewise linear base velocity profile (Balsa, 1987), the phase speed and the fluid speed are equal in the middle of the layer [i.e., U(y = 0) = c so that the critical point is at y = 0] and Balsa (1988) found that the flow is

most sensitive to perturbations which occur near this region. Whereas in the mixing layer, all waves travel at the same speed, in the round jet the waves are dispersive so that different waves travel at different speeds and there is a "critical point" associated with the linearly most unstable wavenumber.

The temporal growth rate and the phase speed as functions of wavenumber for the model base velocity profile with $r_1 = 1$ and $r_2 = 2$ are shown in Figure 10. The disturbance is inviscid, incompressible and axisymmetric and the instability characteristics of the model flow are obtained numerically by solving for the unstable mode (w_2; see discussion below Eq. 3.2-1) when the wavenumber is real. The linear growth rate a_0 is the real part of w_2 while the phase speed c is the (negative) imaginary part of w_2 divided by the (real) wavenumber α. These results agree qualitatively with those for the tanh base profile (see Figure 1), as can be seen by comparing Figure 3 (with $\beta = 0$) and Figure 10. Therefore, the unstable mode of the model flow basically exemplifies the kind of jet flow instability that is in mind. The neutral point is at $\alpha = \alpha_n \simeq 1.036$, the most amplified wavenumber is $\alpha_m \simeq 0.70$, the maximum growth rate is 0.111 and the phase speed of the most amplified wave is 0.742. Since the base flow between $r_1 = 1$ and $r_2 = 2$ is $U(r) = 1 + (1-r^2)/3$ and the "critical point" in the radial direction is that at which the fluid speed and the phase speed are equal, the "critical point" of the most unstable wave is at r = 1.33. It will become clear that in order to elicit the strongest response, the disturbance should be placed near r = 1.33. In other words, $r_{0,max} \approx$ "critical point" associated with the most amplified wavenumber.

The wave-like shape and the amplitude of the wave packet at a typical instant of time (say, t = 40) and at given radial locations are shown in Figure 11. The transverse velocity component v(x, r-fixed, t-fixed) is plotted against the group velocity G (=x/t, t is

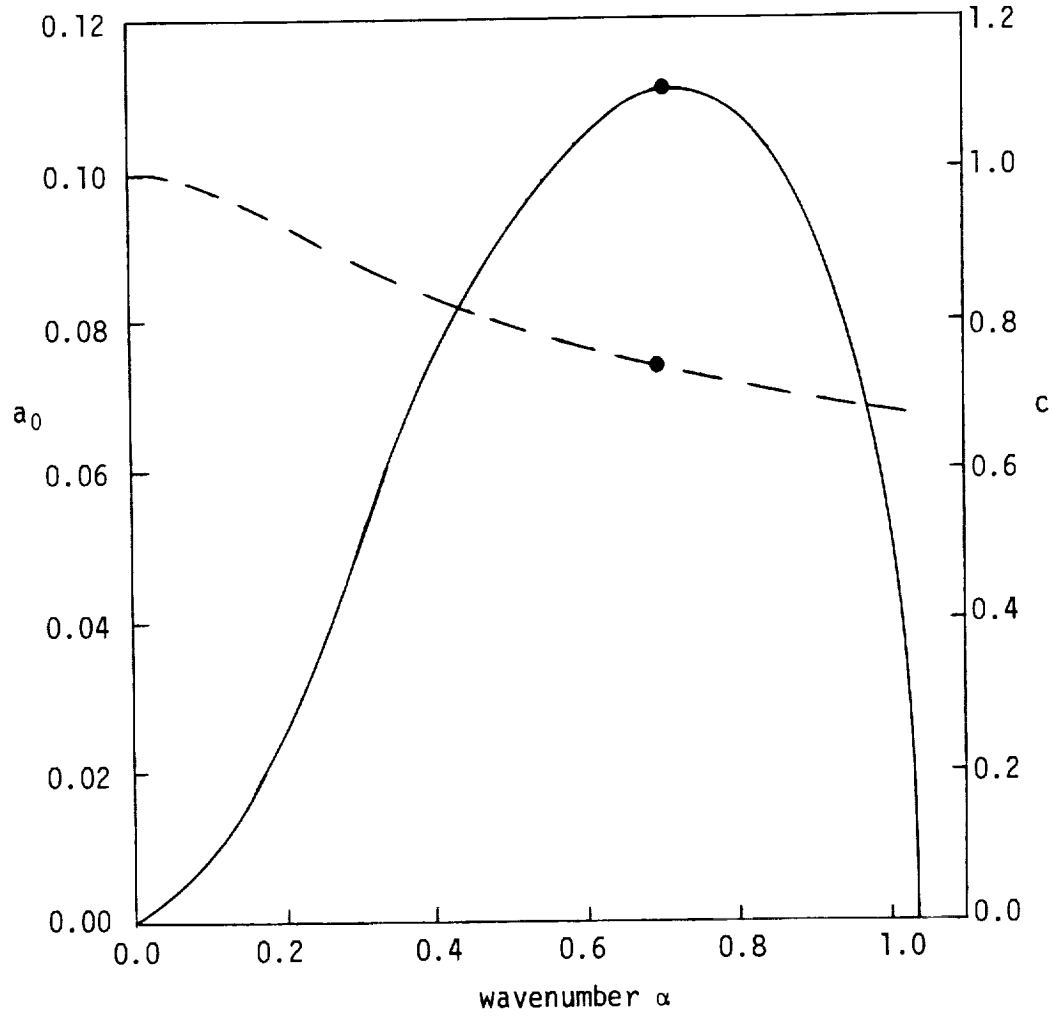

Figure 10. Inviscid instability of the model jet flow with $r_1 = 1$ and $r_2 = 2$: Linear growth rate a_0 (solid line) and phase speed c (dashed line) as functions of wavenumber. $M = 0.0$; $T^* = 1.0$; $\beta = 0$. (● indicates the most amplified wave.)

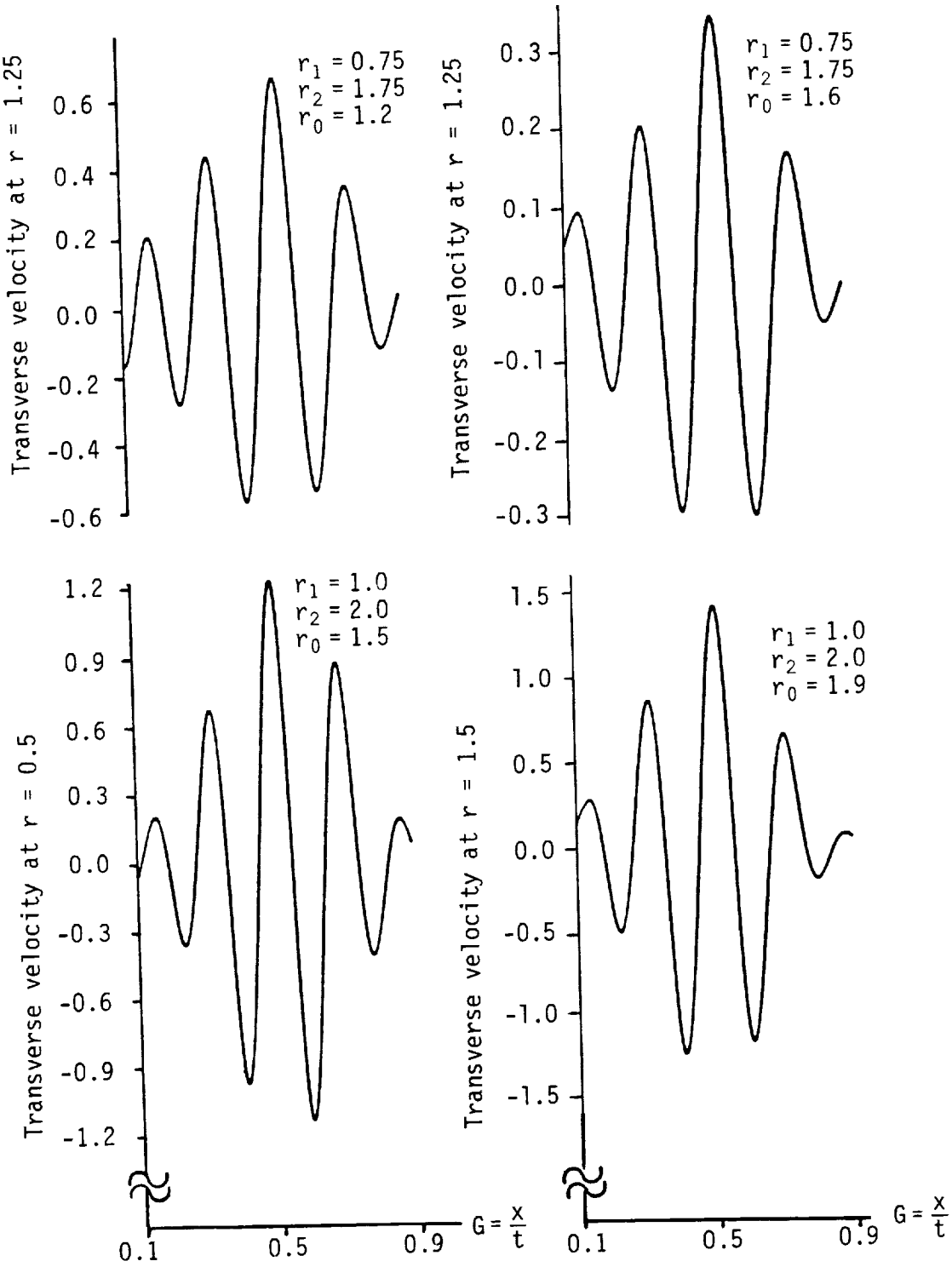

Figure 11. Transverse velocity in wave packet at various radial locations as a function of group velocity for different values of source location and flow geometry. Time = 40.

fixed) for two flow geometries (one with $r_1 = 1$ and $r_2 = 2$ and the other with $r_1 = 0.75$ and $r_2 = 1.75$) and for parametric values of the source location, r_0. Essentially, the packet at each instant of time is contained between the points G = 0 and G = 1, and the amplitude of the packet reaches a maximum for an observer moving at approximately the jet's average speed, G = 0.5. The leading and trailing edges of the packet are defined by $G = x/t = 0 = U_{min}$ and $G = x/t = 1 = U_{max}$, and the disturbance is growing exponentially in time in this interval. The maximum amplitude of the packet v_{max} or the peak velocity at any radial location depends on the source location r_0; for example, when $r_1 = 0.75$ and $r_2 = 1.75$, the peak velocity at the middle of the axisymmetric shear layer (r = 1.25) nearly doubles (changes from about 0.35 to about 0.65) as the source position is changed from $r_0 = 1.6$ (near the outer edge) to $r_0 = 1.2$ (near the middle of the shear layer). An impulsive source in the shear layer ($r_1 < r_0 < r_2$) can produce large fluctuations outside the shear layer; for example, when $r_1 = 1.0$, $r_2 = 2.0$ and $r_0 = 1.5$, the peak velocity at r = 0.5 is about 1.2.

At larger values of time, the general wave-like character of the packet is unaltered, although its amplitude is greater because of the exponential growth associated with the instability of the base flow. Thus, relative to an observer moving with the group velocity, the disturbance grows exponentially in time. But the disturbance measured at any fixed station x eventually decays rapidly with time because the localized disturbance travels away.

In physical terms, the impulsive excitation produces a wave packet (i.e., an amplitude modulated wavetrain of finite extent) whose maximum amplitude v_{max} (see Figure 2) at a fixed radial location, at a fixed large time, and for a given base flow is a function of the source location r_0. The goal of the present receptivity analysis is to obtain

$v_{max}(r_0)$ and to see if the most receptive place, $r_{0,max}$, is related to the "critical point" associated with the most unstable wave of linear stability theory. One may note that the model base flow, with $r_1 = 1.0$ and $r_2 = 2.0$, has such a point at $r \simeq 1.33$, which is towards the inner uniform base flow. On the other hand, for $r_1 = 0.75$ and $r_2 = 1.75$, this "critical point" is at $r = 1.08$.

The "receptivity" of the jet, $v_{max}(r_0)$, as a function of the source location, is shown in Figure 12. The location of the source is changed between the inner and the outer uniform mean profiles and the magnitude of the maximum velocity, v_{max}, is calculated at various locations in the radial direction. Recall that $v = v(x,r,t; r_0)$ and v_{max} is defined by the maximum value of v as x ranges over its values in the interior of the packet at fixed values of r, t and r_0 (see Figure 11). In other words, v_{max} is a function of r, t and r_0; the dependence on t is essentially exponential (therefore uninteresting) because of the intrinsic instability of the base flow. The dependence on the source location, r_0, is given for parametric values of r in Figure 12. In addition, v_{max} also depends on the base velocity profile; hence the dependence on r_1 and r_2.

Figure 12 provides several interesting results about the sensitivity or receptivity of the jet flow to disturbances that are generated at r_0. First, as the source is moved away from the inner flow toward the outer flow, the maximum disturbance velocity at a given radial location first increases and then decreases. This means that there is an optimum place of the source, $r_{0,max}$, which yields the strongest response in the flow. It is interesting to note that the curves are not symmetric about $r = (r_1+r_2)/2$ and they do not attain their maximum values there, which means that the most receptive place of the source is not the middle of the axisymmetric shear layer. In fact, the strongest response is obtained when the impulsive disturbance is placed closer to the high-speed side of the jet

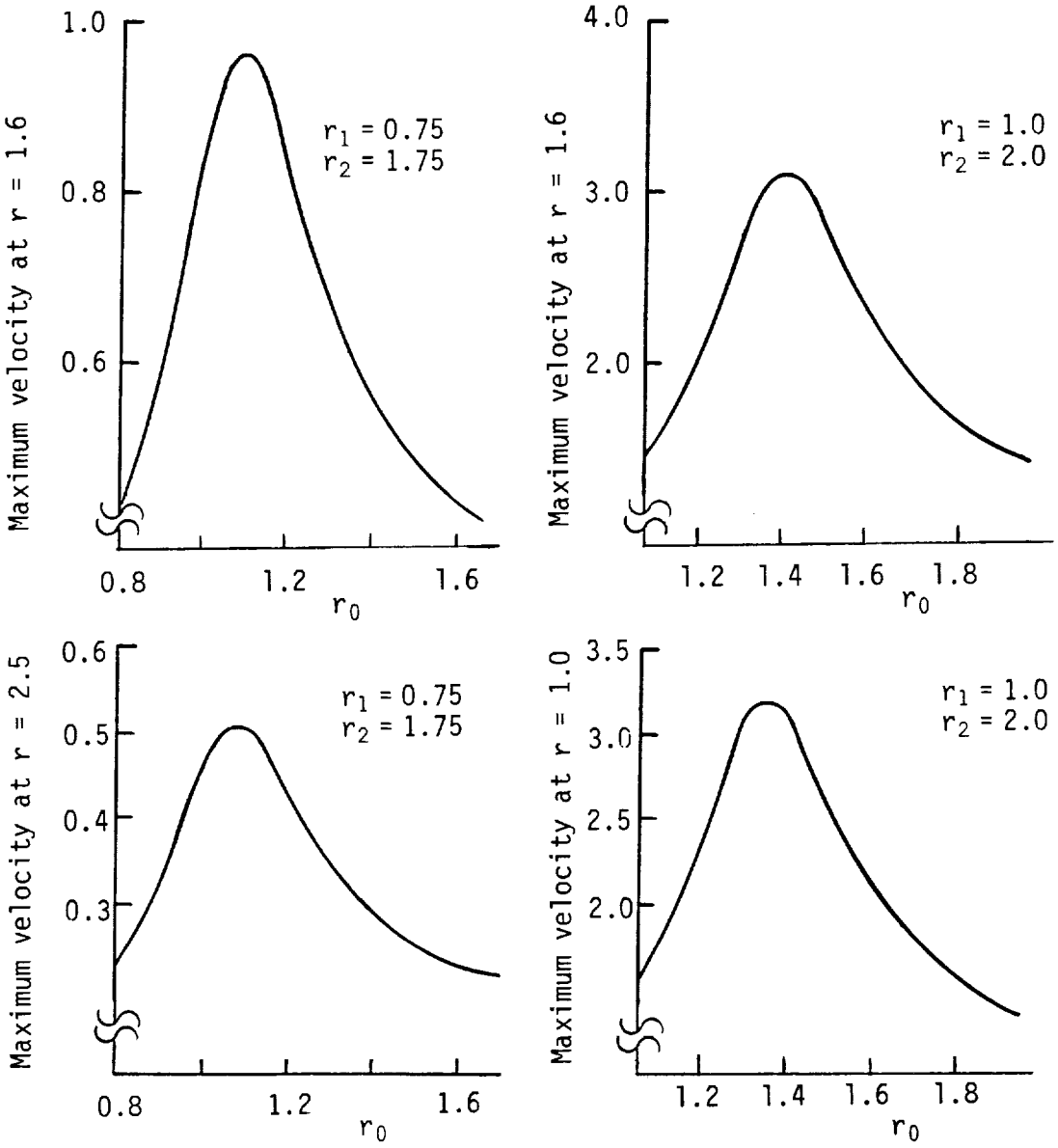

Figure 12. Magnitude of maximum transverse velocity in wave packet at various radial locations as a function of source location for two flow geometries. Time = 40.

or nearer to the inner flow. For example, $r_{0,max}$ is about 1.09 when $(r_1, r_2) = (0.75, 1.75)$ and is about 1.35 when $(r_1, r_2) = (1.0, 2.0)$. Note that $r_{0,max} \approx$ the "critical point" associated with the most unstable wave of linear theory: $U(r = r_{0,max}) \approx c(\alpha = \alpha_m)$ where c is the phase speed of the most amplified wave whose wavenumber is α_m. This simple result is valid for all r_1 and r_2 and is consistent with the result of Balsa (1988), who found that the mixing layer is most sensitive to perturbations which occur near the region at which the phase speed and fluid speed are equal. Finally, the maximum velocity changes fairly rapidly with r_0, except in the vicinity of $r_{0,max}$, which means that the perturbations in the flow field are quite sensitive to the location of the excitation. For example, the peak velocity at $r = 1.6$ and for $(r_1, r_2) = (1.0, 2.0)$ changes from about 1.5 to about 3.0 (nearly doubles) as r_0 is changed from about 1.05 to about 1.35.

In the mixing layer, all unstable waves are convected with the flow at the same phase speed $c = U(y = 0)$ and the flow is very receptive to disturbances that are generated near the centerline of the layer (Balsa, 1988). In the jet, the phase speed depends on the wavenumber and the flow is very receptive to disturbances that are generated near the "critical point" of the most unstable wave. Therefore, in order to elicit the strongest response, the disturbance should be placed at $r_{0,max}$, which is given by

$$U(r_{0,max}) = c(\alpha_m) \tag{4.2-1}$$

where $r_{0,max}$ is the location of the source which results in maximum perturbations at any radial location r, and α_m is the most amplified wavenumber. For the model base flow of Figure 2, $r_{0,max}$ is closer to the high-speed side than to the low-speed side. Equation (4.2-1) provides a simple criterion that is relevant to flow control.

In summary, our current wave packet describes the response of a parallel jet flow that is disturbed by an impulsive source at $x = 0$, $r = r_0$ and $t = 0$. The wave packet is the long time solution of the linearized initial value problem and its amplitude depends on the location r_0 of the perturbation. The long time solution describes not only the general structure of wave packets, but also establishes the explicit connection between the perturbations in the flow and the external disturbances which generate them. The conclusion is a simple one: in order to generate maximum perturbations in the flow, the disturbance should be placed near the "critical point" of the most unstable wave. In other words, the jet flow is most sensitive to perturbations which occur near the region at which the fluid speed and the phase speed of the most amplified wave are equal.

CHAPTER 5

ANALYSIS OF THE MIXING LAYER

In this chapter, the evolution of finite (but small) amplitude disturbances in mixing layers is discussed using both the weakly nonlinear stability theory (Section 2.2) and the (truncated) numerical solutions of the Navier-Stokes equations (Section 2.3). It is the manner in which nonlinearity sets in, and the consequences of its presence, that this analysis seeks to explore. Once a disturbance with some wavenumber and amplitude is superimposed on the base flow, its amplitude grows exponentially in time until nonlinearities generate higher harmonics and wave Reynolds stresses that alter the base flow. This causes the amplitude and frequency of the fundamental wave to go through some dynamical adjustments as discussed previously. In the weakly nonlinear theory, these adjustments are measured by the sign and the magnitude of the Landau constants (a_1, a_2, etc.), and a finite amplitude steady state will be reached if a_1 is negative. The numerical solution, on the other hand, may become steady or oscillatory depending on the wavenumber, initial amplitude of the disturbance and Reynolds number. In order to see the importance of nonlinearities in the critical layer as the neutral wave is approached, and to establish the range of validity of the weakly nonlinear theory, the two solutions are compared for various Reynolds numbers, initial amplitudes and wavenumbers.

The basic objectives of this work are: (1) to understand the nonlinear evolution of disturbances in mixing layers; and (2) to explore the range of validity of the weakly nonlinear theory (Stuart, 1960; Watson, 1960; Schade, 1964; Maslowe, 1977; Herbert, 1983; Huerre, 1980 and 1987). This theory is an asymptotic one valid for small amplitudes and is based on a series expansion in the amplitude in which the leading order solution is that

of the linear problem. Once a given linearly unstable base flow is perturbed by a wave-like disturbance, the disturbance grows (initially) according to linear theory (Drazin and Reid, 1981) until self-interactions create a wave Reynolds stress which will distort the mean flow and alter its stability characteristics.

A weakly nonlinear analysis of the incompressible, two-dimensional and temporally evolving mixing layer consists of expanding the single disturbance in a Fourier series in the axial variable, expanding each Fourier component in terms of the small amplitude A(t) and seeking a Landau-type equation (see Eq. 2.1-11) for the amplitude. The problem is formulated analytically in Section 2.2. In order to see the physical essence of the Landau equation, consider the nonlinear interactions in a flow that is perturbed by an O(A) fundamental disturbance $e^{i\alpha x}$. At $O(A^2)$, the fundamental interacts with itself to generate the second harmonic $e^{2i\alpha x}$ and, with its complex conjugate, to generate the zeroth harmonic $e^{0i\alpha x}$. At $O(A^3)$, the second harmonic interacts with the complex conjugate of the fundamental to reproduce the fundamental. But a far more important interaction, which is invariably ignored in the literature for erroneous reasons, is the interaction of the zeroth harmonic (the so-called mean flow distortion) with the fundamental. This latter interaction also reproduces the fundamental and alters its growth rate. Another objective of this dissertation is to clarify the role of this interaction in the nonlinear stability of free shear flows. Briefly, the nonlinear interactions result in: (1) the generation and distortion of higher harmonics; (2) the distortion of the fundamental; and (3) the distortion of the base flow via the zeroth harmonic. Since the O(A) fundamental wave $e^{i\alpha x}$ is reproduced at $O(A^3)$, $O(A^5)$, $O(A^7)$, etc., it is natural to expand the amplitude A(t) in the form

$$\frac{dA}{dt} = a_0 A + a_1 A^3 + a_2 A^5 + \cdots$$

where the linear growth rate (a_0), the first Landau constant (a_1) and the second Landau constant (a_2) are time-independent but depend on the wavenumber of the disturbance and on the Reynolds number. The initial amplitude A(0) of the disturbance is needed to solve the above first-order nonlinear ordinary differential equation.

The basic steps of the numerical treatment of the mixing layer are discussed in Section 2.3. There we recall that the various steps are: (1) expansion of a single disturbance in a Fourier series in the axial variable; (2) truncation of the series at a given n, where n is the order of the harmonic; and (3) solution of the resulting coupled nonlinear partial differential equations for the Fourier coefficients. These depend on the transverse variable y and time t, and a finite difference scheme is used to solve these equations at a given Reynolds number, wavenumber and initial amplitude. Initially, only the fundamental wave is nonzero and its mode shape and phase speed are obtained by solving (numerically) the Orr-Sommerfeld equation. In the course of time, both the amplitude and the shape of the fundamental change due to nonlinearities. In this work, n = 2, which means that the fundamental and the zeroth and second harmonics are kept and smaller scales of motion (third and higher harmonics) are absent whereas George and Hellums (1972) considered n = 2, 3 and 4 in their work on finite amplitude disturbances in plane Poiseuille flow; Miura and Sato (1978) used n = 1 in their work on the nonlinearly evolving inviscid shear layer.

The disturbance (if unstable) grows while being convected by the flow at the phase speed c, which is somewhere between the maximum and the minimum values of the base flow. For the hyperbolic-tangent family of base profiles, the disturbance propagates at exactly the average velocity; for example, when the base flow is U(y) = tanhy, all waves travel at zero velocity. In the neighborhood of the critical layer, where $U - c \simeq 0$ (the critical layer is at y = 0 for the hyperbolic-tangent profiles), viscous and nonlinear effects

are important. Benney and Bergeron (1969) found the structure of a critical layer in which nonlinearity dominates viscosity and the pattern of the streamlines in this layer resembles the cat's eyes of Kelvin (Drazin and Reid, 1981, p. 141). Outside the critical layer region, the leading order disturbance equation is the Rayleigh equation, and within the critical layer, the leading order flow is the cat's eyes pattern. To understand the relative effects of viscosity and nonlinearity on the instability wave, consider the nonlinear equation (2.2-1) of the perturbation streamfunction, and let the size of the perturbation be A. Near the critical layer, of thickness δ, [the base flow is $U(y) = \tanh y \sim y$ near $y = 0$, $\partial/\partial x \sim 1$, $\partial/\partial y \sim 1/\delta$; Drazin and Reid, 1981, pp. 421-22] the viscous term $\sim A/(\delta^4 \, Re)$, the convection term $\sim A/\delta$ and the nonlinear term $\sim A^2/\delta^3$. A balance between the convection and viscous terms determines the thickness of a linear viscous critical layer to be $\delta \approx Re^{-1/3}$ and a balance between the convection and nonlinear terms determines the thickness of a nonlinear inviscid critical layer to be $\delta \approx A^{1/2}$. These length scales have been similarly derived by Benney and Bergeron (1969) and by Robinson (1974) in their work on nonlinear waves in parallel shear flows. An exceptionally important work on nonlinear critical layers has recently been published by Goldstein and Leib (1988).

In order to establish the range of validity (in terms of amplitude and Reynolds number) in which the weakly nonlinear theory is accurate, the numerical and the weakly nonlinear solutions are compared with each other. Although they both contain only the first few nonlinear interactions (as described previously in terms of Fourier modes), the weakly nonlinear theory makes a further assumption in the form of the amplitude expansion $dA/dt = a_0 A + a_1 A^3 + \cdots$. Putting it slightly differently and in more technical terms, we emphasize that the weakly nonlinear theory assumes *a priori* that the critical layer is viscous. On the other hand, the numerical approach makes no such assumption,

and treats the critical layer as a balance between viscosity and nonlinearities. Such a comparison will give an indication for the breakdown of the weakly nonlinear theory when the amplitude is too large. This comparison is consistent in the sense that only the fundamental, the second harmonic and the mean flow correction (the zeroth harmonic) are kept in both approaches. Therefore, the two solutions should agree well with each other in the limit of small amplitude and Reynolds number. At large amplitudes and higher Reynolds numbers, the results will differ because, in the weakly nonlinear theory, the equations are solved by a perturbation method for small amplitude and the effects of nonlinearities enter in a hierarchial manner. The lowest order solution is the linear one to which corrections are made in a successive fashion to account for nonlinearities. This implies that to lowest order, the critical layer is a viscous one. On the other hand, in the numerical solution, the critical layer is allowed to be fully viscous and nonlinear (within the limits of the truncation after the second harmonic) because we are solving a system of nonlinear equations.

In summary, the analysis in this chapter is concerned with the temporal interactions between an instability mode and its harmonics in mixing layers with hyperbolic-tangent base flows. The first and the second Landau constants are calculated for neutral and for amplified waves, and the amplitude equation (5.2-1) is solved to $O(A^3)$ (see Eq. 5.3-12) to determine the amplitude of the fundamental wave under linear growth and nonlinear saturation. In order to see how the importance of the nonlinearity changes as the neutral wavenumber is approached, to establish the range of validity of the weakly nonlinear theory of Stuart (1960) and Watson (1960), and to describe the evolution of very amplified waves, a numerical solution is obtained and compared to the weakly nonlinear solution for various Reynolds numbers and wavenumbers.

Before discussing the nonlinear instability of the mixing layer, it is worth mentioning some aspects of its linear instability (Betchov and Szewczyk, 1963; Michalke, 1964). The mixing layer is linearly unstable to small disturbances; when it is excited by an oscillatory disturbance of suitable wavenumber, the disturbance extracts energy from the mean flow so that it grows exponentially in time while being convected with the flow. The instability of a given base flow depends on the disturbance wavenumber and on the Reynolds number (based on the momentum thickness). Our typical base flow and its viscous instability characteristics (based on numerical solution of the Orr-Sommerfeld equation) are shown in Figure 13. The linear growth rate a_0 as a function of wavenumber α is shown for different values of the Reynolds number Re and the phase speed of the disturbance c is found to be 0, which means that the critical layer is in the vicinity of $y = 0$. Note that the base flow has an inflection point at $y = 0$ and that the waves are nondispersive (i.e., all waves travel at the same speed).

These linear results, which are in agreement with the numerically obtained results of Betchov and Szewczyk (1963), show that viscosity is stabilizing and that the instability characteristics of the viscous problem at $Re = 200$ and the inviscid one are nearly the same. For example, the maximum growth rates at Reynolds numbers of ∞, 100 and 50 are 0.190, 0.175 and 0.163, respectively. Viscosity reduces the range of unstable wavenumbers by suppressing the growth of short waves and, therefore, leads to a lower neutral point. For example, the neutral wavenumbers at Reynolds numbers of ∞, 200, 100 and 50 are 1.0, 0.969, 0.943 and 0.895, respectively. Viscosity, or molecular diffusion of momentum, tends to smooth out the velocity differences of a disturbance and, in a mechanical sense, dissipates the energy of any disturbance and thereby stabilizes the free shear layer.

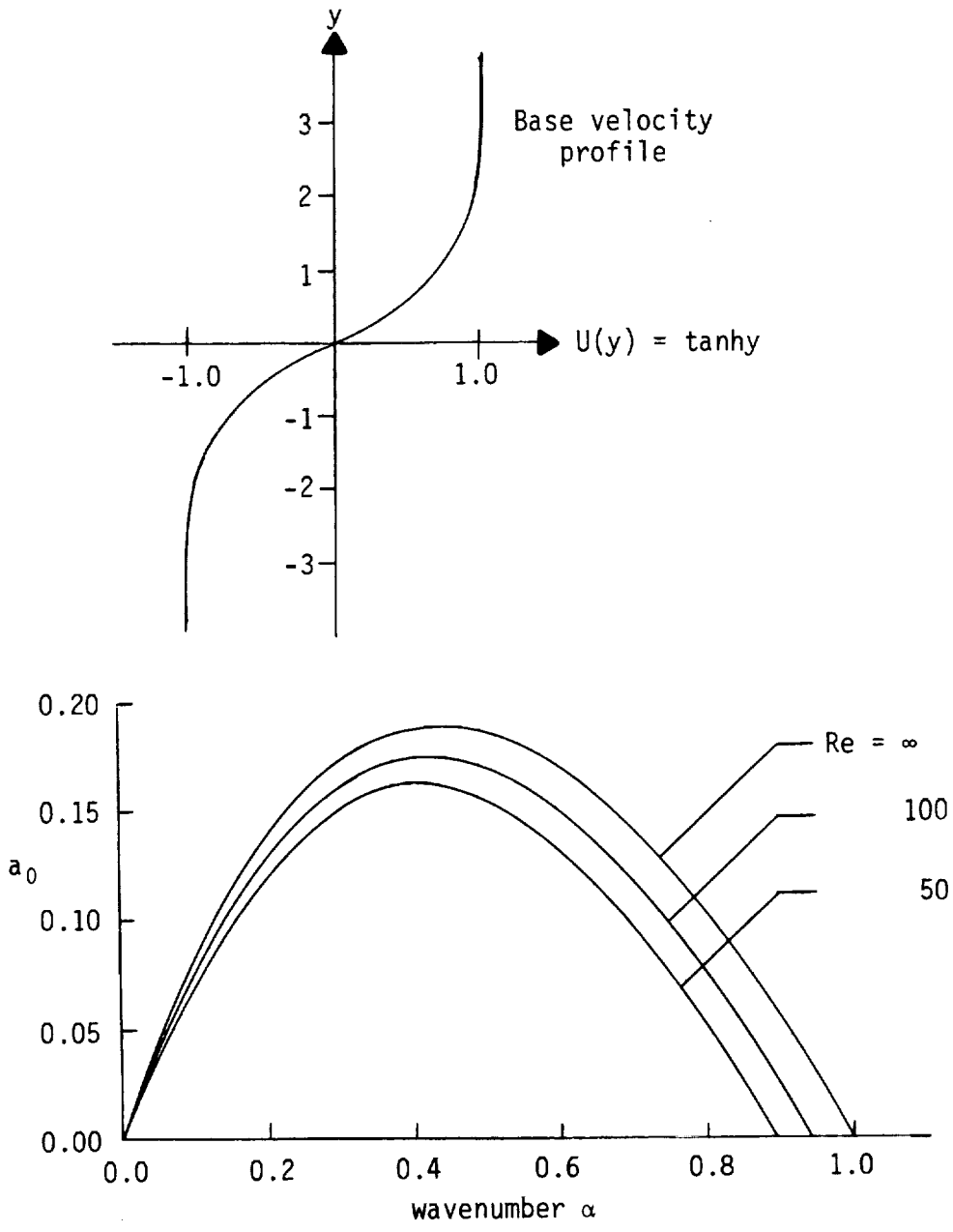

Figure 13. The hyperbolic-tangent base flow and its instability: Linear growth rate a_0 as a function of wavenumber for different values of the Reynolds number Re.

5.1 The First Landau Constant

The mixing layer is unstable; once it is perturbed, the fundamental disturbance grows exponentially in time until it interacts with itself to create a wave Reynolds stress which excites both the zeroth and second harmonics. Once these two harmonics are in the flow, they further interact with the fundamental to modify its exponential growth and such modification is measured by the sign and the magnitude of the first Landau constant a_1. To put it in yet a simpler way, the second term on the right-hand side of the Landau equation ($dA/dt = a_0A + a_1A^3 + \cdots$) is due to the interactions between the fundamental and both the zeroth and second harmonics and may moderate or accelerate the exponential growth of the disturbance according to the sign of a_1.

The generation of the zeroth harmonic causes the mean flow to change in the course of time and, in the spirit of the weakly nonlinear theory (see Eq. 2.2-3), the mean flow is

$$\bar{u}(y,t) = U(y) + A^2(t)\,\phi_{01}'(y) + \cdots \qquad (5.1\text{-}1)$$

where U(y) is the base flow, $\phi_{01}(y)$ is a shape function associated with the distortion of the mean flow, and the prime denotes d/dy. The contributions to the first Landau constant, therefore, come from two nonlinear effects: the interaction of the fundamental with the second harmonic, and the interaction of the fundamental with the zeroth harmonic. The latter is called the mean flow distortion effect (MFD). Both of these interactions are of $O(A^3)$.

There has been a controversy in the literature concerning the effect of the mean flow distortion (MFD) on the growth of the disturbance. Schade (1964) and Maslowe (1977) neglected the mean flow distortion contribution to a_1 by setting the zeroth harmonic

to zero and found the contribution arising from the interaction between the fundamental and the second harmonic to be stabilizing (a_1 was found to be negative for neutral waves). Schade took a hyperbolic-tangent base profile and (by obtaining closed-form solutions of the equations governing the fundamental mode, and the second harmonic) formally calculated a_1 in the limit as $Re \to \infty$, while Maslowe calculated a_1 at low values of Re numerically by using a second-order finite difference scheme. Huerre (1980) concluded that the mean flow distortion is destabilizing but he later (1987) corrected his original work and concluded that the mean flow distortion contribution to the first Landau constant dominates the contribution coming from the interaction of the fundamental with the second harmonic and it is strongly stabilizing. Huerre used the method of multiple scales to obtain a_1 for neutral waves in the limit as $Re \to \infty$ and when the critical layer is viscous.

The first Landau constant (a_1) of the weakly nonlinear stability theory is calculated with and without the presence of the mean flow distortion (MFD). It is found to be negative, indicating that nonlinearities are stabilizing for the mixing layer. The principal contribution to the first Landau constant comes from the MFD and not from the interaction of the fundamental with the second harmonic. An unstable wave will, therefore, saturate into a finite amplitude steady state regardless of the magnitude of the small initial amplitude. The equilibrium amplitude A_e ($A_e^2 = -a_0/a_1$) depends only on the wavenumber and the Reynolds number. At this point in time, the kinetic energy of the disturbance is constant and (in the inviscid limit) the total energy supplied per period from the basic flow to the perturbation flow via the wave Reynolds stresses is zero (in the viscous case, the small viscous dissipation of kinetic energy balances exactly the small energy input into the perturbations from the mean flow via Reynolds stresses; see Drazin and Reid, 1981, p. 425).

The first Landau constant (at the neutral wavenumber) is given, for parametric values of Reynolds number, is shown in Table 1. There is about a 4% difference between the present results and those obtained by Maslowe (1977). We believe the present investigation (which employs a fourth order scheme; $\Delta y = 0.02$; boundary conditions are enforced at $y = \mp 4.0$) is more accurate than Maslowe's (second order scheme with $\Delta y = 0.05$; boundary conditions are enforced at $y = \mp 3.0$). It can be seen from the fourth column that the absolute value of the Landau constant first increases then decreases slightly as the Reynolds number is increased and that the published value of Schade (1964) is approached as $Re \rightarrow \infty$. The inclusion of the mean flow distortion is very stabilizing, especially at higher Reynolds numbers. In Figure 14, the behavior of a_1 as a function of Reynolds number at exactly the neutral points is shown. In the limit of large Reynolds numbers, the dominant contribution to the Landau constant arises from the mean flow distortion. While the harmonic contribution is O(1), the mean flow distortion contribution is $O(Re^{1/3})$. This is consistent with the analysis of Huerre (1987). In particular, the two predictions are:

$$-a_1 \approx \begin{cases} 8.18\ Re^{1/3} & ;\ \text{Huerre (1987)} \\ & \quad (Re \rightarrow \infty) \\ 7.80\ Re^{1/3} & ;\ \text{Present Investigation} \\ & \quad (Re > 20{,}000) \end{cases} \qquad (5.1\text{-}2)$$

The behavior of a_1 as a function of wavenumber for parametric values of shear layer Reynolds numbers is shown in Figures 15 and 16. At large Reynolds numbers, a_1 changes extremely rapidly with wavenumber in the vicinity of the neutral point. Also, in a relative sense, nonlinear effects are more important for near-neutral waves (say, $\alpha \approx 1.0$) than for off-neutral waves (say, $\alpha \approx 0.8$) because of the largeness of the Landau constant computed with MFD. This is due to a competition between a "growth critical layer" [which can be obtained from Eq. 2.2-1 by balancing the terms $\partial(\nabla^2\psi)/\partial t$ and $U\ \partial(\nabla^2\psi)/\partial x$

Table 1. First Landau Constant Calculated at Various Reynolds Numbers and Compared with the Results of Maslowe (1977) and Schade (1964). The Waves are Exactly Neutral. U(y) = tanhy.

Reynolds number (Re)	Neutral Wavenumber (α_n)	First Landau Constant ($-a_1$)		
		Literature* Value (No MFD)	Present Investigation (No MFD)	Present Investigation (MFD)
20	0.7835	0.552	0.584	2.556
30	0.8409	0.786	0.825	4.104
40	0.8738	0.951	1.007	5.578
50	0.8953	1.105	1.147	6.965
75	0.9264	1.350	1.387	10.093
100	0.9431	1.504	1.537	12.831
125	0.9537	1.610	1.638	15.272
150	0.9610	1.685	1.711	17.483
300	0.9798		1.902	27.8
500	0.9877		1.971	37.5
1,000	0.9937		1.997	53.8
2,000	0.9969		1.986	76.0
3,000	0.9979		1.973	92.0
4,000	0.9985		1.950	99.3
10,000	0.9994		1.901	152
∞	1.000	1.698**		

* Maslowe (1977)

**Schade (1964)

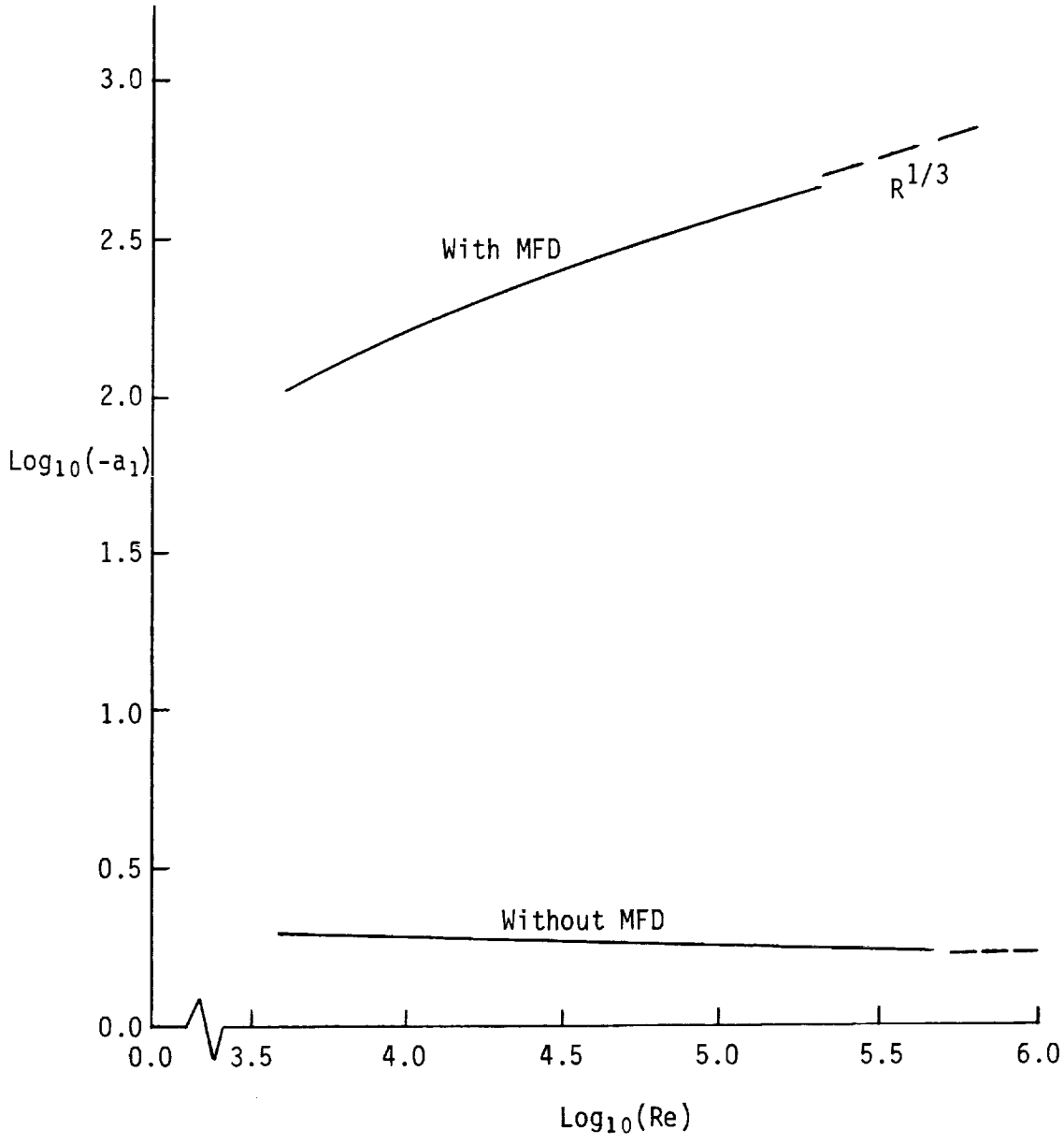

Figure 14. First Landau constant as a function of Reynolds number for neutral waves with and without mean flow distortion (MFD). (Log-Log scale; base 10.) u(y) = tanhy. Dashed lines are Huerre's (1987) results as Re $\rightarrow \infty$.

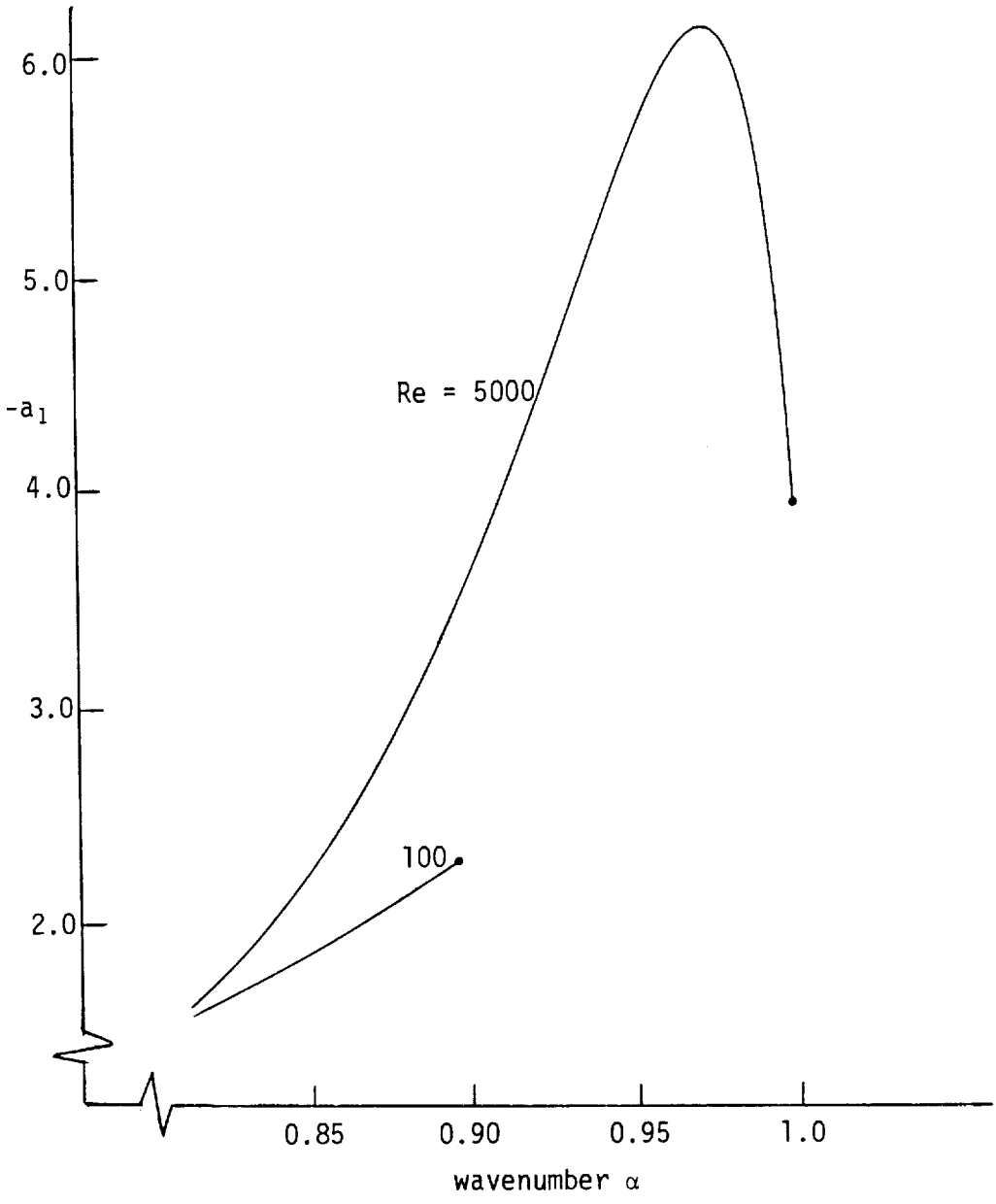

Figure 15. First Landau constant as a function of wavenumber for parametric values of shear layer Reynolds number. (• indicates neutral point.) No mean flow distortion. U(y) = 0.5 (1 + tanhy).

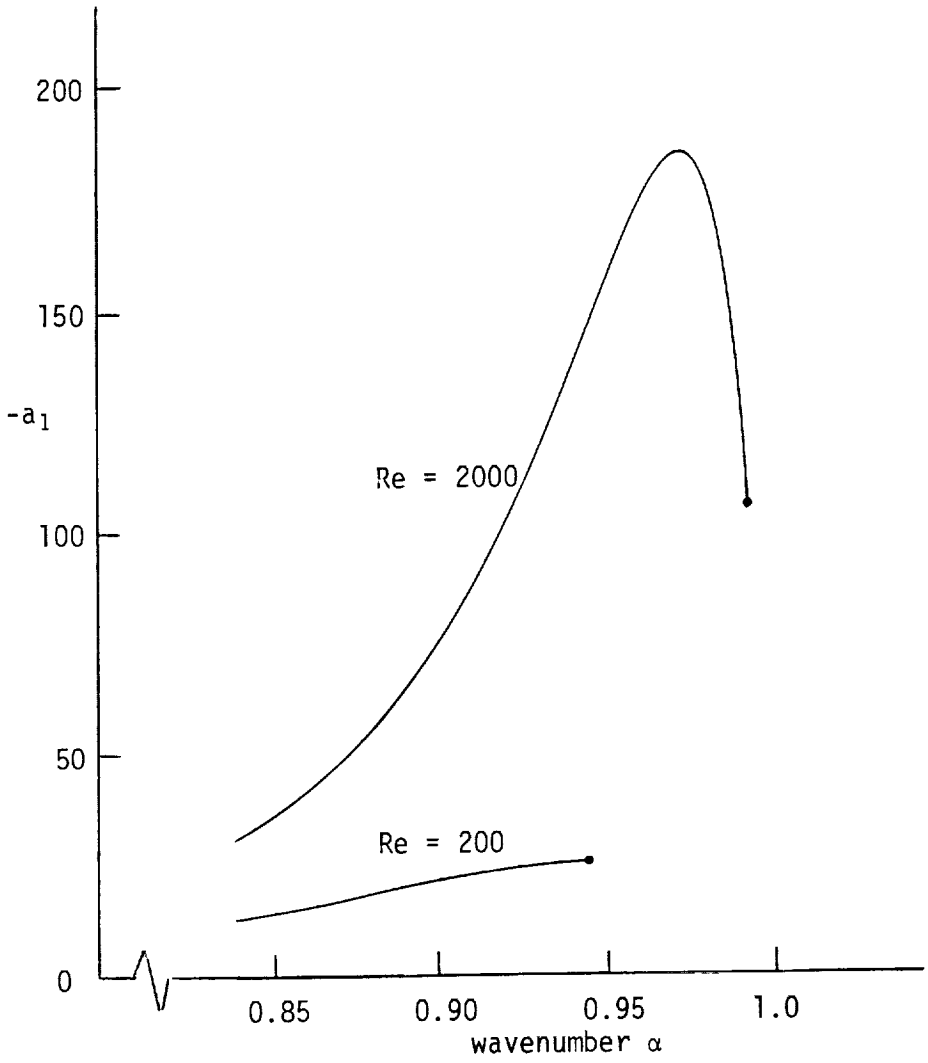

Figure 16. First Landau constant as a function of wavenumber for parametric values of shear layer Reynolds number. (• denotes neutral point.) With mean flow distortion. U(y) = 0.5 (1 + tanhy).

with each other and by noting that, near y = 0, U(y) ~ y ~ δ where δ is the critical layer thickness; Robinson, 1974] of $O(a_0)$ which is important for amplified waves and a viscous critical layer of $O(Re^{-1/3})$ which is important for neutral waves. In other words, in the weakly nonlinear theory, the (inviscid) terms in the momentum equation dominate for amplified waves but the effects of viscosity become more important as the neutral point is approached. Physically, viscosity diffuses any variations in the vorticity and the effect of the viscosity in altering the nonlinear instability of the flow is negligible to first order provided that $a_0 >> Re^{-1/3}$ (Stuart, 1960; Robinson, 1974). This condition, which may also be obtained from a direct comparison of the terms $\partial(\nabla^2\psi)/\partial t$ and $\nabla^4\psi/Re$ in Eq. 2.2-1 after noting that $\partial/\partial t \sim a_0$, means that the time scale for inviscid changes ($1/a_0$; obtained from balancing $\partial/\partial t\ \nabla^2\psi$ with $U(\partial/\partial x)\nabla^2\psi$ in the growth critical layer) must be much smaller than the time scale for viscous diffusion in order to neglect the effects of viscosity.

There are many conclusions which can be drawn from Figures 15 and 16. First, at any (unstable) wavenumber considered, the value of the first Landau constant is much larger in the presence of the mean flow distortion. This means that it is the changes in the mean flow induced by the Reynolds stresses, and not the birth of the second harmonic, that contribute the most to slowing the growth of the fundamental. Second, at large Reynolds numbers, the maximum value of the first Landau constant ($-a_{1max}$) is attained just before the neutral wave; for example, at Re = 5000 (no MFD), the neutral wave is $\alpha_n = 0.998$, but $-a_{1max}$ is at $\alpha_{max} = 0.965$. To the right of α_{max}, the Landau constant is dominated by a viscous critical layer while to the left, a_1 is dominated by a growth critical layer. This argument is similar to the classical boundary layer concept in the sense that the Landau constant behaves almost inviscidly until forced to adjust to viscous effects just before the neutral wave, at a distance that depends on the magnitude of the Reynolds

number. Finally, at low Reynolds numbers, the Landau constant "feels" viscous effects throughout the entire wavenumber range and behaves in a monotonic fashion. In other words, the sharp peak or boundary layer is completely diffused.

Generally, the maximum value of the Landau constant ($-a_{1max}$) is reached just before the neutral wave. The behavior of $-a_{1max}$ as a function of Reynolds numbers is shown in Figure 17. It can be seen that the absolute value of a_{1max} increases with increasing Reynolds number and that the mean flow distortion is very stabilizing. The maximum value of the Landau constant changes from $O(Re^{1/4})$ when the mean flow distortion is absent to O(Re) when the mean flow distortion is included. Note that nonlinear effects are more important for a near-neutral wave than for either precisely neutral or moderately amplified waves.

The strongly stabilizing effect of the mean flow distortion can be explained by following the shape of the distorted mean velocity profile in the vicinity of the critical layer during the course of time. At $t = 0$, the mean velocity is U(y) - this is the base flow. For $t > 0$, the mean flow remains $\bar{u}(y,t) = U(y)$ when the mean flow distortion is neglected and becomes less steep when the mean flow distortion is included [see Eq. (5.1-1)]. In other words, the inclusion of the mean flow distortion results in a more diffused (less steep) and, therefore, a more stable flow as time goes on. Basically, the mean velocity gradient will be reduced near the middle of the shear layer during the growing period of the amplitude as soon as the zeroth harmonic is born. The fundamental will then be convected into more and more stable profiles until a steady-state (i.e., saturation where $A = A_e$) is reached.

Figure 18 shows how the mean velocity profile $\bar{u}(y,t)$ is modified with time. The initial amplitude $A(t = 0)$ of the fundamental disturbance (with $\alpha = 0.8$) is 0.005 and (at

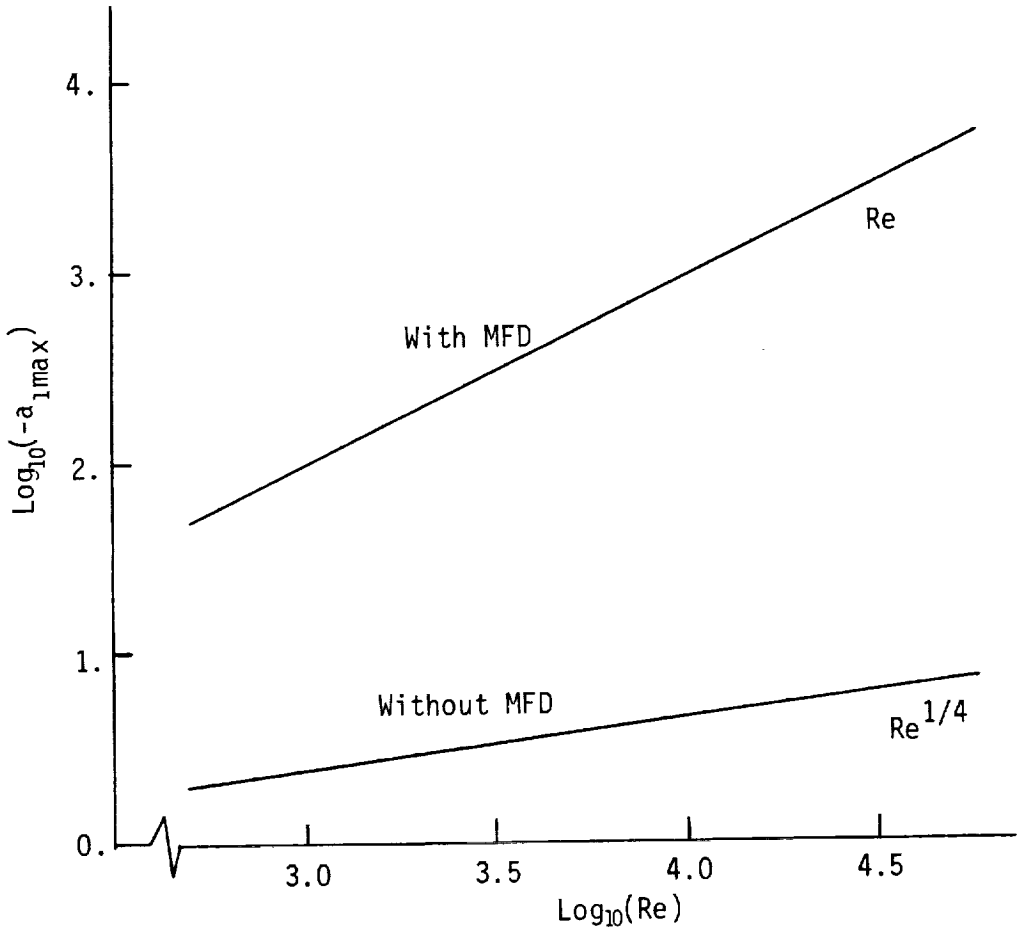

Figure 17. Maximum value of first Landau constant as a function of Reynolds number with and without mean flow distortion (MFD). (Log-Log scale.) U(y) = tanhy. The waves are slightly unstable in the linear sense.

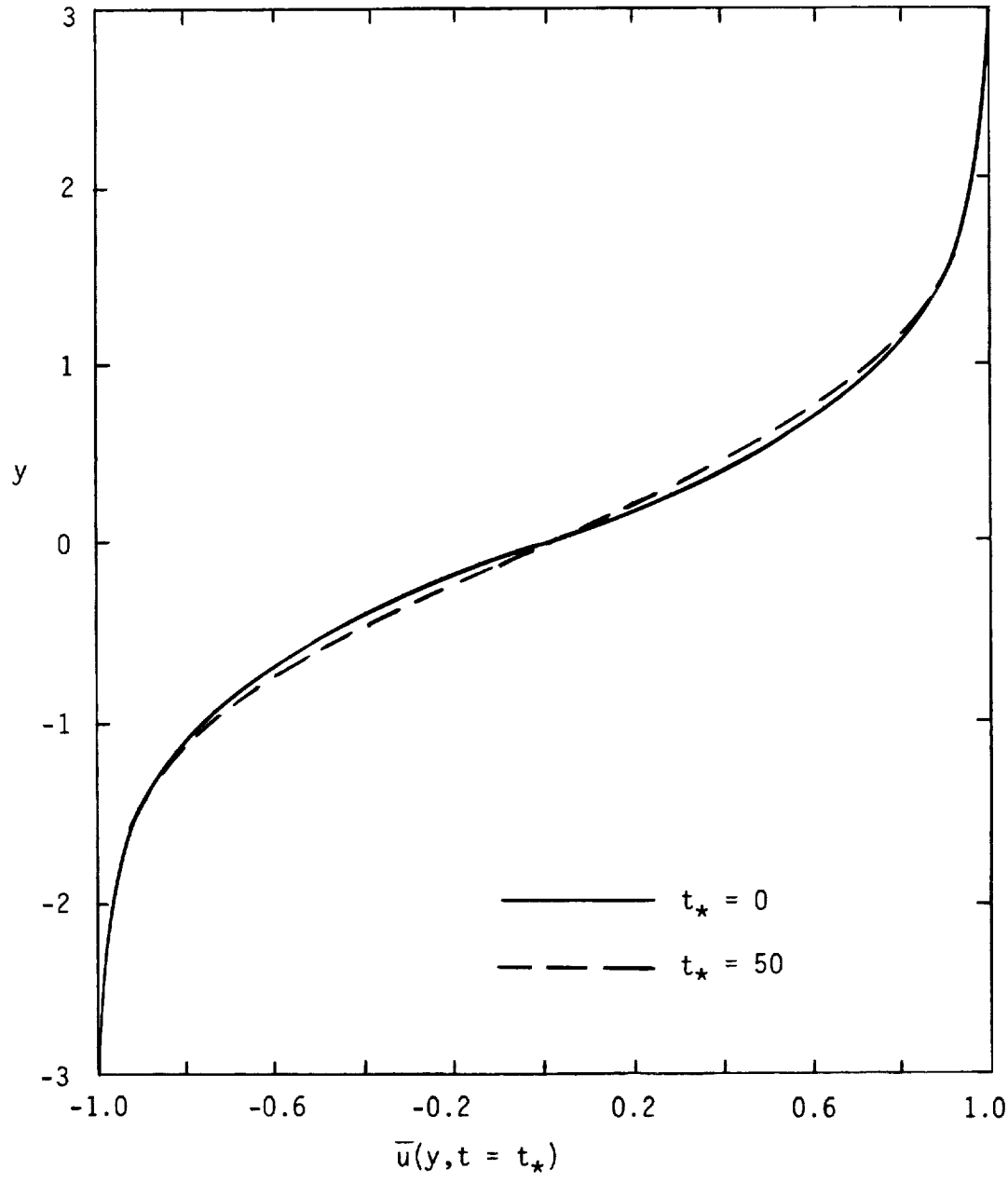

Figure 18. The mean velocity profile $\overline{u}(y,t)$ along the y-axis at two different times. Base flow is $u(y,0) = \tanh y$. $\alpha = 0.8$. Re = 5000. A(0) = 0.005. A(50) = 0.097.

Re = 5000) the linear growth rate and the first Landau constant are 0.107 and -11.2, respectively. Although the overall pattern of the mean flow is not drastically changed, the gradient ($\partial\bar{u}/\partial y$) is seen to be sufficiently modified in the vicinity of the center of the shear layer. As time goes on, the mean velocity increases below y = 0, decreases above y = 0, and remains the same at y = 0. For example, the mean velocities $\bar{u}(y = -0.6, t = t_*)$ at $t_* = 0$, 30 and 50 are -0.537, -0.523 and -0.515, respectively. It may be noted that the mean flow remains nearly the same far above and below the critical point (say, for $|y| > 1.5$), and that the mean flow near the middle of the shear layer keeps changing until a new steady flow is established. In this case, an equilibrium state is reached when the nondimensional time $t \approx 70$ and the amplitude, then, is $A_e = 0.098$.

In summary, the results of this section are: (1) the first Landau constant is negative indicating that nonlinearities are stabilizing so that the exponential growth rate of the fundamental disturbance will be reduced in time until a steady state is established; (2) the dominant contribution to the first Landau constant comes from mean flow distortion and not from the interaction between the fundamental and the second harmonic; (3) the mean flow distortion is very stabilizing because the disturbance is continually being convected into flow regions with smaller maximum vorticity; and (4) in a relative sense, nonlinear effects are most significant for very slightly amplified waves because of the competition between a linear inviscid "growth critical layer" (which dominates for amplified waves) and a linear viscous critical layer (which dominates in the vicinity of the neutral point at high Reynolds numbers).

5.2 The Second Landau Constant

Linear theory is ordinarily concerned only with very small-amplitude disturbances, so nonlinear effects in this case are typically of minor significance. The weakly nonlinear

theory, however, is concerned with the way cumulative nonlinear effects modify the instability of the flow. In an unstable flow, with increasing time, higher harmonics develop, the mean flow continues to change, and the fundamental disturbance keeps adjusting its shape and growth rate. The precise way in which this happens depends on the level of viscosity, and the amplitude and length scale of the disturbance. While the first Landau constant modifies the growth rate of the nonlinear disturbance at $O(A^2)$, the second Landau constant (a_2) modifies the growth at $O(A^4)$. We may think of $(A^{-1}\, dA/dt)$ as the instantaneous growth rate which obeys

$$\frac{1}{A}\frac{dA}{dt} = a_0 + a_1 A^2 + a_2 A^4 + \cdots \qquad (5.2\text{-}1)$$

In other words, the second Landau constant gives a further correction to the amplitude equation due to nonlinear effects. The first Landau constant provides a measure of the deviation from linear growth rate due to: (1) the interaction between the fundamental and the second harmonic; and (2) the interaction between the fundamental and the zeroth harmonic or the mean flow. The second Landau constant provides a measure of the further correction to the growth rate due to: (1) the interaction between the second harmonic and the third harmonic; (2) the interaction between the second harmonic and the reproduction (at order A^3) of the fundamental; (3) the interaction between the fundamental and the square (at order A^4) of the second harmonic; (4) the interaction between the fundamental and the mean flow distortion (at order A^4); and (5) the interaction between the primary mean flow distortion and the reproduced (at order A^3) fundamental.

The second Landau constant is calculated for neutral and near-neutral waves with and without the mean flow distortion. In simple terms, the absence of the mean flow

distortion means that the zeroth harmonic (n = 0) is set to zero artificially so that the mean flow remains the same in the course of time.

The behavior of a_2 as a function of wavenumber is shown in Figures 19 and 20. It can be seen that most of the contribution to the second Landau constant arises from mean flow changes and not from harmonic interactions because the values of a_2 with MFD become very large. For neutral and very slightly amplified waves, a_2 is positive, indicating that higher order interactions are destabilizing, but for certain wavenumbers (say, $\alpha \approx 0.87$; with MFD) a_2 is negative. In general, a_2 may be positive or negative depending on the wavenumber, but for neutral and very near neutral waves, a_2 is always positive.

The behavior of a_2 as a function of the Reynolds number at exactly the neutral wavenumber is shown in Figure 21. Without the mean flow distortion, a_2 is found to be equal to approximately 4.13 Re in the limit of large Reynolds numbers (Re > 2000). The mean flow distortion is very destabilizing in the sense that it changes the order of the positive a_2 from Re to Re^2.

The weakly nonlinear theory is an asymptotic theory valid for small amplitudes and its convergence depends on the magnitudes of the Landau constants and on the amplitude A(t) of the fundamental wave. For exactly neutral waves ($a_0 = 0$) and at high Reynolds numbers, the first Landau constant $a_1 \sim Re^{1/3}$ and the second Landau constant $a_2 \sim Re^2$ which means that (since $dA/dt = a_0A + a_1A^3 + a_2A^5 + \cdots$) the weakly nonlinear theory is meaningful provided that

$$Re^{5/3} A^2 << 1 \qquad (5.2\text{-}2)$$

and this implies that the theory breaks down (cannot describe the evolution of finite amplitude disturbances) in the limit as $Re \to \infty$. In this case, the critical layer is dominated by nonlinearities and a nonlinear critical layer theory is needed (Goldstein and Leib, 1988).

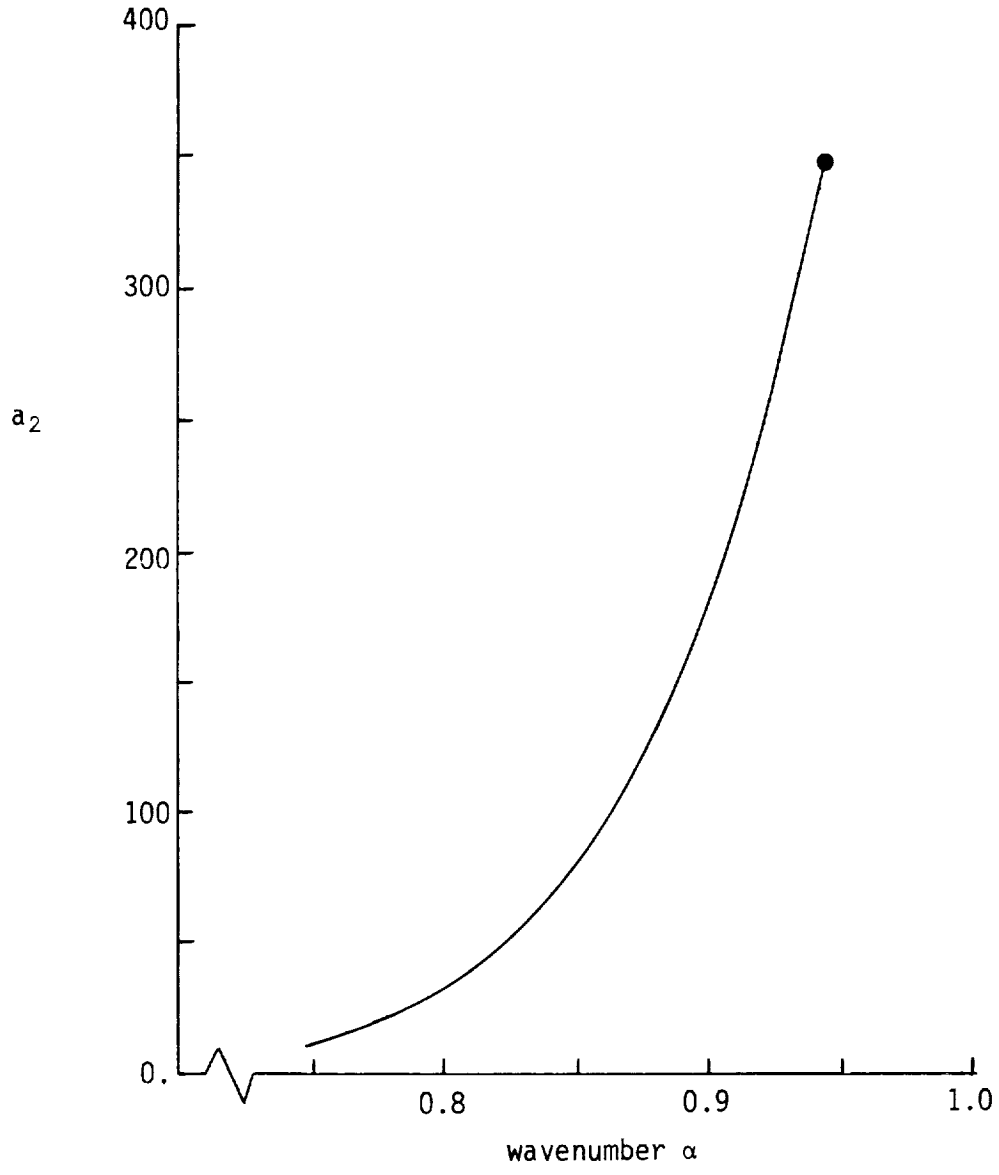

Figure 19. Second Landau constant as a function of wavenumber. (● indicates neutral wave.) No mean flow distortion. U(y) = 0.5 (1 + tanhy). Re = 200.

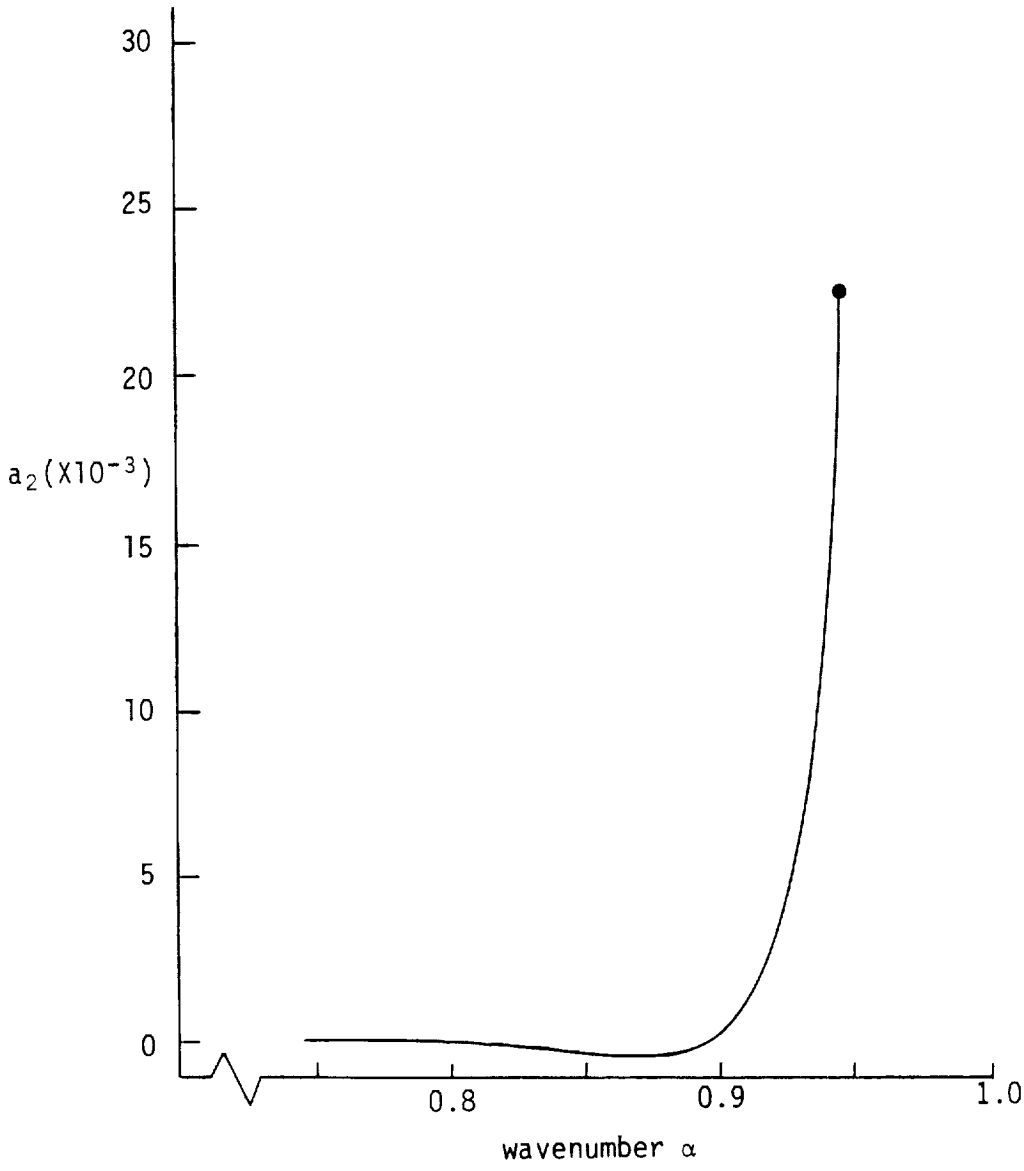

Figure 20. Second Landau constant as a function of wavenumber. (● indicates neutral point.) With mean flow distortion. U(y) = 0.5 (1 + tanhy). Re = 200.

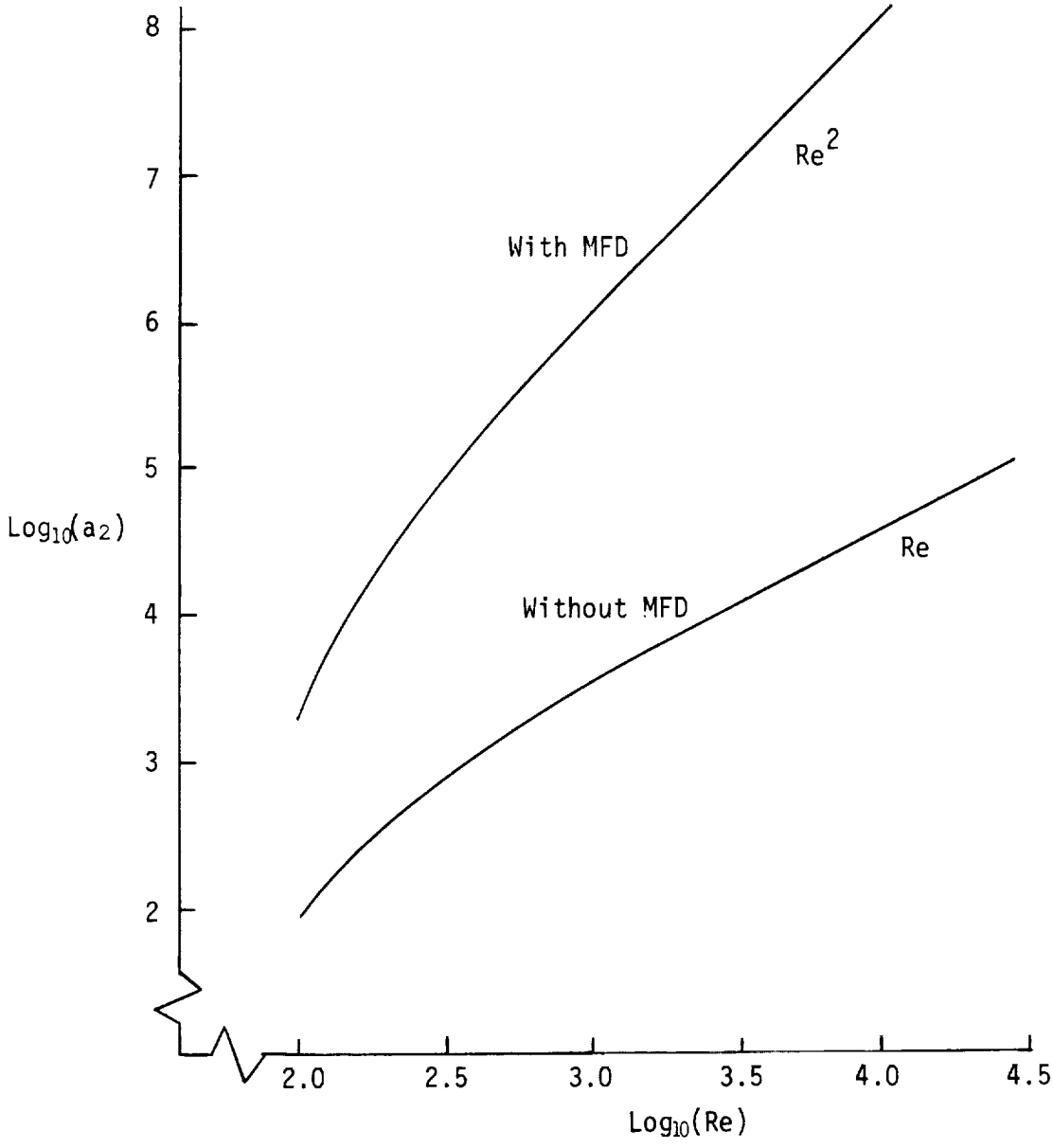

Figure 21. Second Landau constant as a function of Reynolds number for neutral waves with and without mean flow distortion (MFD). (Log-Log scale.) U(y) = 0.5 (1 + tanhy).

The modified mean velocity profile $\bar{u}(y,t)$ is composed of the initial mean velocity U(y) and mean flow corrections arising from nonlinearities and, in the spirit of the weakly nonlinear theory, is given by

$$\bar{u}(y,t) = U(y) + A^2(t)\,\phi_{01}'(y) + A^4(t)\,\phi_{02}'(y) + \cdots \qquad (5.2\text{-}3)$$

The physics embedded in this equation is the following. A linear (very small amplitude) disturbance does not alter the mean flow until it has grown to an appreciable size. Then, while the primary Reynolds stress tends to diffuse the flow because ϕ_{01}' is positive below y = 0 and negative above y = 0, higher order interactions tend to steepen the flow since ϕ_{02}' is negative just below y = 0 and positive just above y = 0. This is why the mean flow distortion is stabilizing at $O(A^2)$ and destabilizing at $O(A^4)$. The fact that very significant changes in the mean flow take place in the course of time render the weakly nonlinear theory invalid in describing the evolution of finite amplitude disturbances at large Reynolds numbers. Essentially, the amplitude is constructed by inequality (5.2-3). Figure 22 shows the mode shapes $\phi_{01}'(y)$ and $\phi_{02}'(y)$ as functions of y (the prime denotes d/dy) and it can be seen that nonlinearities distort the mean flow near the critical point (y = 0) but do not significantly broaden the mixing layer (in time). Note that the higher order distortions are concentrated closer and closer to the critical layer.

The frequency of the disturbance at finite amplitudes is governed by (see Eq. 2.1-11)

$$\frac{d\gamma(t)}{dt} = \omega_0 + \omega_1\,A^2(t) + \omega_2\,A^4(t) + \cdots \qquad (5.2\text{-}4)$$

This means that, in general, nonlinear finite amplitude interactions modify the frequency of the nonlinear disturbance in the course of time. But the calculated complex Landau

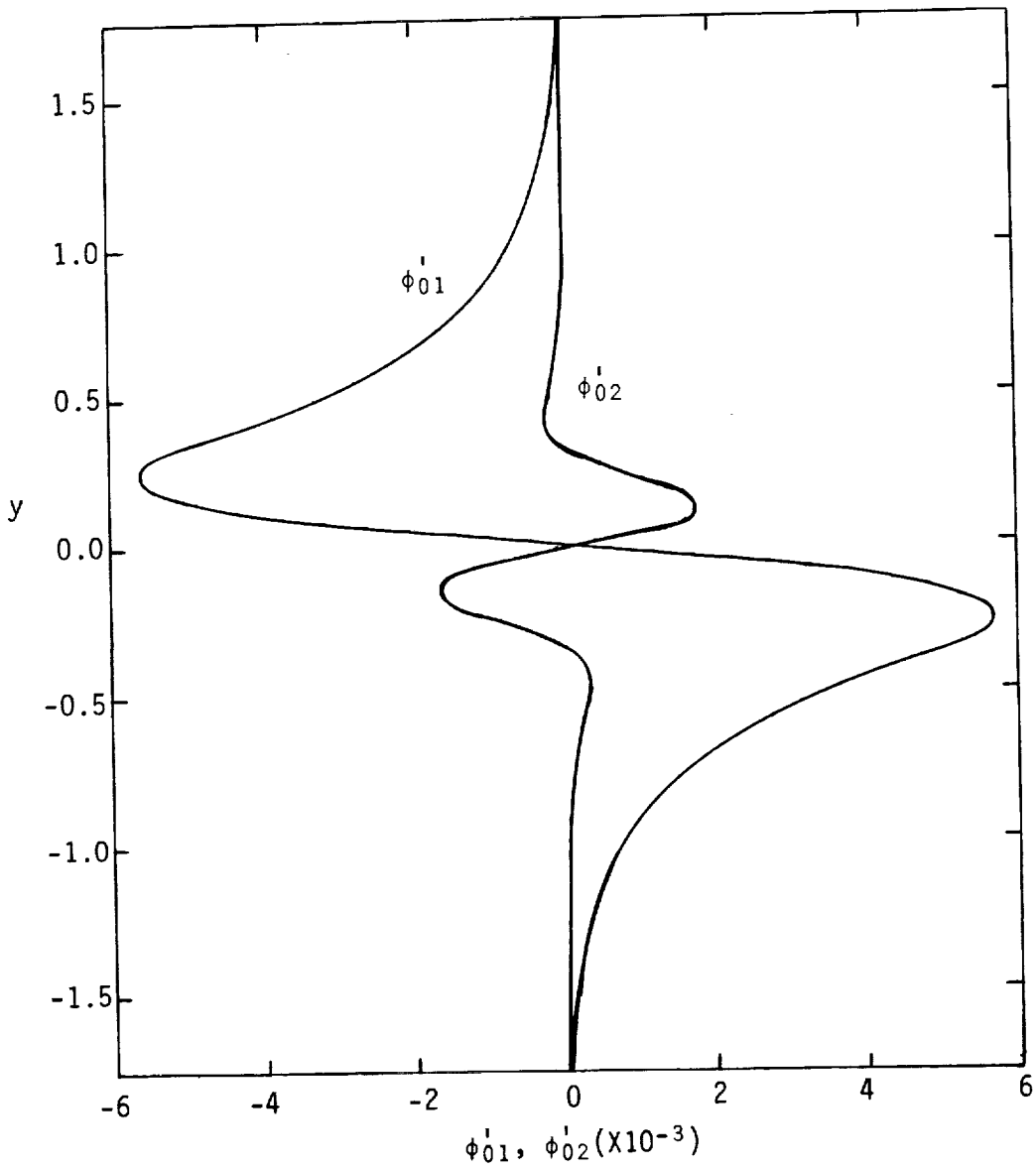

Figure 22. Mode shapes $\phi'_{01}(y)$ and $\phi'_{02}(y)$ as functions of y. Base flow is U(y) = tanhy. α = 0.8. Re = 1000. (a_0, a_2, a_2) = (0.105, -9.26, 568).

constants ($\lambda_n = a_n - i\omega_n$, n = 1,2) are found to be real which shows that nonlinearities do not modify the frequency when the hyperbolic-tangent family of mean velocity profiles is employed. This is due to the mean vorticity symmetry about y = 0; it is clearly a special case. It is well known that the frequency of a nonlinear oscillator depends on its amplitude.

In summary, the results of this section are: (1) the second Landau constant may be positive or negative depending on the wavenumber α, but for exactly neutral or very slightly amplified waves it is positive, which means that higher order nonlinear interactions are destabilizing; (2) the mean flow distortion generated by nonlinear interactions at order A^4 tends to increase the maximum vorticity in the mixing layer by increasing the mean velocity gradient near the middle of the layer in the course of time and, therefore, is destabilizing; (3) most of the contribution to the second Landau constant arises from mean flow changes and not from the interaction of higher harmonics. Nonlinearities distort the mean flow near the middle of the shear layer (note that the critical and inflection points coincide and they both are at y = 0); and (4) the weakly nonlinear theory breaks down in describing the evolution of finite amplitude waves at large Reynolds numbers.

5.3 Numerical Versus Weakly Nonlinear Solutions

In comparing the solutions obtained from the numerical calculations with those from the weakly nonlinear stability theory, only the fundamental, the second harmonic, and the mean flow correction are retained in both. However, the results are, by no means, identical because the numerical solution treats the critical layer differently from the weakly nonlinear theory. In the former, the critical layer is fully viscous and nonlinear (within the assumptions of the truncation after the second harmonic). While in the weakly nonlinear theory, the effects of nonlinearities enter in a hierarchical manner the critical layer is a

viscous one. Note that the $O(A^3)$ correction to the shape of the fundamental in the weakly nonlinear theory is also retained here because this change is accounted for in the numerical solution. Furthermore, the comparison is made for the hyperbolic-tangent family of mean velocity profiles for which the phase velocity of the disturbance and the imaginary part of the first Landau constant are zero.

5.3.1 The Numerical Solution

The details of the analysis are given in Section 2.3. The perturbation streamfunction, axial velocity ($u = \partial\psi/\partial y$), transverse veloctiy ($v = -\partial\psi/\partial x$), and vorticity are, respectively,

$$\psi(x,y,t) = \phi_0(y,t) + \left[\phi_1(y,t)\, e^{i\alpha x} + \phi_2(y,t)\, e^{2i\alpha x} + cc\right] \tag{5.3-1}$$

$$u(x,y,t) = \phi_{0y}(y,t) + \left[\phi_{1y}(y,t)\, e^{i\alpha x} + \phi_{2y}(y,t)\, e^{2i\alpha x} + cc\right] \tag{5.3-2}$$

$$v(x,y,t) = -\left[i\alpha\phi_1(y,t)\, e^{i\alpha x} + 2i\alpha\phi_2(y,t)\, e^{2i\alpha x} + cc\right] \tag{5.3-3}$$

$$\Omega(x,y,t) = \omega_0(y,t) + \left[\omega_1(y,t)\, e^{i\alpha x} + \omega_2(y,t)\, e^{2i\alpha x} + cc\right] \tag{5.3-4}$$

where cc stands for the complex conjugate of the preceding terms in an equation. The system of nonlinear partial differential equations satisfied by ϕ_0, ϕ_1 and ϕ_2 is given by (2.3-2) to (2.3-4). Clearly, ϕ_0, ϕ_1, ϕ_2 are the first three Fourier coerficients in the expansion of the perturbation streamfunction.

The initial given parallel mean velocity profile U(y) is modified by nonlinearities so that the instantaneous mean velocity profile (averaged over a wavelength) is given by

$$\bar{u}(y,t) = U(y) + \phi_{0y}(y,t) \tag{5.3-5}$$

The amplitude of the fundamental is defined by

$$A(t) = |\phi_1(0,t)| \tag{5.3-6}$$

so that it is essentially the magnitude of the fundamental component of the transverse velocity divided by the wavenumber at y = 0.

5.3.2 The Weakly Nonlinear Solution

The corresponding physical quantities obtained from the weakly nonlinear theory are given in Section 2.2. We write

$$\psi(x,y,t) = A^2(t)\,\phi_{01}(y) + \{[A(t)\,\phi_{10}(y) + A^3(t)\,\phi_{11}(y)]\,e^{i\alpha x} + A^2(t)\,\phi_{20}(y)\,e^{2i\alpha x} + cc\} \tag{5.3-7}$$

$$u(x,y,t) = A^2(t)\,\phi'_{01}(y) + \{[A(t)\,\phi'_{10}(y) + A^3(t)\,\phi'_{11}(y)]\,e^{i\alpha x} + A^2(t)\,\phi'_{20}(y)\,e^{2i\alpha x} + cc\} \tag{5.3-8}$$

$$v(x,y,t) = -\{i\alpha[A(t)\,\phi_{10}(y) + A^3(t)\,\phi_{11}(y)]\,e^{i\alpha x} + 2i\alpha\,A^2(t)\,\phi_{20}(y)\,e^{2i\alpha x} + cc\} \tag{5.3-9}$$

$$\Omega(x,y,t) = -A^2(t)\,\phi''_{01}(y) - \{A(t)\,[\phi''_{10}(y) - \alpha^2\,\phi_{10}(y)]\,e^{i\alpha x} + A^3(t)\,[\phi''_{11}(y) - \alpha^2\,\phi_{11}(y)]\,e^{i\alpha x} + A^2(t)\,[\phi''_{20}(y) - 4\alpha^2\,\phi_{20}(y)]\,e^{2i\alpha x} + cc\} \tag{5.3-10}$$

and

$$\bar{u}(y,t) = U(y) + A^2(t)\,\phi'_{01}(y) + \cdots \tag{5.3-11}$$

The solution of the amplitude equation (5.2-1) to $O(A^3)$ is

$$A^2(t) = \frac{A^2(0)\, e^{2a_0 t}}{1 + \frac{a_1}{a_0} A^2(0)\,(1-e^{2a_0 t})} \tag{5.3-12}$$

The mean value of the vorticity is

$$\bar{\Omega}(x,y,t) = -U'(y) + \Omega(x,y,t) \tag{5.3-13}$$

Our principal objective now is to obtain the time evolution of the flow field by solving the previous equations (i.e., the numerical approach and the weakly nonlinear theory) and comparing these results to gain additional insights into the saturation of the fundamental and into the behavior of the weakly nonlinear theory. In order to do this, the governing equations are solved at given values of wavenumber, Reynolds number and initial amplitude A(0). The results are presented in the following two forms:

1. x is specified ($0 \le x \le 2\pi/\alpha$).

   y is specified.

   A, u, v and $\bar{u}$ are plotted as functions of time.

2. t is specified.

   Lines of constant total vorticity ($\bar{\Omega}(x,y,t)$ = constant) are plotted in the x-y plane for $0 \le x \le 4\pi/\alpha$ and $-1.6 \le y \le 1.6$.

5.4 Saturation and Vorticity Roll-Up

There are many general features of the weakly nonlinear theory and the numerical solutions. First, both show the validity of linear theory for short initial times at small amplitudes. Initially, the fundamental wave grows according to linear theory until near-

neutral nonlinearity sets in relatively slowly for near-neutral waves and more rapidly for very amplified waves. Second, while the weakly nonlinear solution always yields a steady saturated state, the numerical solution may evolve into a quasi-steady (oscillatory) state depending on the amplitude of the initial disturbance, Reynolds number and wavenumber. For example, at large initial amplitudes, the flow will evolve into an oscillatory state characterized by an alternating energy exchange between the mean flow and the perturbation field. The mean velocity gradient is reduced while the disturbance is growing and is increased during the decay. The peak saturation amplitude is nearly independent of the initial excitation amplitude. Third, both solutions show that most of the contribution to the nonlinear behavior arises from changes in the mean flow and not from higher harmonics although the second harmonic is moderately important. Finally, the agreement between the two calculations is better at low and moderate Reynolds numbers. The disagreement, which occurs at either large Reynolds numbers or at large amplitudes, seems to have its origin in the fact that the weakly nonlinear theory, which is based on a viscous critical layer, predicts too much change in the mean flow. At low Reynolds numbers, the agreement is excellent except for very amplified waves. At large Reynolds numbers, the agreement is good except for very nearly neutral and very amplified waves.

The amplitude of the fundamental disturbance as a function of time for two unstable waves of different wavenumbers in a tanh shear layer is shown in Figures 23, 24 and 25. The Reynolds numbers in these figures are 500, 2000 and 5000 respectively, and the initial amplitude is 0.005. For nondimensional times up to 10 to 20, depending on the wave and Reynolds numbers, the exponential growth of the disturbance is predicted very well by linear stability theory (dashed line). At these times, the amplitude is about 0.06 for the more unstable disturbance (α = 0.7; Re = 500 and 2000) and is about 0.01 for the

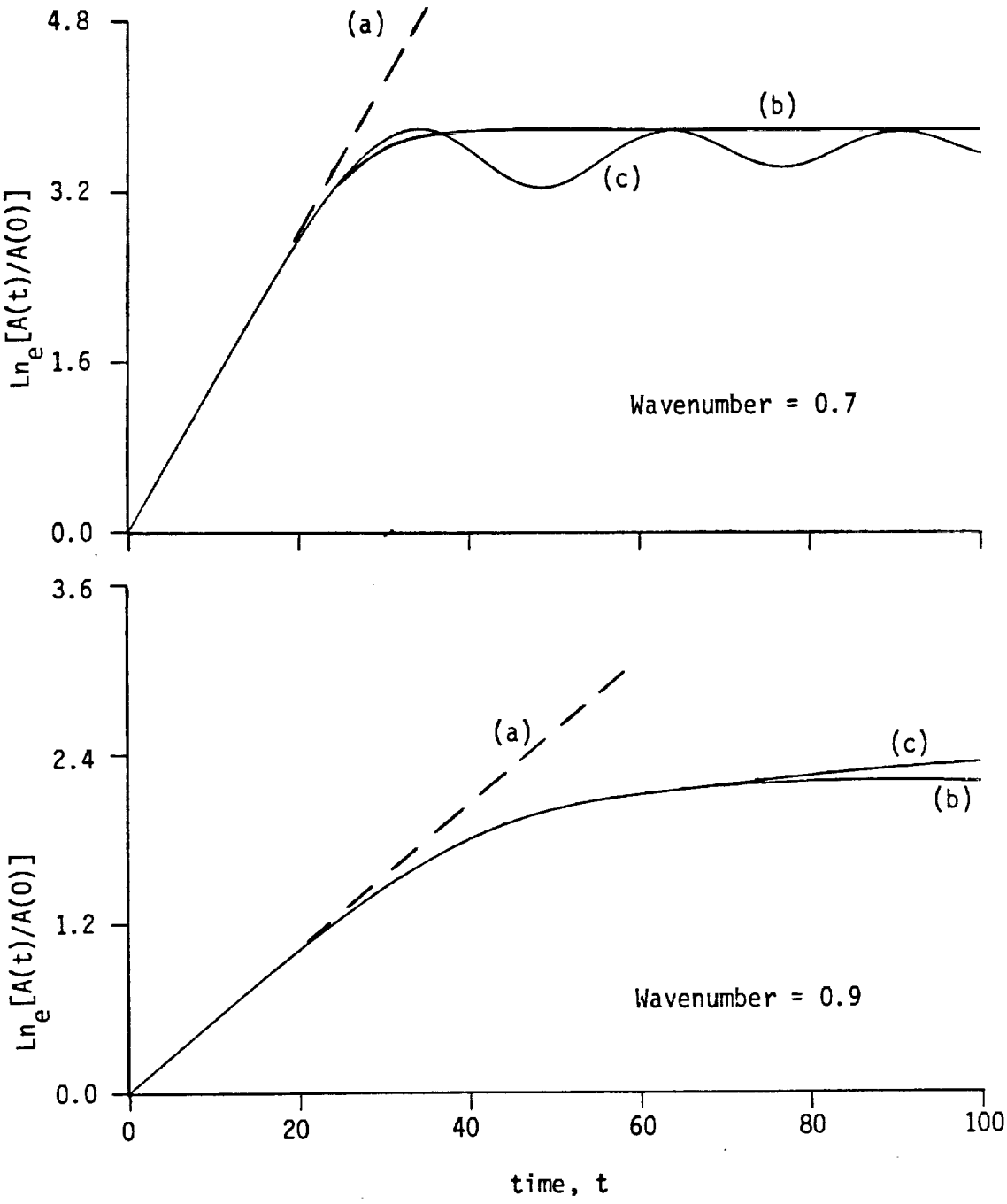

Figure 23. Amplitude of the fundamental as a function of time. (a) Linear theory, (b) weakly nonlinear theory, and (c) numerical calculations. U(y) = tanhy. Re = 500. A(0) = 0.005.

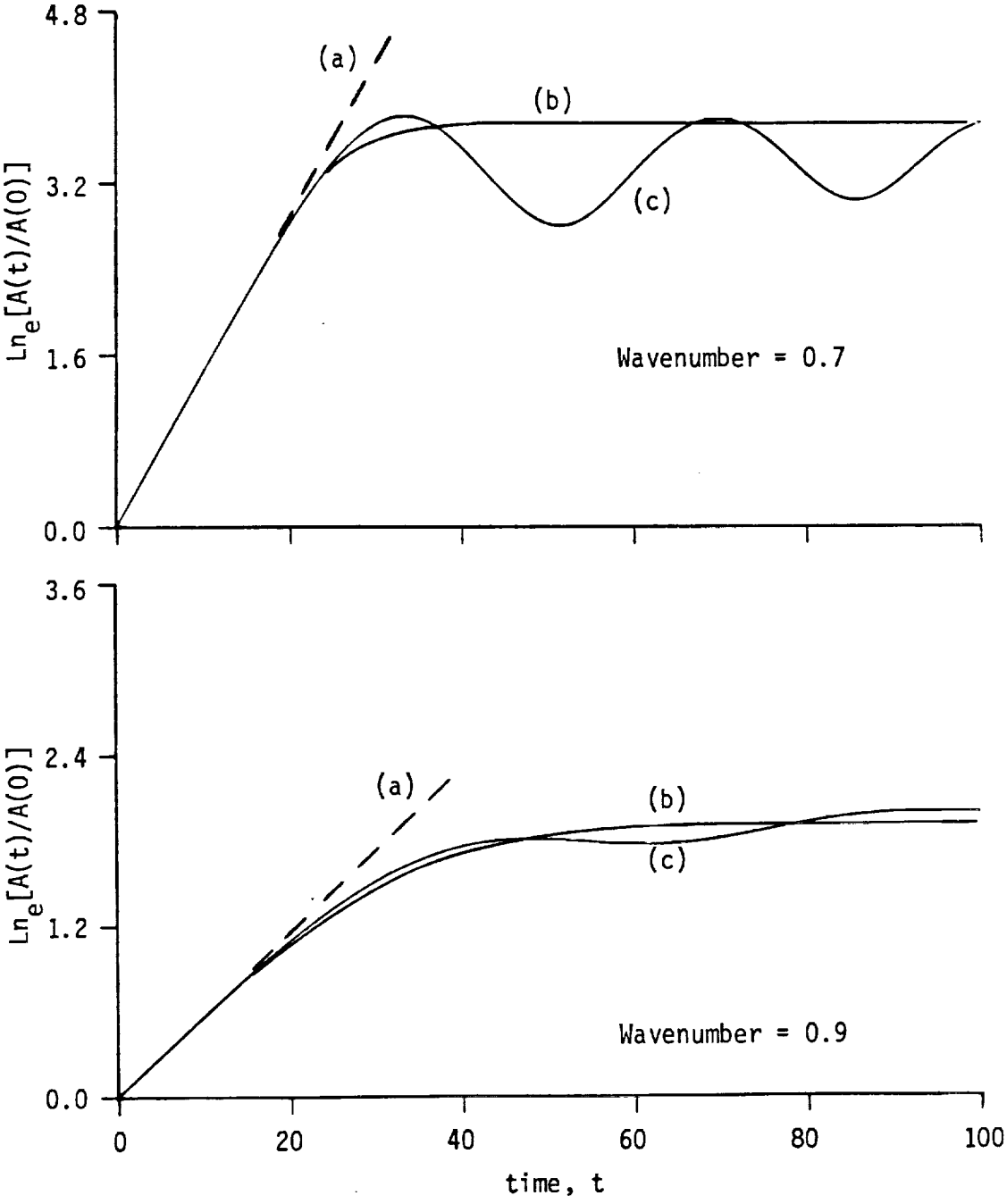

Figure 24. Amplitude of the fundamental as a function of time. (a) Linear theory, (b) weakly nonlinear theory, and (c) numerical calculations. U(y) = tanhy. Re = 2000. A(0) = 0.005.

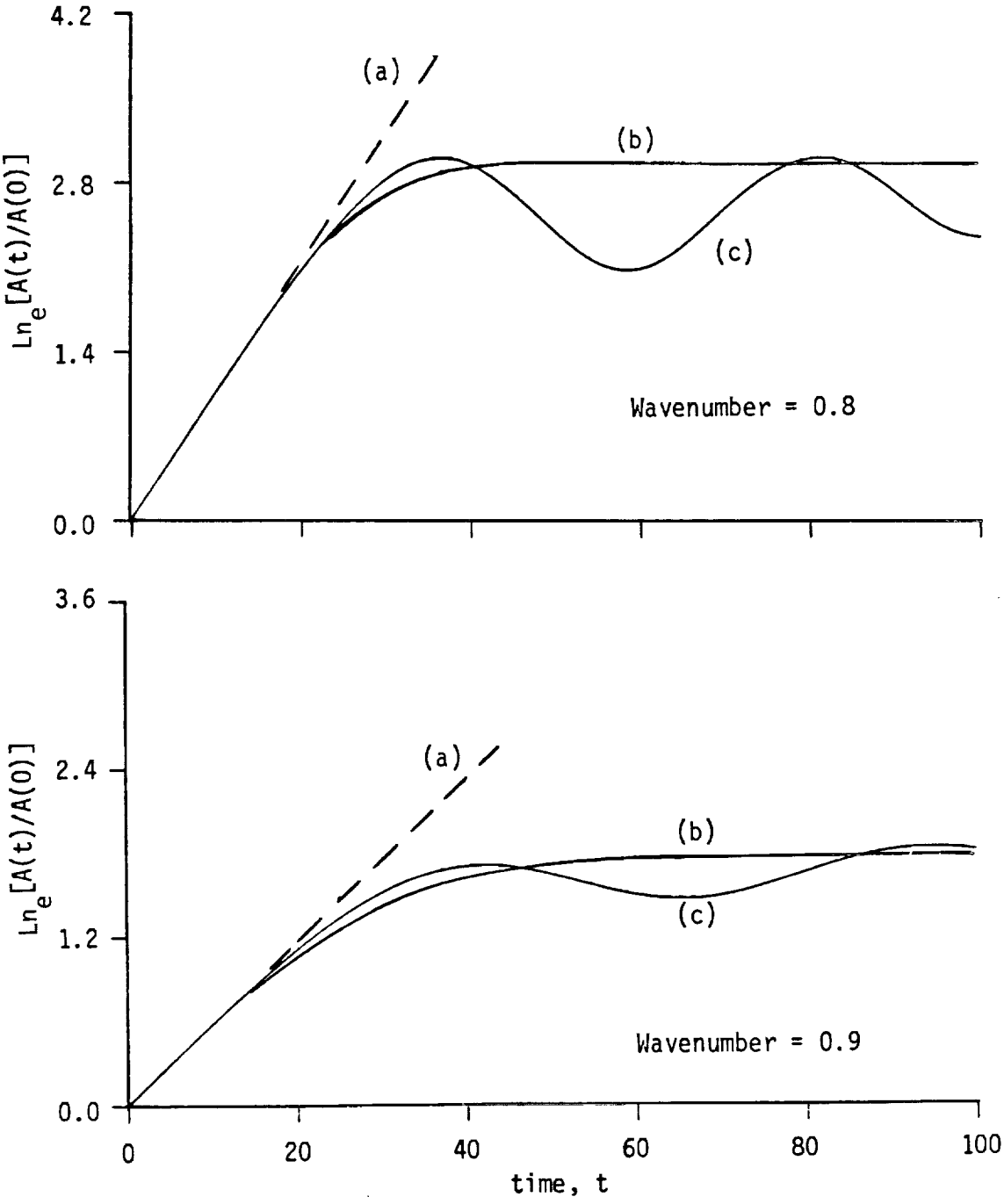

Figure 25. Amplitude of the fundamental as a function of time. (a) Linear theory, (b) weakly nonlinear theory, and (c) numerical calculations. U(y) = tanhy. Re = 5000. A(0) = 0.005.

near-neutral disturbance (α = 0.9). For larger values of time, nonlinear effects set in very quickly at large amplitudes and more slowly at small amplitudes. The saturation amplitude predicted by the weakly nonlinear theory is slightly higher than the average of the oscillations predicted by the numerical simulation. The physical interpretation of these oscillations is given by Browand and Ho (1983). It should be noted that the weakly nonlinear theory cannot predict the oscillatory energy exchange between the modes and the mean flow because the Landau constants are time-independent [see (5.3-12)]. The agreement between the numerical and the weakly nonlinear solutions gets better as the neutral wavenumber is approached, as expected from theoretical considerations (Stuart, 1960). It may be noted that the agreement between the two solutions is also better at low and moderate Reynolds numbers.

In Figure 26, the amplitude as a function of time is shown for four unstable waves (α = 0.70, 0.90, 0.95 and 0.98; the neutral wave is α_n = 0.999). The initial amplitude is 0.002 and the Reynolds number is 5000. There are many conclusions which can be drawn from this figure. First, both the numerical and the weakly nonlinear solutions show the validity of linear theory for short initial times (say, up to $t \approx 20$). Second, the agreement between the two solutions improves as the neutral point is approached (note that the amplitude of the oscillations of the numerical solution diminishes as the neutral wavenumber is approached). Third, for moderately amplified waves (α = 0.7, say) the amplitude oscillations of the numerical solution are large (say, the amplitude varies between $A \approx 0.06$ and $A \approx 0.20$). The temporal calculations of Miura and Sato (1978) show the same trend. Physically the amplitude oscillation is due to the temporal variations of the mean velocity profile (the mean velocity gradient at y = 0 is reduced during the period in which the amplitude is growing, while it steepens during the other half of the cycle).

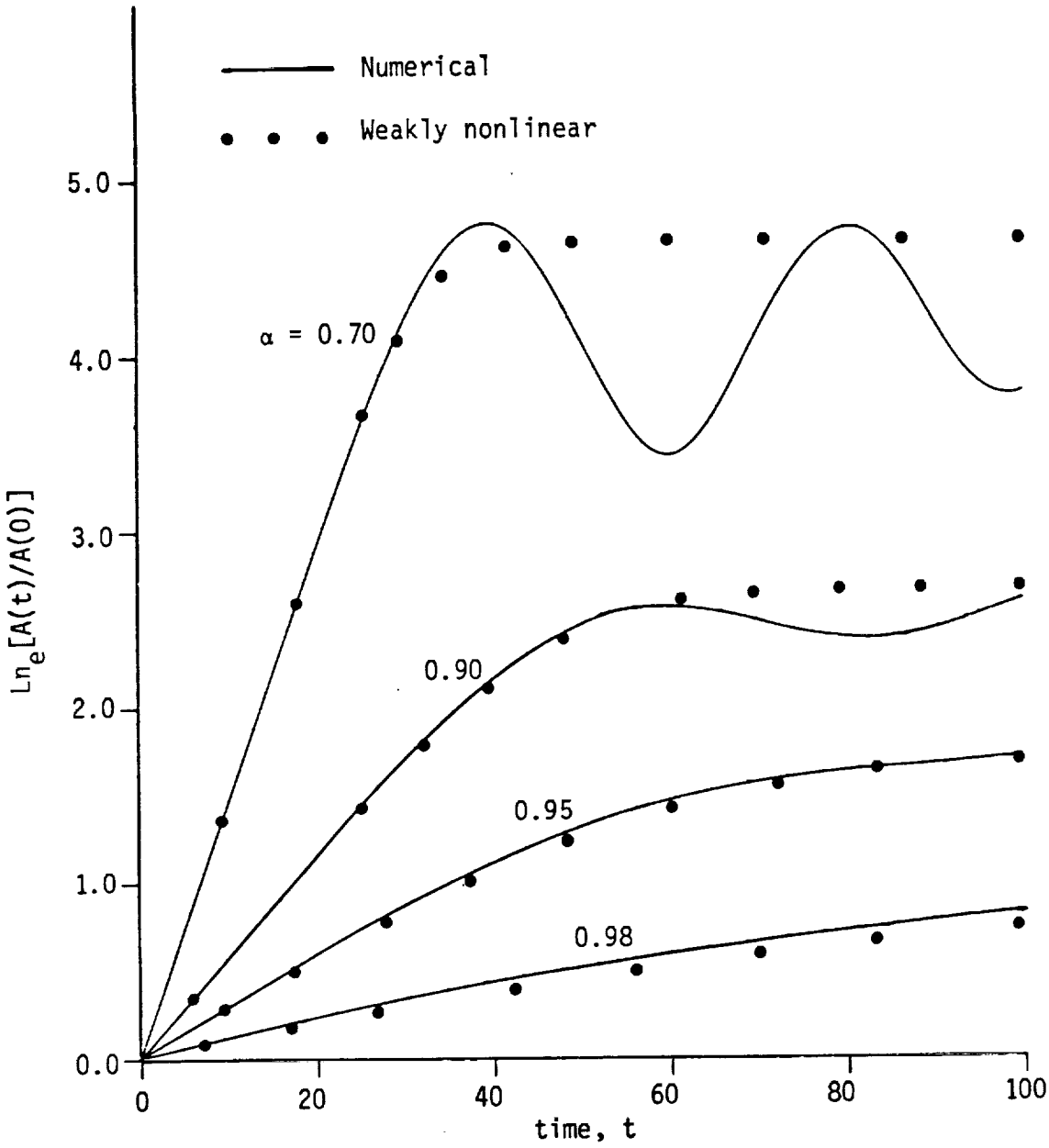

Figure 26. Amplitude of the fundamental as a function of time for four unstable waves. U(y) = tanhy. Re = 5000. A(0) = 0.002.

Finally, at very nearly neutral waves (say, $\alpha = 0.98$), the amplitude predicted by the weakly nonlinear theory is slightly lower than that predicted by the numerical calculations.

In Figures 27 and 28, the amplitude A(t), the perturbation axial velocity [$u(x,y,t) = \partial\psi/\partial y$], the perturbation transverse velocity [$v(x,y,t) = -\partial\psi/\partial x$] and the instantaneous mean velocity [$\bar{u}(y,t) = U(y) + A^2(t)\, d\phi_{01}^{(y)}/dy$] in the weakly nonlinear theory and $\bar{u}(y,t) = U(y) + \phi_{0y}(y,t)$ in the numerical solution] are plotted as functions of time for a moderately unstable wave ($\alpha = 0.7$; Figure 27) and for a near-neutral wave ($\alpha = 0.9$; Figure 28) at an arbitrarily but representative point (i.e., x and y are fixed). According to the weakly nonlinear theory, the mean flow decreases to yield saturation and according to the numerical solution, the mean flow initially decreases then oscillates to yield an oscillatory field. The mean flow starts decreasing at a nondimensional time of about 15 when the amplitude is about 0.03. After this time, nonlinearities set in quickly but the mean velocity is reduced much more in the weakly nonlinear calculation. For example, the predicted mean velocities in the numerical and the weakly nonlinear calculations at time equal to 35 [(i.e., $\bar{u}(0.16,35)$] are 0.130 and 0.063 respectively. At this time, the predicted amplitude in both calculations is about 0.20. Although the amplitude A(t) and the perturbation velocities (u and v) agree well with each other (up to t = 35, say) the modified mean flow is different in the two solutions. The weakly nonlinear theory exaggerates the distortion of the mean flow but as the neutral wavenumber is approached, the agreement gets much better. In Figure 28, the same physical quantities at the same transverse location above the center of the shear layer are plotted as functions of time. The wave is nearly neutral with wavenumber of 0.9 and the Reynolds number is 500. The agreement between the two calculations is almost perfect in this case because the amplitude is small, which results in slow changes in the mean velocity and, therefore, the slow setting in of nonlinearities.

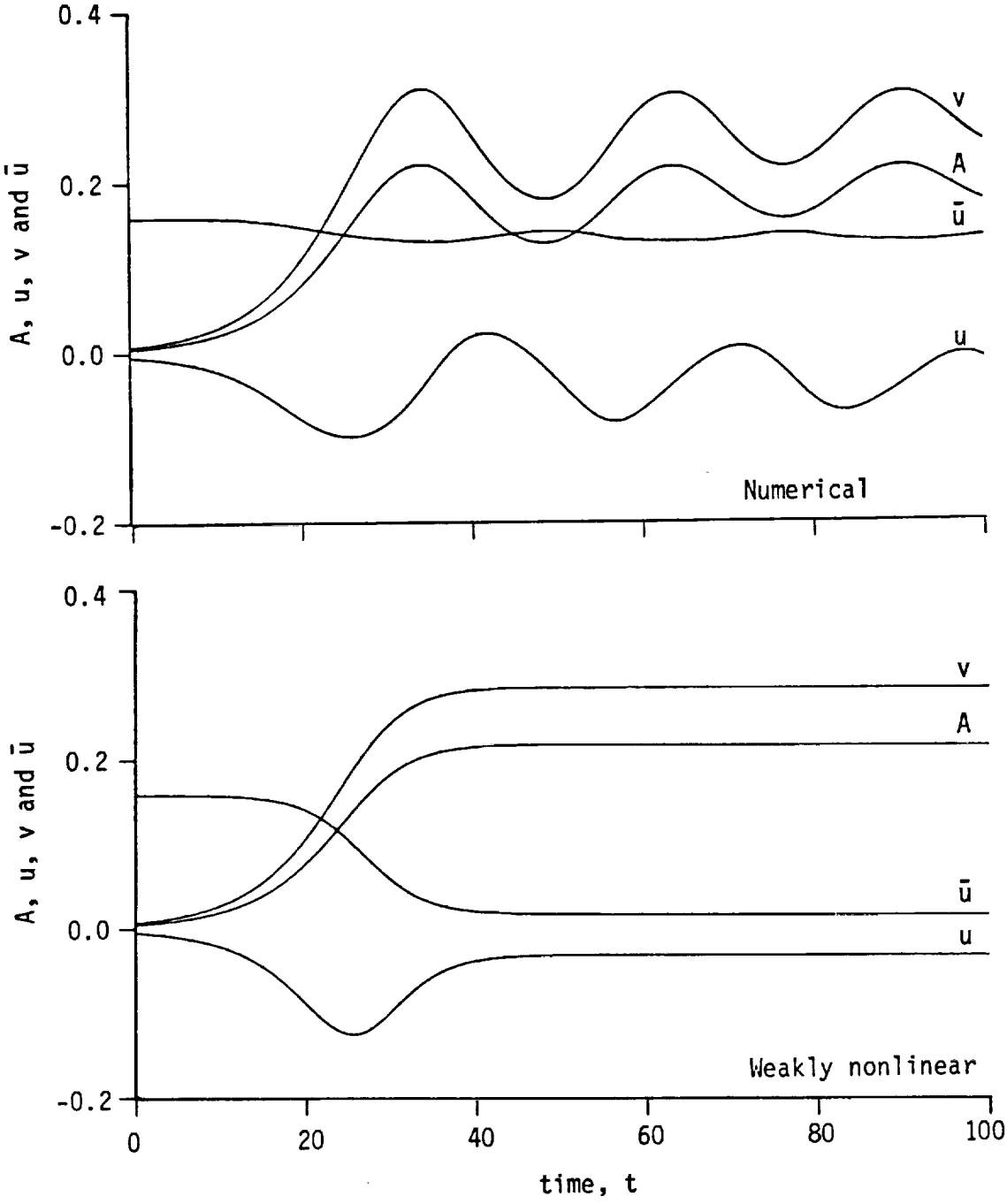

Figure 27. Amplitude, perturbation velocities and modified mean flow as functions of time calculated at $y = 0.16$ and $x = \pi/(2\alpha)$. $U(y) = \tanh y$. $Re = 200$. $\alpha = 0.7$. $A(0) = 0.005$.

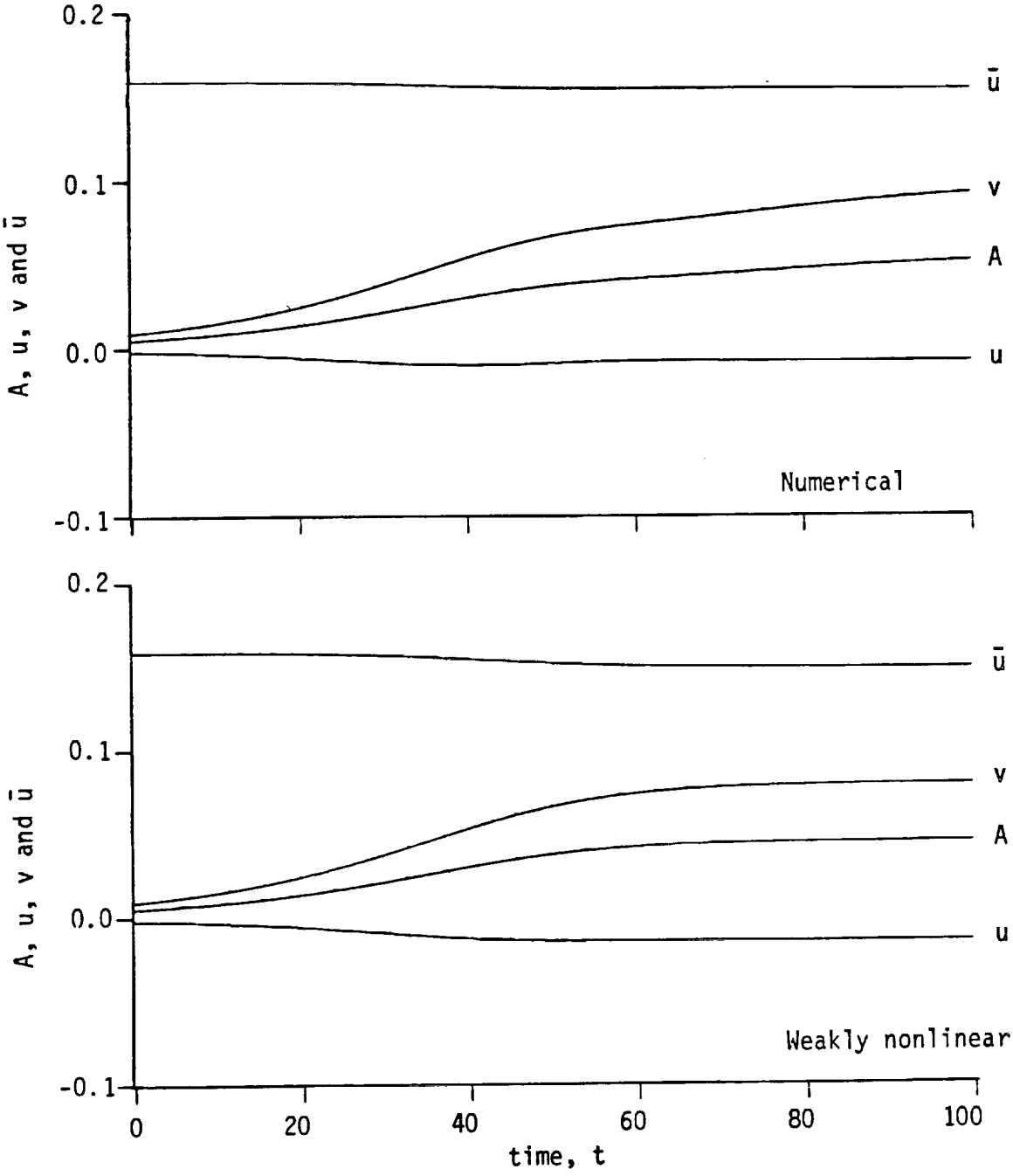

Figure 28. Amplitude, perturbation velocities and modified mean flow as functions of time calculated at $y = 0.16$ and $x = \pi/(2\alpha)$. $U(y) = \tanh y$. $Re = 500$. $\alpha = 0.9$. $A(0) = 0.005$.

Large nonlinearities result in a strong interaction between the mean flow distortion and the fundamental mode. In Figure 29, the amplitude of the fundamental, as a function of time, for nearly the most amplified wave in a tanh shear layer is shown. The Reynolds number is 1000 and the linear growth rate is 0.186. At an initial amplitude of 0.05, the disturbance grows according to linear theory up to a nondimensional time of about 7 and then attains a maximum amplitude of 0.6 (note that the velocity ratio across the shear layer is two) at time equal to 20. After this time, it oscillates about an amplitude of 0.4 with a period equal to about 32. At an initial amplitude of 0.01, the behavior is very similar except that the action of nonlinearities is delayed. The lack of dependence of the peak saturation amplitude on the initial excitation amplitude has also been observed experimentally by Freymuth (1966). The numerical temporal calculations of Metcalfe and co-workers (1987) show the same trend. In addition, the average value of the oscillations is also insensitive to the initial amplitude; the oscillatory solution represents the locking onto a nonlinear limit cycle.

Shear flows characterized by inflectional profiles are highly unstable so that small perturbations grow exponentially to large fluctuations in relatively short times (in this work, the flow is assumed to be spatially periodic and evolves in time). The primary instability of free shear flows is the Kelvin-Helmholtz instability mechanism (discussed in Batchelor, 1967, p. 516; Drazin and Reid, 1981) which applies, in general, to inviscid flows possessing a vorticity minimum. Through this mechanism, beyond the region of exponential growth, instability waves evolve into a periodic array of concentrated spanwise vortices connected by thin vorticity layers or braids. This pattern of vorticity is known as "Kelvin cat's eyes". Basically, the roll-up of the shear layer is due to the accumulation of vorticity at certain spatial regions.

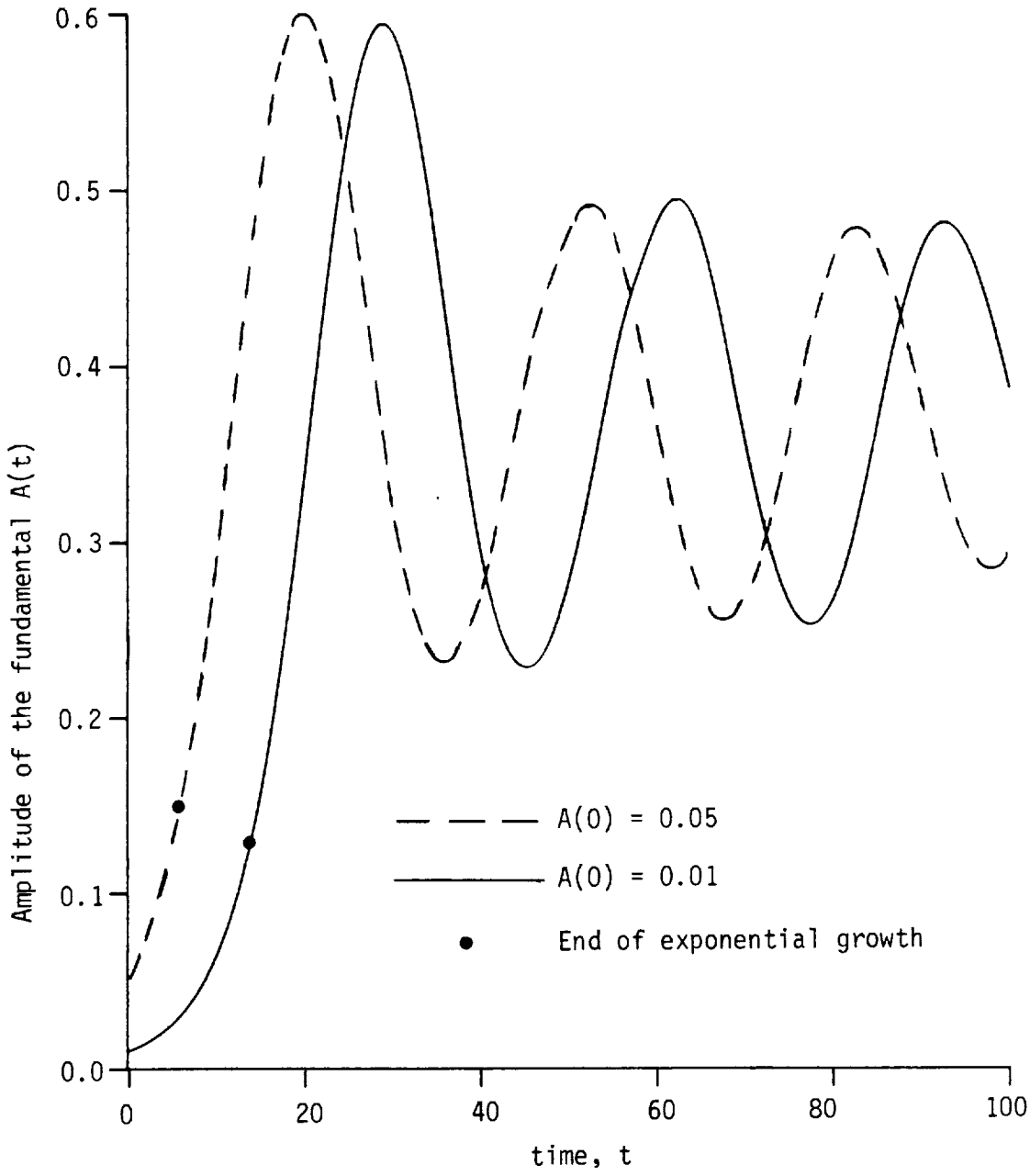

Figure 29. Amplitude of the fundamental as a function of time for two initial amplitudes. U(y) = tanhy. Re = 1000. α = 0.5. The linear growth rate is 0.186.

In Figure 30, the contours of constant total vorticity, as calculated from the weakly nonlinear theory, are shown for two different times. The evolving disturbance has a wavenumber equal to 0.6 and is superimposed on the mean velocity U(y) = 0.5 tanhy. The Reynolds number is 500 and the initial amplitude is 0.01. The linear growth rate for this wave is 0.082 and the maximum amplitudes obtained from the weakly nonlinear theory and the numerical simulation are 0.182 and 0.188 respectively. In the upper picture, we see the oscillatory pattern in the vortex contours, as expected from linear stability theory. Note that the contours are increasingly distorted as the "critical" layer at y = 0 is approached. This remark suggests that the most significant perturbations occur near the "critical" layer even when the instability wave is quite unstable. Because of viscosity, the vorticity contours can actually close on themselves and form small islands. In the bottom picture, we show how the contours begin to roll-up. Near the critical layer, these contours "overturn" and start to form the cat's eyes (which are nicely shown in Figure 31). The weakly nonlinear theory becomes quite inaccurate for the vorticity (which is the second derivative of streamfunction) at times larger than about 25. Clearly, however, the weakly nonlinear theory can describe the initial stages of the nonlinear roll-up of vorticity. In Figure 31, the vorticity contours from the numerical calculations are shown for large times. For small times, the contours are very similar to those of the weakly nonlinear theory shown in Figure 30. As time is increased, the roll-up process continues in an orderly manner. At time equal to 30, the amplitude and the minimum vorticity are 0.102 and -0.59 respectively, while they are 0.187 and -0.65 at time equal to 50. It is obvious that the roll-up of vorticity is a typical nonlinear effect.

The numerically calculated vorticity contours are similar to those obtained by Corcos and Sherman (1984) and by Metcalfe and co-workers (1987). It is worth noting that

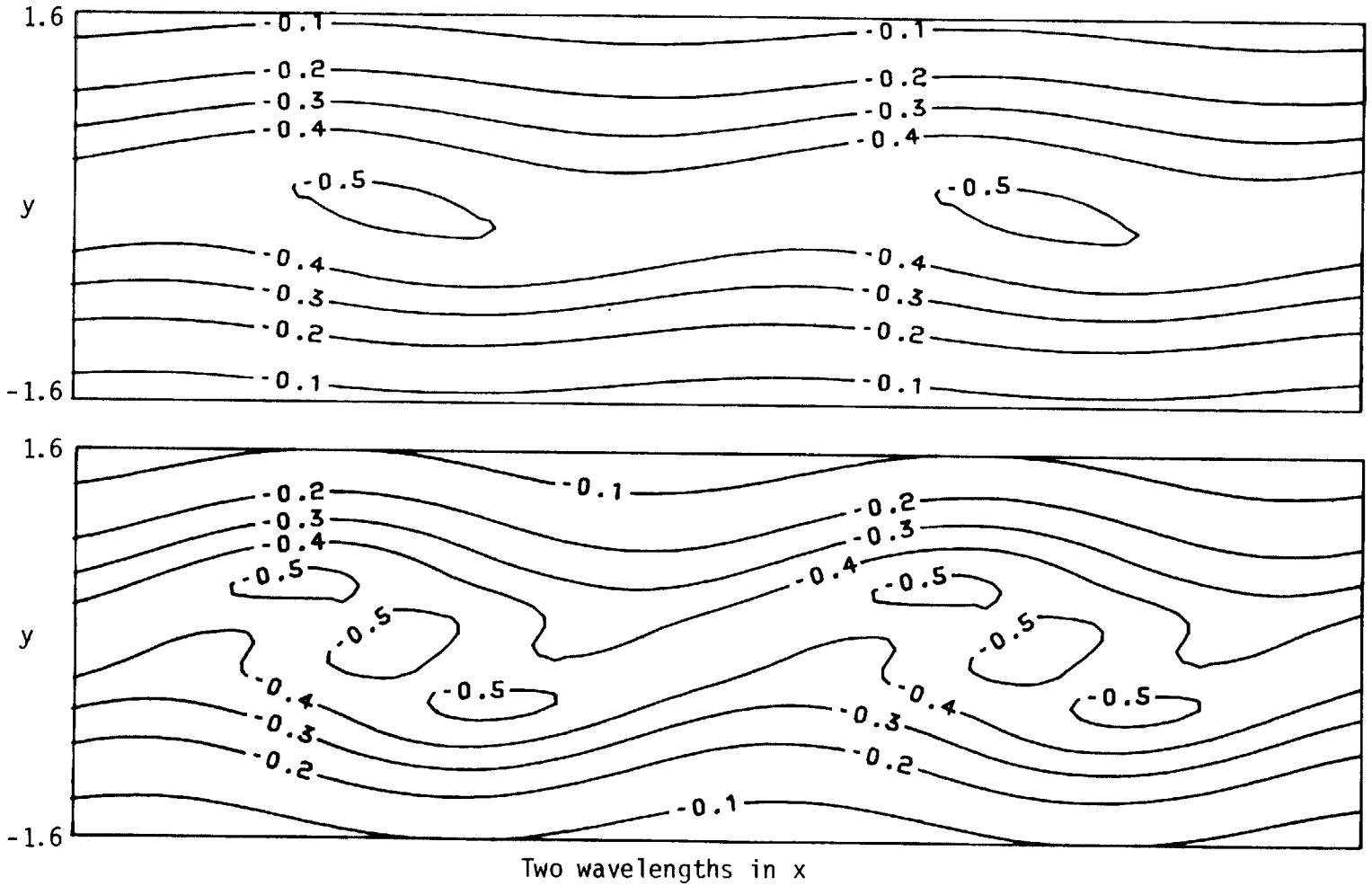

Figure 30. Contours of constant total vorticity calculated from the weakly nonlinear theory. U(y) = 0.50 tanhy. Re = 500. α = 0.6. A(0) = 0.01. Time is equal to 10 in the top plot and is equal to 20 in the bottom one.

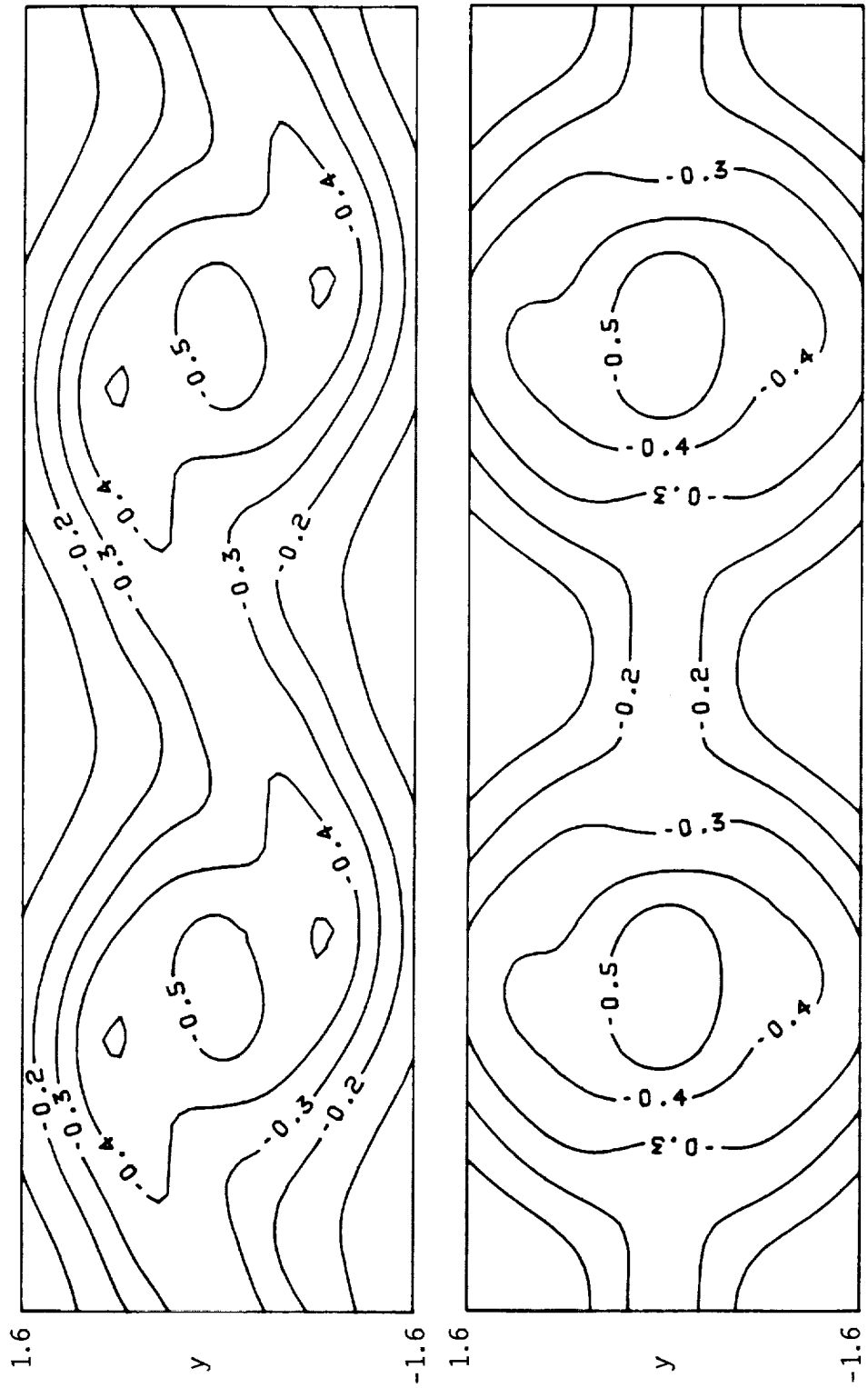

Figure 31. Contours of constant total vorticity calculated from the numerical solution. U(y) = 0.5 tanhy. Re = 500. α = 0.6. A(0) = 0.01. Time is equal to 30 in the top plot and is equal to 50 in the bottom one.

the present calculation is not an exact solution of the Navier-Stokes equations since short scales of motion, namely the third and higher harmonics, are not included.

In summary, the principal results of this section are: (1) at small amplitudes and at moderate Reynolds numbers, the weakly nonlinear theory describes well the saturation of the fundamental, the distortion of the mean flow and the initial stages of vorticity roll-up; (2) the weakly nonlinear theory breaks down at either large amplitudes or large Reynolds numbers because in these two cases the theory predicts too much distortion of the mean flow; (3) at large amplitudes, the numerical solution predicts flow oscillations due to a periodic energy exchange between the fundamental and the mean flow, with the second harmonic playing a less important role; and (4) the numerical solution, which is an approximate one, describes the roll-up of the shear layer reasonably well.

CHAPTER 6

NONLINEARITIES IN HEATED SUBSONIC JETS

The central issues surrounding this part of the work are the relative importance of the compressibility and heating of the jet in the subsequent evolution of weak nonlinear disturbances. Thus, the Landau constants will not only depend on the Reynolds number and axial wavenumber, but also on the jet temperature, Mach number and disturbance azimuthal mode number. The wave Reynolds stresses, which now include density fluctuations as well, distort the mean velocity and temperature profiles of the jet and, therefore, alter its stability characteristics. In heated compressible flows, the additional physical process involved is that of the reversible work of compression which contributes, along with energy exchange between the mean and perturbation flows via the Reynolds stress and the viscous dissipation of kinetic energy, to the rate of change of the kinetic energy of the perturbation flow in the mechanical energy balance. In the following analysis, it is apparent that nonlinearities are responsible for slowing the exponential amplification of the disturbance with time, and that compressible and heated jets are more stable than incompressible cold jets. In the numerical calculations, the momentum thickness (θ_*) and the specific gas constant (κ) are arbitrarily taken to be 0.2 and 1.4 respectively.

To repeat, the basic objectives of this work are: (1) to understand the nonlinear evolution of disturbances in round jets; (2) to explore the effect of compressibility (increasing the Mach number M; $0 \leq M < 1.0$) on the weakly nonlinear evolution of disturbances in round jets; (3) to understand the effect of heating (increasing the jet temperature ratio T^*; $T^* \geq 1$); (4) to investigate the effect of the azimuthal mode number

(β = 0,1); and (5) to explore the applicability of the weakly nonlinear theory to heated subsonic jets where both quadratic and cubic nonlinearities exist.

There are several distinctive features of the heated subsonic round jet. First, the waves are dispersive so that waves with different wavenumbers are convected with the flow at different speeds. This is because the symmetry of the base vorticity about the "critical" point is broken and, as a result, the frequency of oscillation, $d\gamma/dt$, will depend on the amplitude of the disturbance. Because of heating, the generalized inflection point is no longer at the inflection point determined by the base velocity profile and the phase speed of a (nonsingular) neutral mode is no longer given by the value of U where the derivative of $[r\ U'/(\beta^2 + \alpha^2 r^2)]$ vanishes (prime denotes d/dr) (Batchelor and Gill, 1962).

In the present work, we shall consider only subsonic flows and will look for modes which move at subsonic speeds with respect to the ambient, as well as with respect to the fluid on the jet centerline. These modes are regular in the sense that the perturbation pressure and the radial component of the velocity are finite, although the density and temperature become infinite (because we have neglected heat conduction; we kept the viscous diffusion term in Eq. (2.1-5) in order to treat neutral waves) at the critical point when the wave is exactly neutral. The axial component of the velocity is finite for the axially symmetric mode (β = 0) and is infinite for all other modes. When the mode is supersonic, singular neutral modes are also possible; we shall not look at these because our flow is assumed to be subsonic.

Second, cubic nonlinearities exist when the jet flow is either subsonic or hot, which means that the O(A) fundamental disturbance $e^{i\alpha x}$ interacts with itself (say, $e^{i\alpha x}\, e^{i\alpha x}\, e^{-i\alpha x}$, as exemplified by the term ρuv), to reproduce itself at $O(A^3)$. In other words, cubic nonlinearities will force the fundamental to modify its growth rate even in

the absence of the second harmonic and the mean flow distortion; and third, the vortex stretching term (Batchelor, 1967, p. 267; the change of vorticity by vortex stretching is, roughly speaking, a consequence of the conservation of angular momentum; vortex stretching does not occur in two-dimensional flows), which represents amplification or contraction of the vorticity vector by the strain rate is nonzero for azimuthal disturbances.

In order to see the physical essence of the nonlinear adjustments, consider the nonlinear interactions in a flow that is perturbed by an O(A) fundamental wave $e^{i\alpha x}$. Due to quadratic nonlinearities, the fundamental interacts with itself to generate an $O(A^2)$ second harmonic $e^{2i\alpha x}$ and with its complex conjugate to generate an $O(A^2)$ zeroth harmonic $e^{0i\alpha x}$ (this is the mode that distorts the mean profiles). At $O(A^3)$, the second harmonic interacts with the fundamental to generate the third harmonic $e^{3i\alpha x}$ and to reproduce the fundamental, and the zeroth harmonic interacts with the fundamental to reproduce the fundamental. Also, due to cubic nonlinearities, the fundamental interacts with itself to reproduce itself at $O(A^3)$. The first Landau constant, which measures the fundamental's deviation from linear growth is, therefore, due to: (1) the interaction between the fundamental and the second harmonic; (2) the mean flow distortion, and (3) the interaction of the fundamental with itself via cubic nonlinearities.

6.1 Isothermal Incompressible Jets

The jet is unstable; once it is perturbed, the fundamental disturbance grows linearly in time until it interacts with itself to create a wave Reynolds stress which excites both the zeroth (thus inducing a distortion of the mean flow) and second harmonics. Once these two harmonics are in the flow, they interact with the fundamental to modify its exponential growth and such modification is measured by the sign and the magnitude of the first Landau constant a_1. In the isothermal imcompressible jet, cubic nonlinearities are

absent and the nonlinear contribution to the growth rate arises from the mean flow distortion and from the interaction between the fundamental and the second harmonic. The generation of the zeroth harmonic causes the mean flow to change in the course of time so that the instantaneous mean velocity profile is given by

$$\bar{u}(r,t) = U(r) + A^2(t)\, u_{01}(r) + O(A^4)$$

where U(r) is the base flow and $u_{01}(r)$ is the mode shape associated with the distortion of the mean flow.

The Landau constant of the cold incompressible jet is found to be negative, which means that the amplitude, A(t), of the instability wave will saturate into an equilibrium amplitude. The saturation amplitude A_e ($A_e^2 = -a_0/a_1$) is independent of the small initial amplitude, but depends on the axial and azimuthal wavenumbers and on the Reynolds number. Most of the contribution to the first Landau constant arises from the changes in the mean flow, but while the minor contribution from the interaction between the first two harmonics stabilizes axisymmetric disturbances, it destabilizes first azimuthal ones.

In Figure 32, the behavior of the first Landau constant as a function of Reynolds number is shown at the neutral wavenumber. The flow is cold ($T^* = 1$) and incompressible (M = 0) and the disturbance is axisymmetric. The first Landau constant is negative (with and without MFD) indicating that nonlinearities are stabilizing so that the exponential growth of the fundamental disturbance will be reduced in time until a steady state is established. The mean flow distortion is very stabilizing. At large Reynolds numbers, the dominant contribution to a_1 comes from mean flow changes and not from the interaction between the fundamental and the second harmonic. While the second harmonic contribution is O(1), the mean flow distortion contribution is a strong function of Reynolds number.

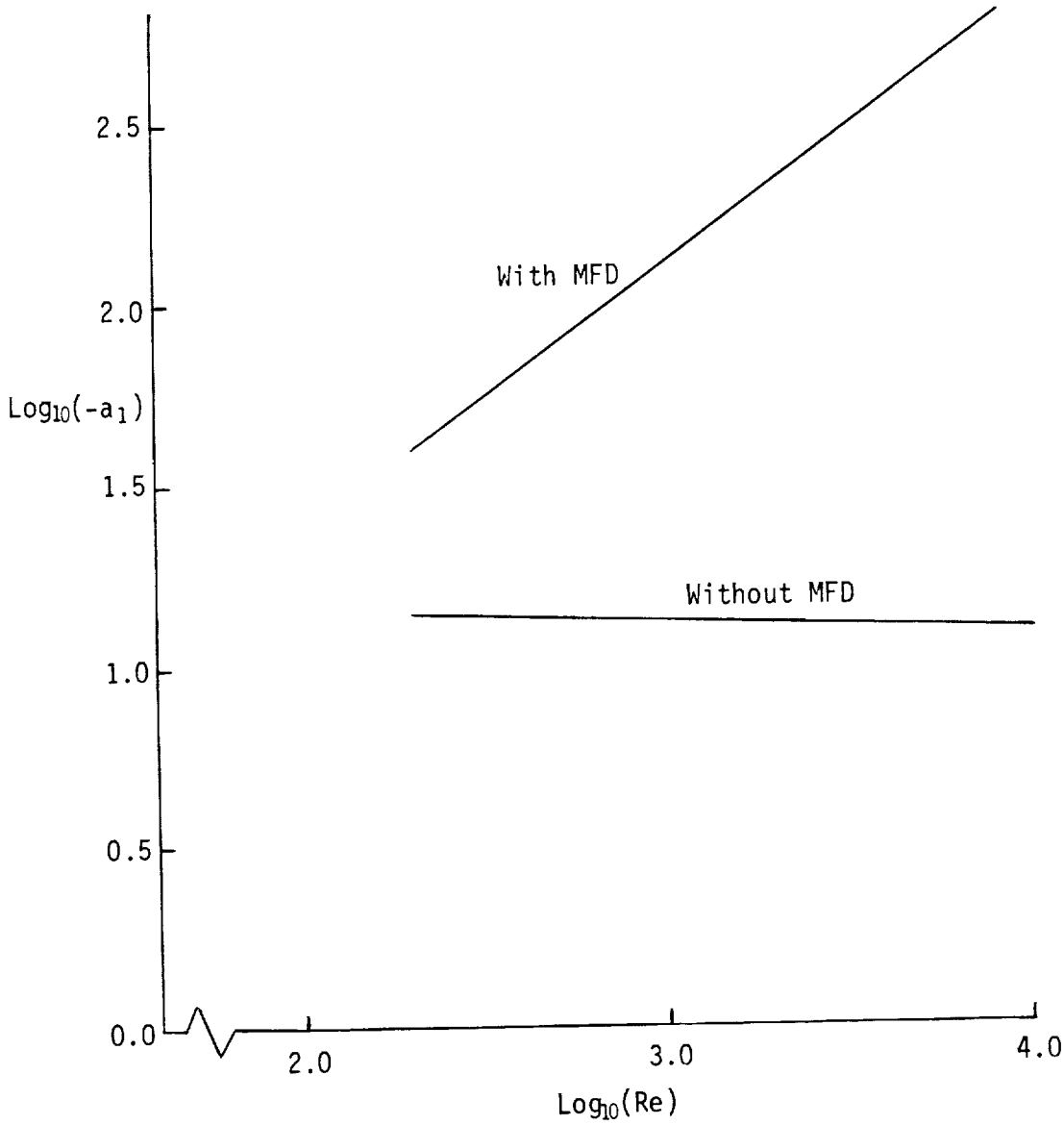

Figure 32. First Landau constant as a function of Reynolds number for neutral waves with and without mean flow distortion (MFD). $\beta = 0$, M = 0.0, $T^* = 1.0$.

In Figure 32, we saw values of the "total" first Landau constant. In order to show the contribution of the interaction between the first and second harmonics, we display the values of $(-a_1)$ (Figure 33) due to this effect alone. The Landau constant is negative for neutral as well as amplified waves so that this interaction alone can slow down the linear growth, and bring the flow into a saturated state. At exactly the neutral wave, the Landau constant is nearly the same for these two Reynolds numbers (see also Figure 32). The Landau constant increases in magnitude as the most amplified wave is approached which implies that the interaction between the first and second harmonics counteracts the increase in the linear instability of the flow as the wavenumber is reduced from its neutral value to that associated with the maximum (linear) growth rate.

Nonlinearities modify the frequency of the fundamental wave at $O(A^2)$ and such modification is measured by the sign and the magnitude of the imaginary part of the Landau constant, which depends on the flow parameters and on the mode number. A typical result is shown in Figure 34 when the Reynolds number is 500. As far as the real part, a_1, of the Landau constant is concerned, this latter figure is the counterpart of Figure 33 when the effect of the mean flow distortion is included. Note also the similarities between the behaviors of the (real part) of the Landau constants for jets and mixing layers (Figures 34 and 16). The imaginary part of the Landau constant is quite insensitive to wavenumber except in the immediate vicinity of the neutral wavenumber.

In summary, the results of this section are: (1) nonlinearities modify both the amplitude and frequency of a small disturbance in a jet, but the dominant contribution to the first Landau constant comes from the distortion of the mean flow (and not from the interaction between the fundamental and the second harmonic); (2) nonlinearities are stabilizing so that the growth rate of the fundamental will be reduced in time until a

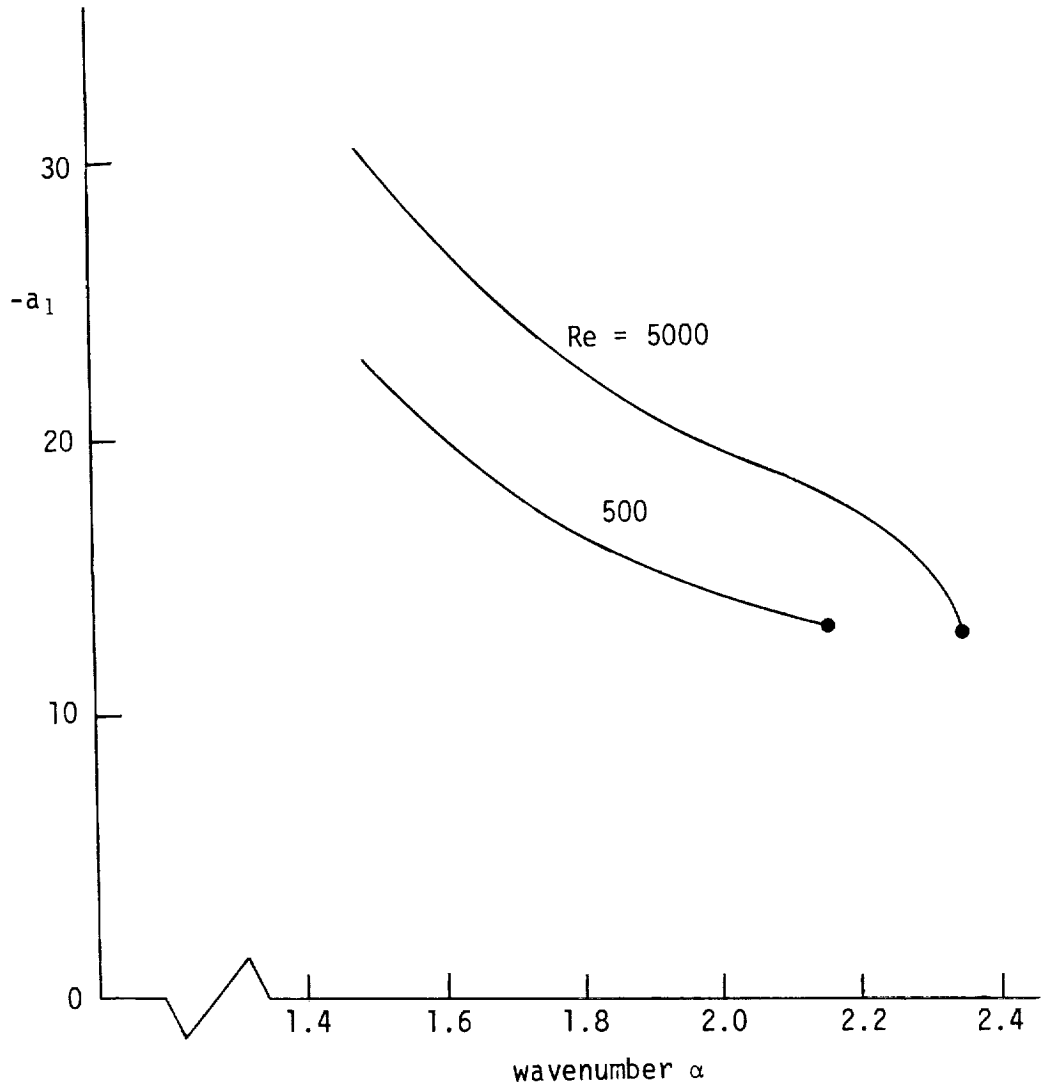

Figure 33. First Landau constant as a function of wavenumber for parametric values of jet Reynolds number. Axisymmetric mode. $T^* = 1.0$, $M = 0.0$. No mean flow distortion. (● indicates neutral point.)

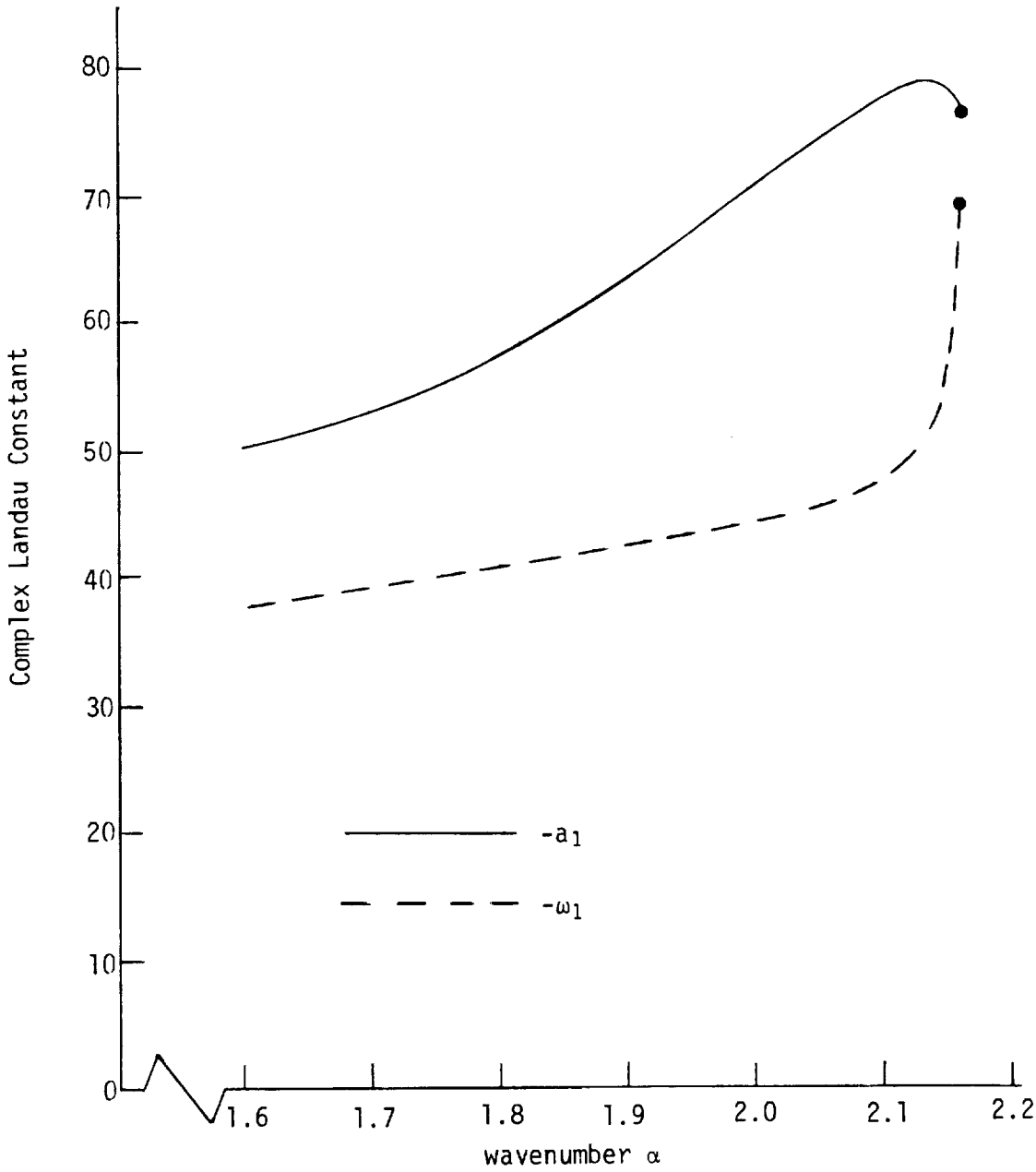

Figure 34. Complex Landau constant as a function of wavenumber. Axisymmetric mode. Re = 500, M = 0.0, $T^* = 1.0$. Mean flow distortion included. (● denotes neutral wave; $\alpha_n = 2.16$.)

steady state is established; (3) in a relative sense, nonlinear effects are more important for near-neutral waves than for off-neutral waves because the Landau constant is quite large for near-neutral waves; and (4) our weakly nonlinear theory becomes increasingly inaccurate as the Reynolds number tends to infinity.

6.2 Heating and Mach Number Effects

In this section, the dependence of the Landau constant on wavenumber for various temperature ratios and Mach numbers is discussed in order to shed light on the weakly nonlinear behavior of a disturbance in heated and compressible jets. The results show that heating is very stabilizing (i.e., the Landau constant is negative and increases in magnitude with increasing T^*) and compressibility (increasing M) is slightly stabilizing for weakly unstable waves. This holds for both axisymmetric and first azimuthal modes with and without the mean flow distortion.

A heated or compressible jet is unstable; once it is perturbed, the fundamental disturbance grows exponentially in time until it interacts with itself to generate a second harmonic and a zeroth harmonic. Once these two harmonics are in the flow, they interact with the fundamental to modify its exponential growth. The major difference between this and the incompressible case is the presence of cubic terms (such as ρuu in the momentum equation). Because of cubic nonlinearities, the fundamental will interact with itself to modify its own growth. In simple terms, the cubic (i.e., the second) term on the right-hand side of the Landau equation ($dA/dt = a_0A + a_1A^3 + \cdots$) is due to the interactions between the $O(A)$ fundamental and both the $O(A^2)$ zeroth and the $O(A^2)$ second harmonics and to the interaction of the fundamental with itself via cubic nonlinearities. When the flow is either hot or compressible, both the mean velocity and the mean temperature profiles will be distorted (via the zeroth harmonic) due to the generation of

wave Reynolds stresses. The mean flow distortion is always stabilizing because it tends to reduce the velocity gradients near the center of the jet shear layer.

The behavior of the Landau constant at a low Mach number, as a function of wavenumber for three values of the jet temperature ratio, is shown in Figure 35, when the disturbance is axisymmetric and the mean flow distortion is not included. It can be seen that a heated jet becomes increasingly stabilized as the neutral wavenumber (denoted by the vertical dashed lines) is approached. Since for moderately amplified waves (say, $1.4 \leq \alpha \leq \alpha_n$), the linear growth rate (a_0) decreases with heating (see Figure 7) while ($-a_1$) increases with heating (and since the equilibrium amplitude is $A_e = \sqrt{a_0/(-a_1)}$), heating will severely reduce the overall growth of the disturbance. In other words, under linear growth and nonlinear saturation, a heated jet is much more stable than a cold one.

Although our calculations are carried out for a parallel base flow using temporal theory, they may be applied to a laboratory situation in the following way. First, time is really an age variable which, in a typical experiment, becomes the downstream distance (say, x). In essence, here we are making use of an idea of Gaster in which x (of a spatial calculation) and t (of a temporal calculation) are related by $x = U_c t$ where U_c is some suitable convection speed. Now suppose a jet is perturbed by a periodic oscillation at some frequency near the most amplified frequency. As this wave propagates downstream, it becomes less and less unstable because of the divergence of the base flow. This divergence is caused by viscous or turbulent stresses (due to the fine grain motion) acting on the base flow. In terms of our temporal theory, the excitation occurs at some wavenumber (say, $\alpha = 1.4$, Figure 35) and as the wave develops in time, its wavenumber increases (i.e., the wave approaches its neutral point). As this happens, and as the amplitude of the wave increases to the point where (weak) nonlinear effects become

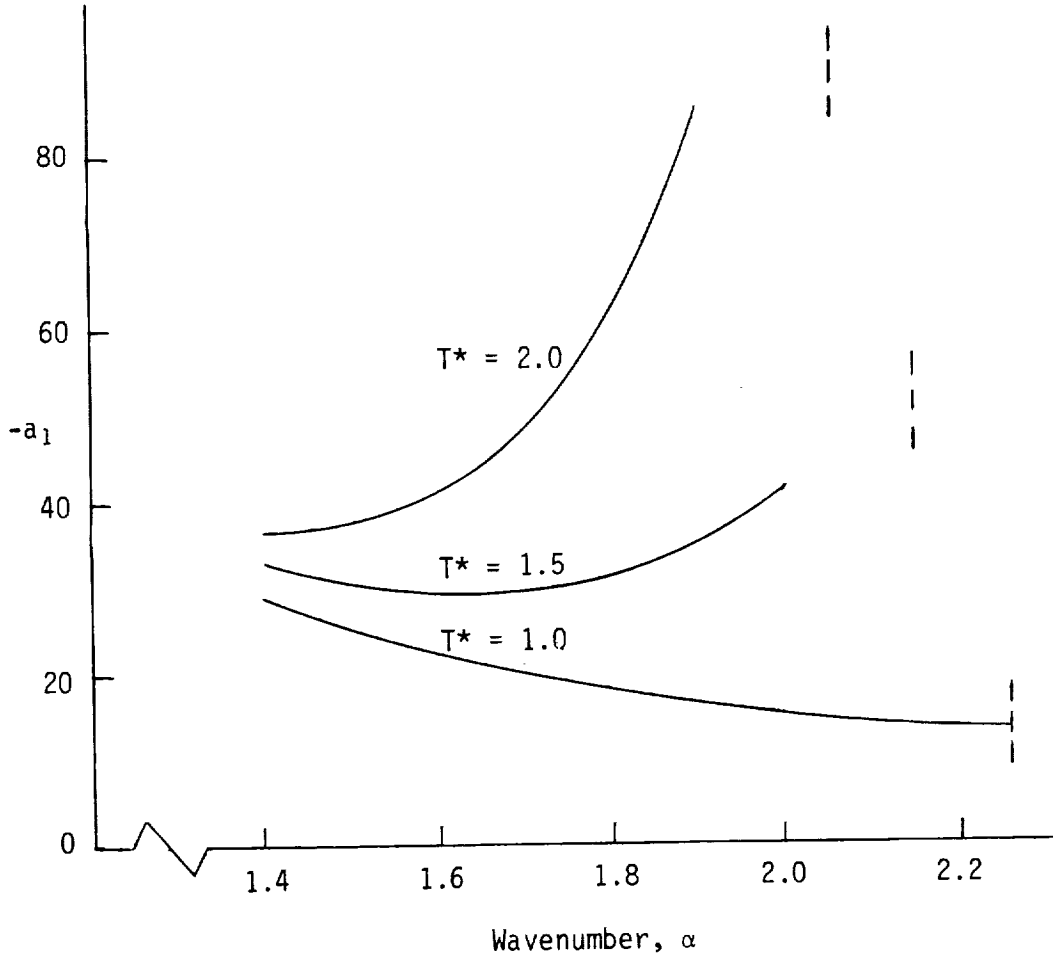

Figure 35. Landau constant as a function of wavenumber for parametric values of jet temperature ratio, T^*. Axisymmetric mode. Re = 1000. M = 0.1. No mean flow distortion. Vertical dashed lines denote neutral points.

important, a heated jet becomes considerably less unstable than a cold one. Therefore, the saturation amplitude in a heated jet can be expected to be much smaller than in a cold jet, and the various secondary instabilities (i.e., resonances and vortex pairing) are, therefore, less important.

Figure 36 shows the behavior of a_1 as a function of wavenumber for two temperature ratios for the first azimuthal mode when the mean flow distortion is not included. It is interesting to note that when the jet is cold (i.e., $T^* = 1$), the first Landau constant is positive for unstable wavenumbers, which means that the second harmonic alone is destabilizing (i.e., will force the fundamental to increase its growth rate) but heating changes the sign of a_1 and is, therefore, once again stabilizing. It can also be seen that heating becomes increasingly stabilizing as the neutral point is approached. For a fixed wavenumber (say, $\alpha = 1.8$), the linear growth rate decreases (see Figure 7) while $-a_1$ increases with heating, which means that heating greatly suppresses the overall growth of the disturbance.

The dependence of the Landau constant on Mach number is shown in Figure 37 for $\alpha = 1.3$, which is approximately the most unstable wave. The magnitude of the Landau constant decreases slightly with increasing Mach number at this wavenumber. On the other hand, for larger wavenumbers (i.e., for weakly amplified waves with $1.8 < \alpha < \alpha_n$, say), increasing the Mach number increases the magnitude of the Landau constant, but only slightly. The linear growth rates of weakly amplified waves, however, decrease with increasing Mach number, which means that, under linear amplification and nonlinear saturation, the equilibrium amplitude of the fundamental is lower for a subsonic jet than for an incompressible one; much of this reduction in amplitude comes from a reduction in the linear growth rate a_0.

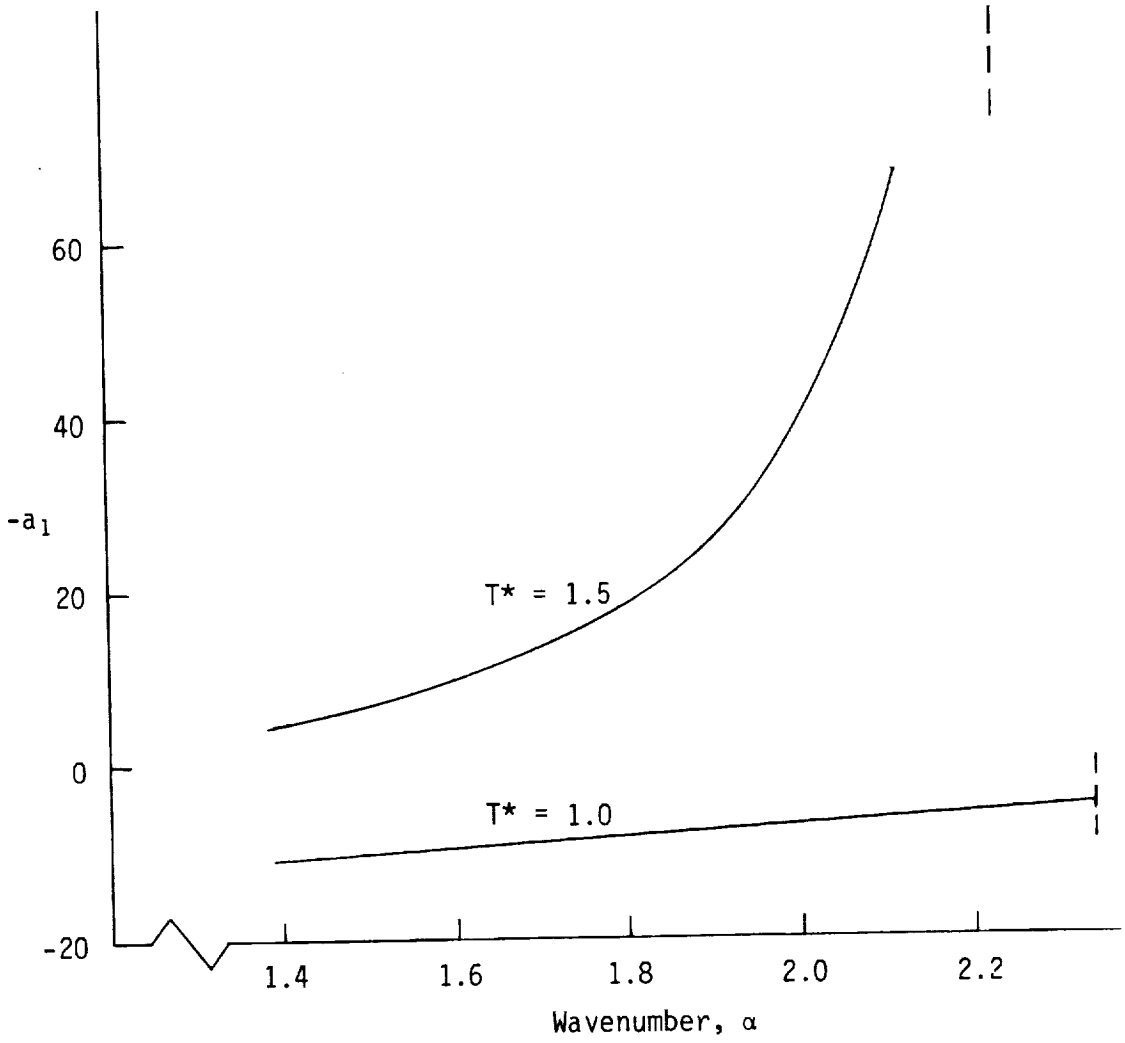

Figure 36. Landau constant as a function of wavenumber for parametric values of jet temperature ratio, T^*. First azimuthal mode. Re = 1000. M = 0.0. No mean flow distortion. Vertical dashed lines denote neutral points.

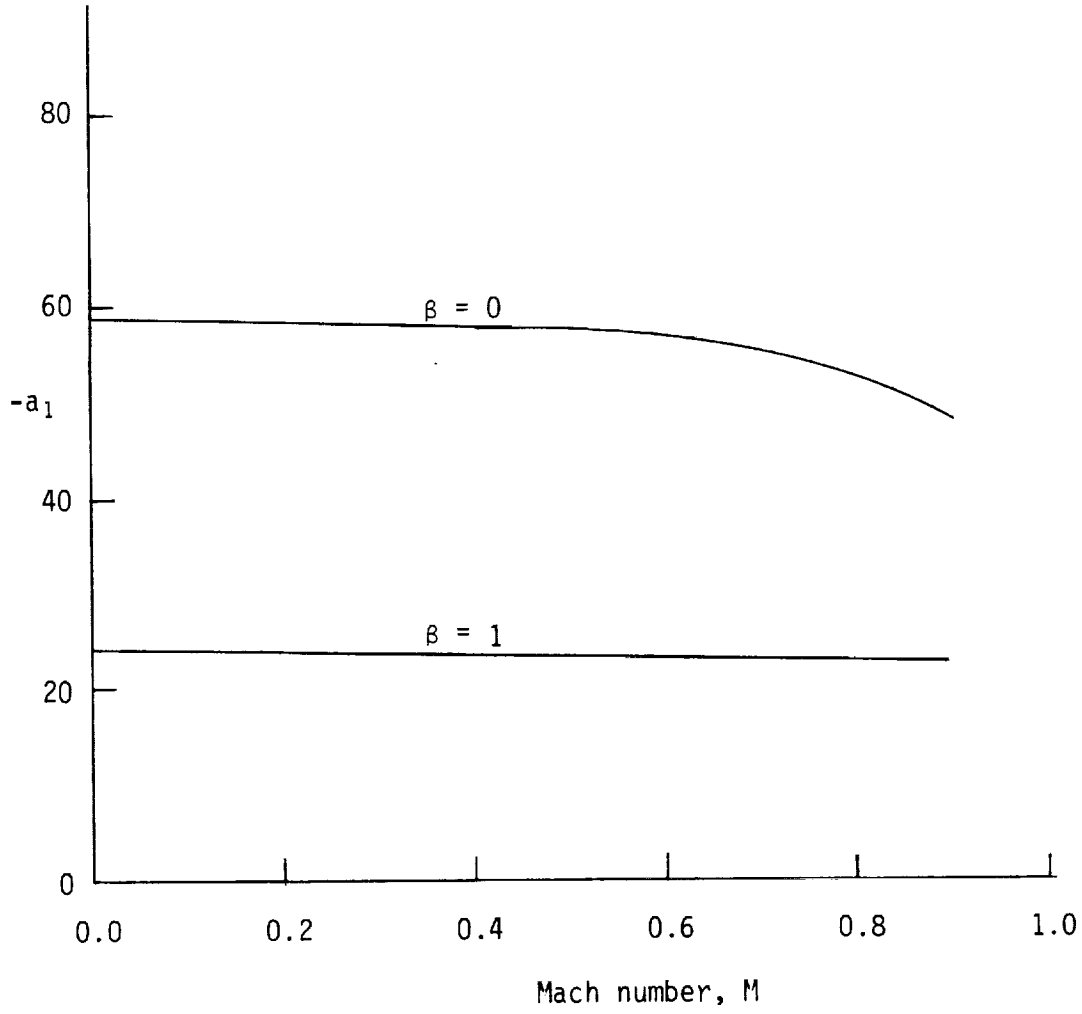

Figure 37. Landau constant as a function of Mach number for the axisymmetric and the first azimuthal modes at an axial wavenumber of 1.3. Re = 1000. $T^* = 1.0$. Mean flow distortion included.

Linear stability calculations (see Chapter 4) indicate that, for given flow parameters and axial wavenumber, the linear growth rate of the first azimuthal mode is larger than that of the axisymmetric mode. On the other hand, the nonlinear calculations (see Figure 37, for example) show that the magnitude of the Landau constant is larger for the axisymmetric mode. This means that the $\beta = 1$ mode is the dominant one in the sense that it will result in higher saturation amplitudes and, therefore, produce a significant distortion of the mean flow. Hence, the primary nonlinearity in a jet is expected to be in the first azimuthal mode for our base velocity profile.

In order to isolate the effects of heating, compressibility and mode number on the subsequent evolution of a disturbance, consider the typical behavior of a weakly amplified mode which is "deposited" into the flow at time $t = 0$ with an initial amplitude of 1%. The mode has an axial wavenumber of 1.6. The linear growth rate and the first Landau constants are calculated, as described previously, and the Landau (amplitude) equation is integrated to find the amplitude $A = A(t)$. Its behavior is shown in Figure 38 for various combinations of azimuthal mode numbers, Mach numbers and temperature ratios. In all cases, the disturbance amplitude levels off and tends to the equilibrium amplitude, A_e, whose values are shown on the right-hand side.

There are two important points to note: first, at large values of time, our base flow will be dominated by the first azimuthal mode (the dashed lines are generally above the solid ones), and second, heating reduces the equilibrium amplitude quite significantly.

In the weakly nonlinear theory, the distortion of the mean flow is proportional to A^2 (the instantaneous mean velocity is $\bar{u}(r,t) = U(r) + A^2(t)\, u_{01}(r) + \ldots$, the instantaneous mean density is $\bar{\rho}(r,t) = R(r) + A^2(t)\, \rho_{01}(r) + \ldots$, where $R(r)$ is the base density and $\rho_{01}(r)$ is the mode shape associated with the distortion of the mean density). Because of this, in

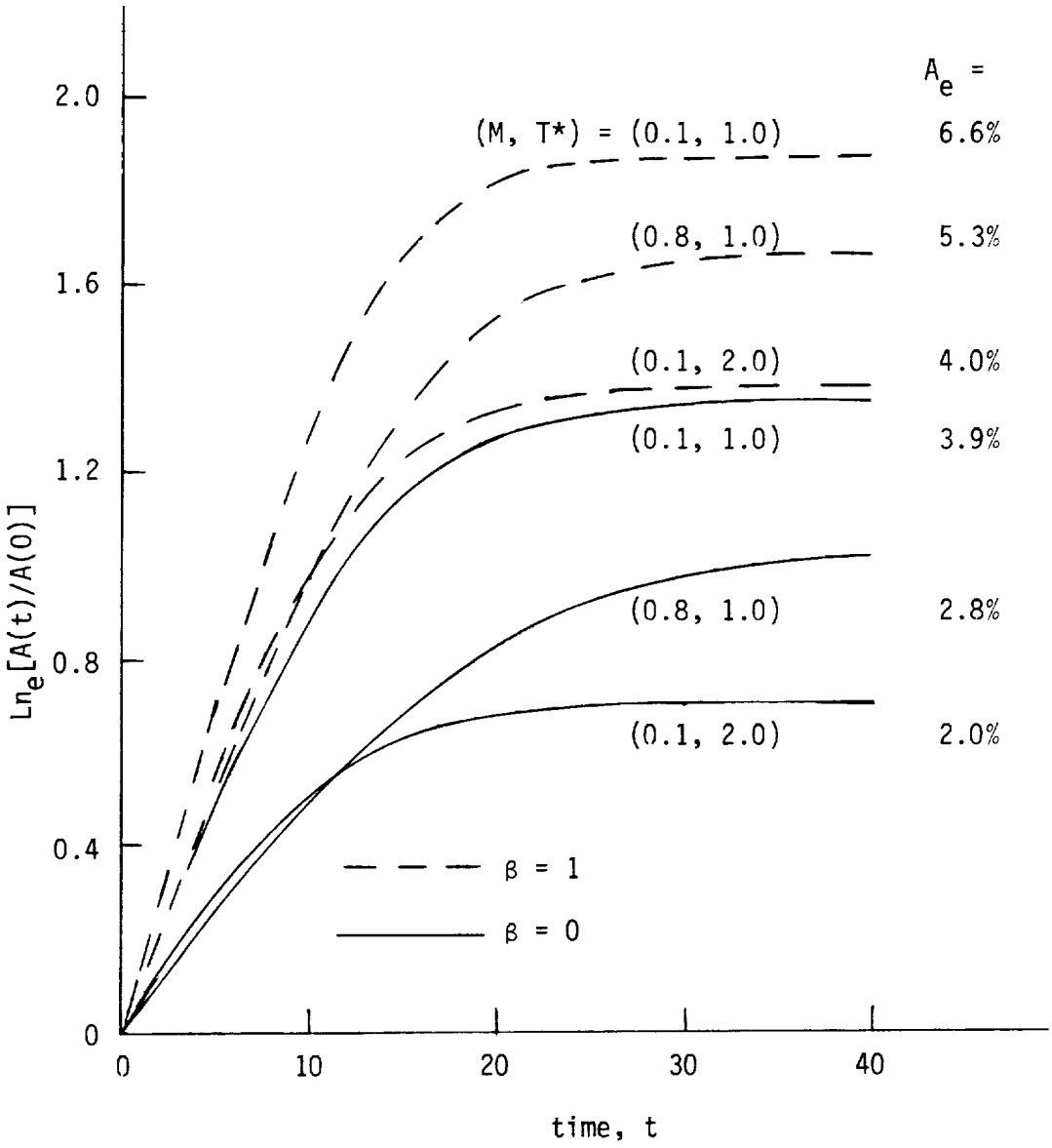

Figure 38. Amplitude of the fundamental as a function of time for the axisymmetric and the first azimuthal modes at two Mach numbers and temperature ratios. A_e is the equilibrium amplitude. Mean flow distortion included. Re = 2000. α = 1.6. A(0) = 1%.

view of Figure 38, the induced velocity and density distortions will be smaller for heated (or subsonic) jets than for cold (or incompressible) ones. Therefore, excitation at a given amplitude will have less effect on a heated (or subsonic) jet than on a cold (or incompressible) one.

While linear theory is concerned with very small-amplitude disturbances, weakly nonlinear theory is concerned with the way cumulative (small) nonlinear effects modify the instability of the flow. The jet is unstable so that, with increasing time, higher harmonics develop, the mean flow continues to change, and the fundamental disturbance keeps adjusting its shape, growth rate and frequency until a steady state is established. The precise way in which this happens depends (for given Re, α) on the jet Mach number, temperature ratio, and mode number (see Figure 38).

In short, the results of this section are: (1) heating and compressibility suppress the nonlinear growth rate of weak instability modes. This is summarized in Figure 39, where the saturation amplitude is plotted as a function of jet Mach number and temperature ratio; (2) excitation of a given amplitude will have less effect on heated (or subsonic) jets because of the small mean flow changes (which are proportional to A^2); and (3) under linear growth and nonlinear saturation, the first azimuthal mode is the dominant one for the representative base flow for which we have carried out our calculations.

6.3 Vorticity Roll-Up

Flows characterized by inflectional profiles are generally unstable so that small perturbations grow to large fluctuations in relatively short times (in this work, the flow is assumed to be spatially periodic and evolving in time). The basic vorticity distribution, which possesses a minimum, is (inviscidly) unstable to small perturbations via the Kelvin-Helmholtz instability mechanism (Batchelor, 1967). Thus, instability waves grow

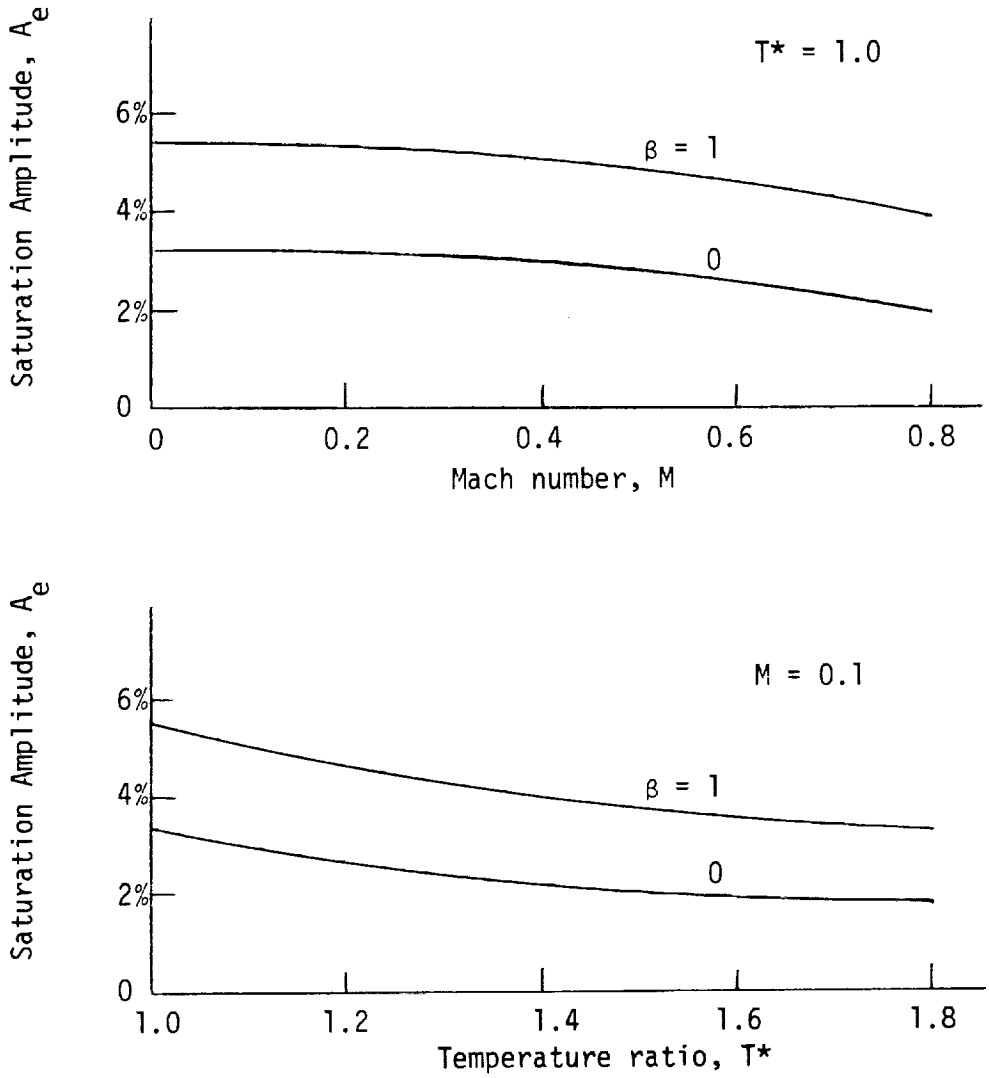

Figure 39. Saturation amplitude (A_e) of the instability wave as a function of jet Mach number and temperature ratio for the axisymmetric and the first azimuthal modes. α = 1.7. Re = 5000. A(0) = 1%. Mean flow distortion included.

exponentially with time (initially) and the redistribution of vorticity causes the jet shear layer to roll-up and form distinct vortices (Ahuja et al., 1982). Most of the vorticity is concentrated in a thin annulus near the middle of the jet shear layer and, of course, the large scale vortices convect with the flow at a speed which depends on the wavenumber, Reynolds number, jet Mach number and temperature.

Initially, the flow is made up of the base flow and a small disturbance but, as time increases, the amplitude of the fundamental keeps increasing exponentially until nonlinear interactions generate higher harmonics and distort the base flow. The flow will then be made up of all the harmonics of the fundamental and a distorted (time-dependent) mean flow. Therefore, the vorticity will constantly change until a final steady-state is reached. In this work, the solution contains only an O(A) fundamental wave, an $O(A^2)$ second harmonic and an $O(A^2)$ mean flow distortion. In the round jet, nonlinearities also modify the frequency of the disturbance.

Consider the axisymmetric disturbance ($\beta = 0$); then, the perturbation axial velocity u(x,r,t), the perturbation radial velocity v(x,r,t) and the total azimuthal component of vorticity $[-U'(r) + \partial v/\partial x - \partial u/\partial r]$ are

$$u(x,r,t) = \left[A(t)\, u_{10}(r)\, e^{i(\alpha x-\gamma)} + A^2(t)\, u_{20}(r)\, e^{2i(\alpha x-\gamma)} + c.c.\right] + A^2(t)\, u_{01}(r) \tag{6.4-1}$$

$$v(x,r,t) = \left[A(t)\, v_{10}(r)\, e^{i(\alpha x-\gamma)} + A^2(t)\, v_{20}(r)\, e^{2i(\alpha x-\gamma)} + c.c.\right] + A^2(t)\, v_{01}(r) \tag{6.4-2}$$

$$\bar{\Omega}(x,r,t) = -U' + \left[A(i\alpha v_{10} - u'_{10})\, e^{i(\alpha x-\gamma)} + A^2(2i\alpha v_{20} - u'_{20})\, e^{2i(\alpha x-\gamma)} + c.c.\right] - A^2\, u'_{01} \tag{6.4-3}$$

where the shape of the linear mode is given by (u_{10}, v_{10}), the shape of the second harmonic is given by (u_{20}, v_{20}) and the shape of the mean flow distortion is given by (u_{01}, v_{01}).

The time (and amplitude) dependent phase, γ, is obtained from

$$\frac{d\gamma}{dt} = \omega_0 + A^2(t)\,\omega_1 + O(A^4)$$

where $\omega_1 = -\mathrm{Im}(\lambda_1)$ is minus the imaginary part of the first complex Landau constant, λ_1. For a given wave and Reynolds number (α = 1.6, β = 0, Re = 5000), the mode shapes and Landau constant are obtained numerically and the amplitude and phase equations are integrated with the initial conditions A(0) = 0.01, $\gamma(0)$ = 0. This enables us to obtain the instantaneous (total) vorticity, as given by (6.4-3). In Figures 41, 42 and 43, we show contours of constant vorticity. But first, we look at Figure 40, which displays the behavior of the amplitude, A = A(t), and the values of time (denoted by the dots) at which the vorticity controus are actually shown. We plot these contours for three combinations of Mach number and temperature ratio.

In each of these figures, (41, 42 and 43), we see an oscillatory contour well outside a central region, say r $\approx$ 0.9. Within this central region (r $\approx$ 0.9), the vorticity shows a tendency to roll-up at the larger values of time. For example, in Figure 41 (bottom), this roll-up may be identified by examining the third contour from the bottom which exhibits "wave breaking" or an "S" shape at a certain axial location. It is clear that at this relatively large Reynolds number (= 5000), our weakly nonlinear theory does not adequately represent the vorticity, although it does indicate the tendency towards roll-up and a nonlinear stage. Clearly, most of the difficulty arises in a central region (say, r $\approx$ 0.9). This is where the critical layer is, and it needs to be treated as a separate entity with its

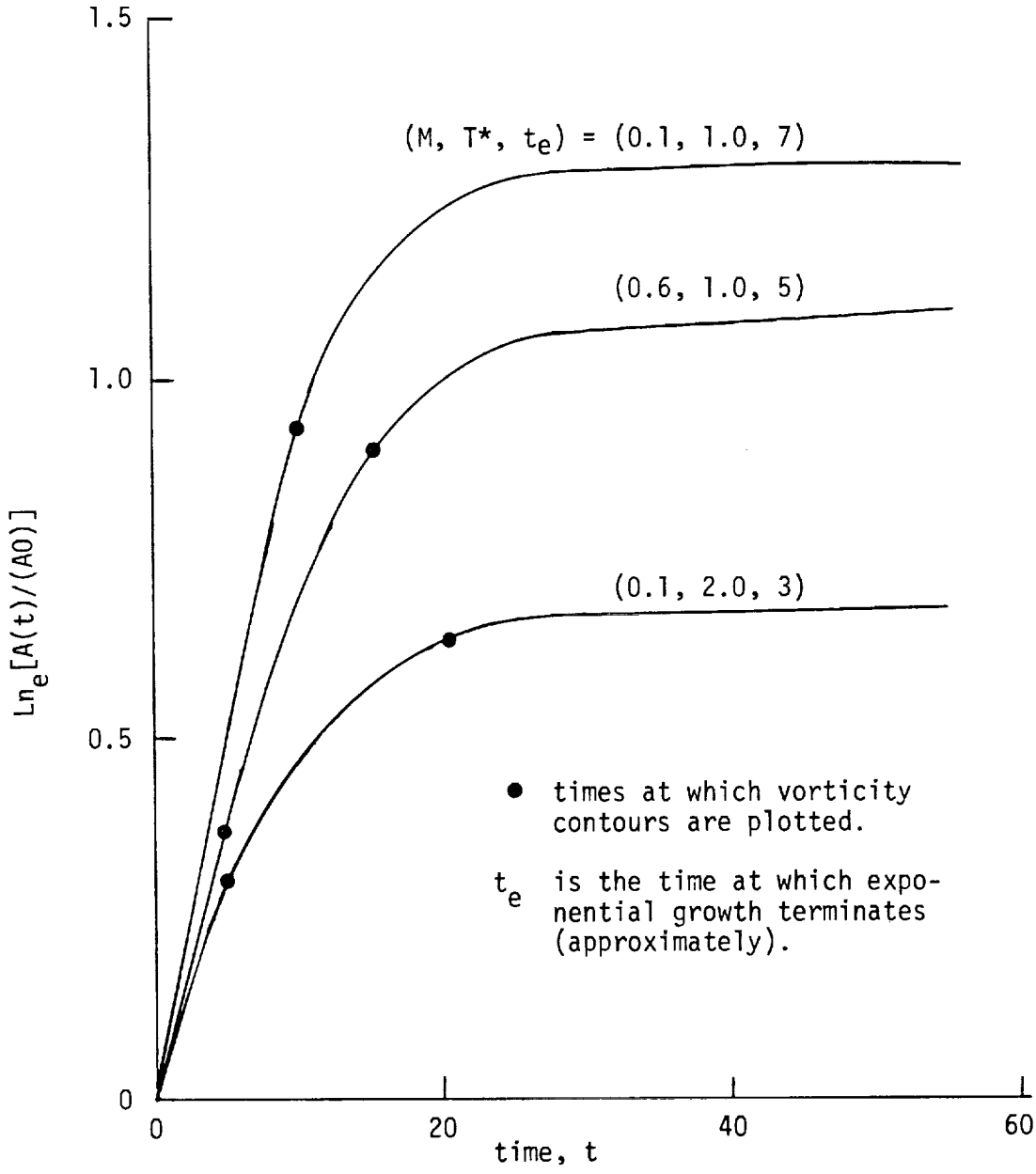

Figure 40. Amplitude of the fundamental as a function of time for two values of jet Mach number and temperature ratio. α = 1.6. β = 0. Re = 5000. A(0) = 1%.

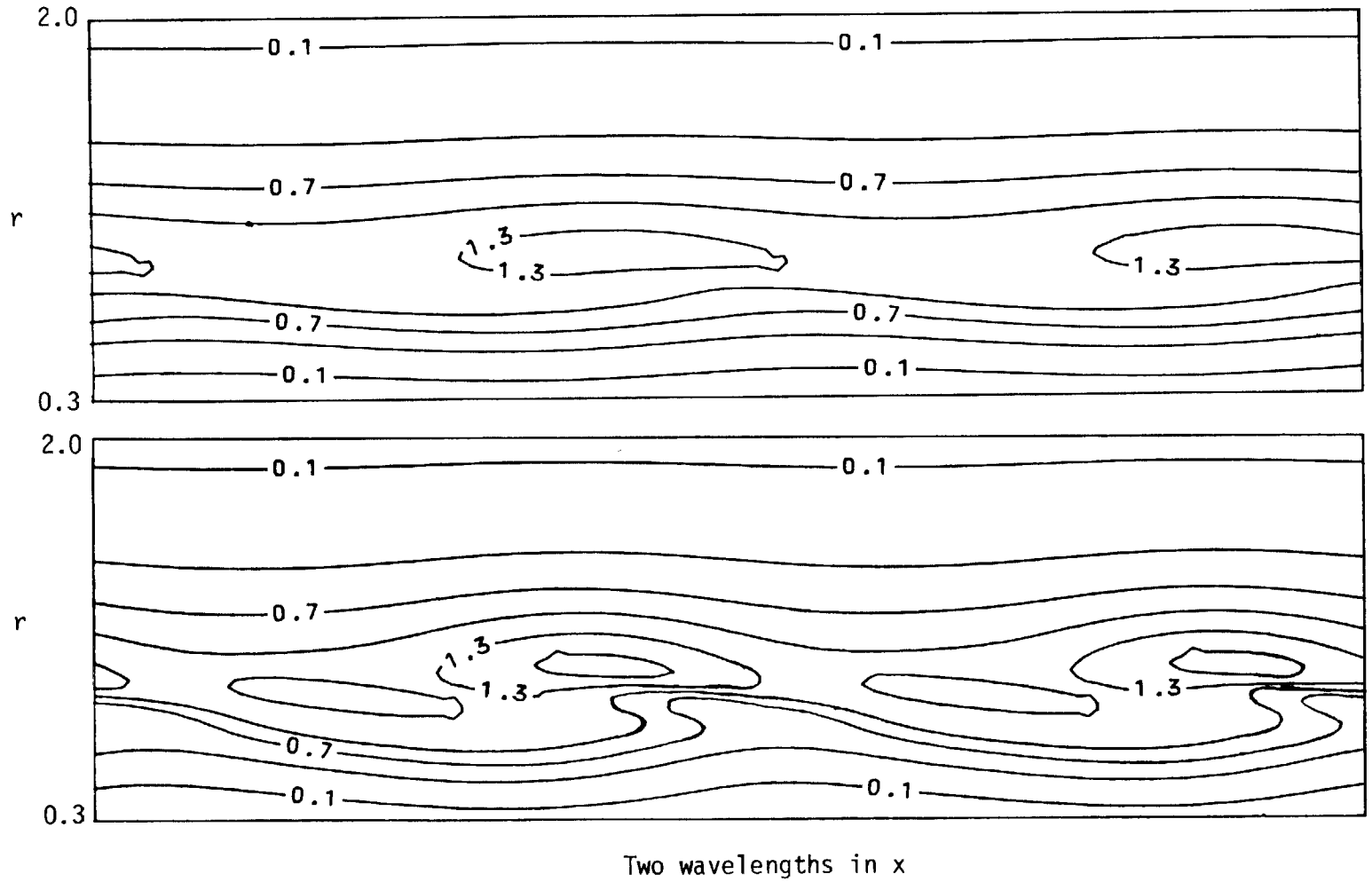

Figure 41. Contours of constant vorticity at two values of time. Time is equal to zero in the top plot and is equal to 10 in the bottom one. $\alpha = 1.6$. $\beta = 0$. Re = 5000. A(0) = 1%. M = 0.1. $T^* = 1.0$.

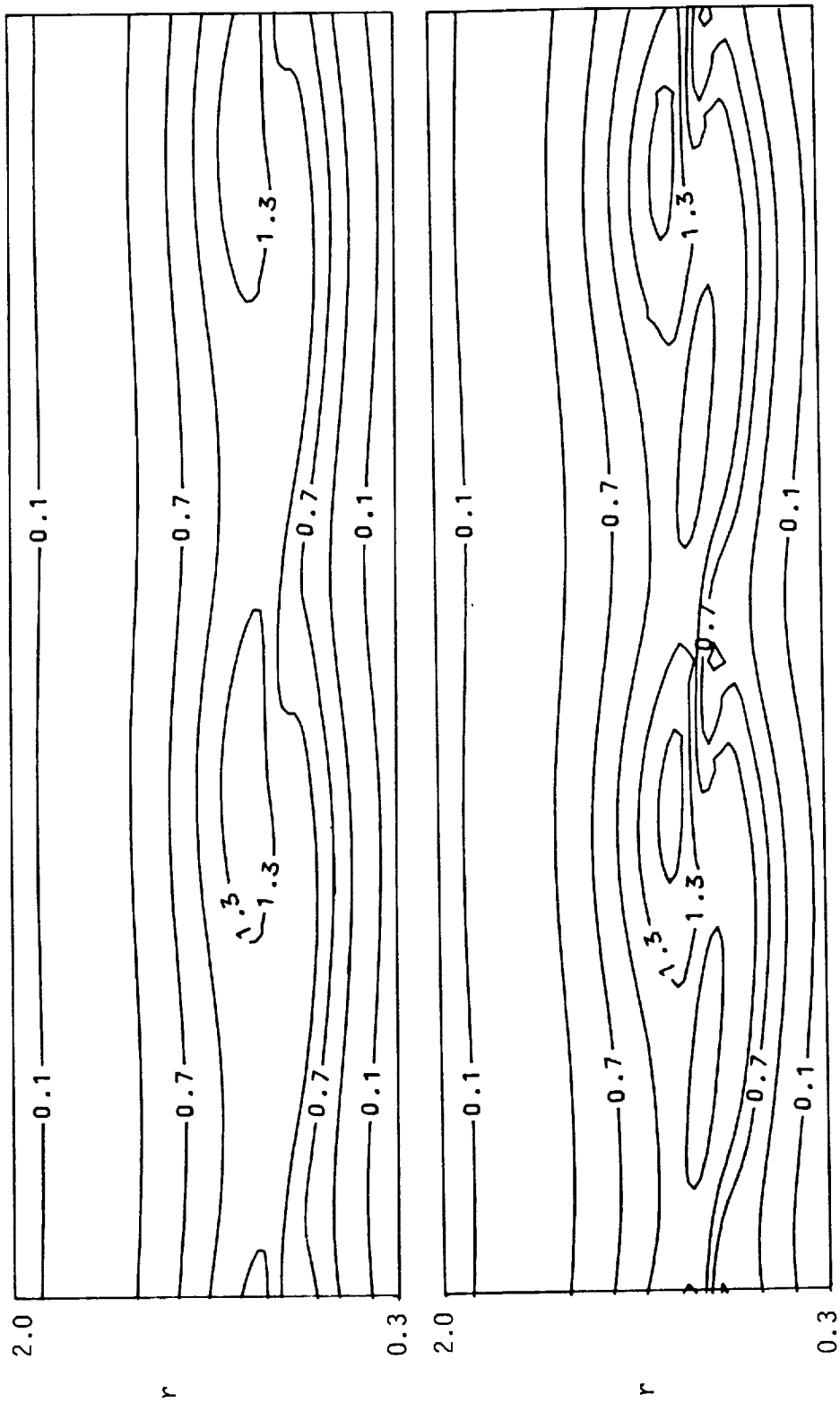

Figure 42. Contours of constant vorticity at two values of time. Time is equal to 5 in the top plot and is equal to 15 in the bottom one. $\alpha = 1.6$. $\beta = 0$. Re = 5000. A(0) = 1%. M = 0.6. $T^* = 1.0$.

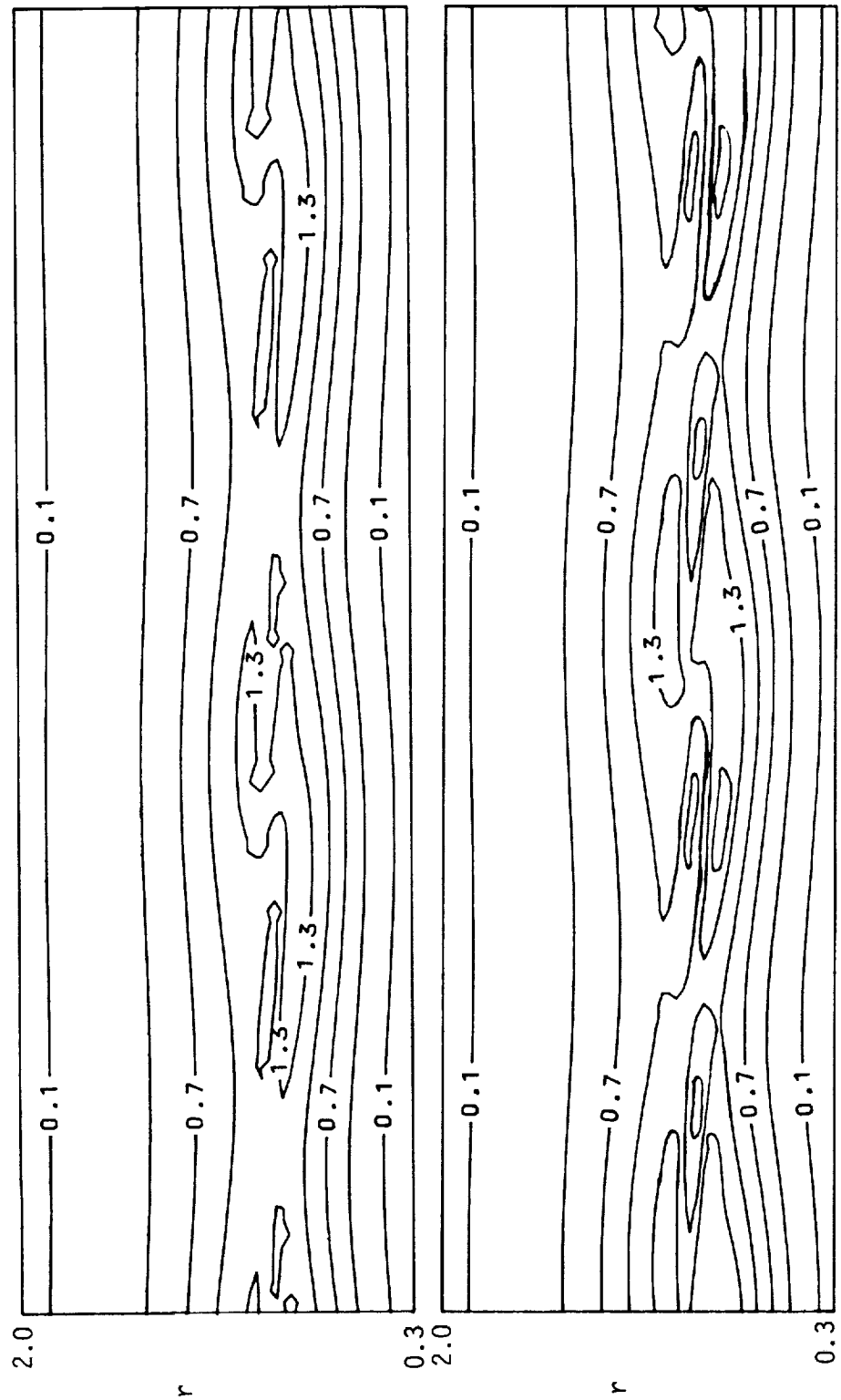

Figure 43. Contours of constant vorticity at two values of time. Time is equal to 5 in the top plot and is equal to 20 in the bottom one. $\alpha = 1.6$. $\beta = 0$. Re = 5000. A(0) = 1%. M = 0.1. $T^* = 2.0$.

own length scale which depends on the amplitude. At high Reynolds numbers, this leads to a complementary theory which involves a nonlinear and nonequilibrium critical layer (Goldstein and Leib, 1988).

CHAPTER 7

SUMMARY AND DISCUSSION

In the previous chapters, some aspects of linear and nonlinear instability in mixing layers and heated jets were discussed. A receptivity analysis was carried out in order to see how the flow response varies with the location of an imposed excitation. The equations of motion of a jet flow that is excited by a compact pulse were solved to yield a wave packet of slowly changing amplitude which emerges downstream as a result of the instability. The long time solution of the initial value problem provides information not only on the structure of the packet (which consists of a few oscillations and is convected downstream by the mean flow), but also on the relationship between the magnitude of the disturbances in the jet and the location of the (localized and impulsive) input disturbance. This magnitude depends in a nontrivial manner on the location of the excitation and there is an optimum position for which little energy input will produce large perturbations. It was found that maximum response is generated when the source is placed at a point where the fluid velocity equals the phase velocity of the most amplified wave of the packet.

In Chapter 5, the nonlinear evolution of disturbances in mixing layers was analyzed using both the weakly nonlinear stability theory and a numerical solution of the Navier-Stokes equations. This solution retained the first few Fourier modes for reasons that were given in the main body of that chapter. Once an unstable base flow is perturbed by a wave-like disturbance, the disturbance grows initially according to linear stability theory until nonlinear interactions generate higher harmonics and wave Reynolds stresses which will distort the mean flow and alter its stability characteristics. The solution, thereafter,

may become steady or oscillatory depending on the wavenumber, the initial amplitude of the disturbance and the Reynolds number.

The weakly nonlinear theory is an asymptotic theory valid for small amplitudes in which the effects of nonlinearities enter in a hierarchical manner. The lowest order solution is the linear one to which corrections are made in a successive fashion. Our numerical solution, on the other hand, involves a truncation of Fourier modes but places no explicit restriction on the amplitude of the disturbance. The two solutions were compared for various wave and Reynolds numbers in order to establish the range of validity of the weakly nonlinear theory.

In nonlinear hydrodynamic stability theory, a perturbed mixing layer is represented as a superposition of interacting instability waves that propagate and amplify in time. Beyond the region of linear growth, instability waves evolve into more or less discrete vortices composed of several Fourier modes. The established vortex structure may be steady or may oscillate in time, depending on the amplitude of the perturbations and on the Reynolds number.

The analysis in Chapter 5 was concerned with the temporal interactions between instability modes in mixing layers and the main conclusions are:

1. Nonlinearities stabilize the growth of the fundamental instability wave, but the dominant effect arises from mean flow changes and not from higher harmonics.

2. At small initial amplitudes, the flow will evolve into a steady (saturated) state, while at large initial amplitudes, the flow will evolve into an oscillatory state characterized by an alternating energy exchange between the mean flow and the perturbation (fundamentals and harmonics).

3. At small amplitudes and at moderate Reynolds numbers, the weakly nonlinear theory describes well the saturation of the fundamental, the distortion of the mean flow and the initial stages of vorticity roll-up. The agreement between the numerical results and the weakly nonlinear theory is very good.

4. The two-dimensional numerical simulations describe well the (intrinsically nonlinear) roll-up of the shear layer. Beyond the region of linear growth, instability waves evolve into a periodic array of compact vortices. The oscillatory final state was observed by other workers as well.

The weakly nonlinear theory was extended to heated and compressible round jets where both quadratic and cubic nonlinearities exist. The quadratic and cubic wave Reynolds stresses generated by self-interactions will distort the mean velocity and temperature profiles and, therefore, alter the jet instability characteristics. The nonlinear evolution of the flow will depend not only on the axial wavenumber, the azimuthal wavenumber and the Reynolds number, but also on the jet Mach number and temperature.

The analysis in Chapter 6 was concerned with the temporal interactions between instability modes in heated subsonic round jets and the main conclusions are:

1. According to weakly nonlinear theory, heating and compressibility suppress the growth of instability waves so that an external excitation of a given amplitude will have less effect when the jet is hot or compressible.

2. Under exponential growth and nonlinear saturation, the first azimuthal mode of excitation is the dominant one for the base profiles considered in this study.

3. The weakly nonlinear theory describes qualitatively the initial stages of the roll-up of vorticity.

The weakly nonlinear theory has always been applied to neutral instability modes which are superimposed on isothermal mixing layers. Using the formalism of Herbert (1983), we have applied this theory to unstable waves.

A most remarkable finding is that at high Reynolds numbers, the Landau constants vary extremely rapidly in the vicinity of the neutral wavenumber. This rapid variation, for the most part, comes from the distortion of the mean flow and definitely implies that a weakly nonlinear theory at $Re = \infty$ must contain a fully nonlinear critical layer which evolves in space and time. Outside this critical layer, nonlinearities may be described in a hierarchical manner in which the lowest order term is provided by linear theory. The onset of the full nonlinearity in the critical layer is quite sudden (because the Landau constants vary rapidly near the neutral wavenumber); this explains why linear stability theory is so successful in predicting the position of the roll-up (in time or space).

APPENDIX A

MEAN JET PROFILES

The mean velocity, density and pressure profiles of the heated subsonic jet are:

$$\underset{\sim}{U} = (U(r), 0, 0),\ U(r) = 0.5 \left[1 - \tanh\left(\left(r - \frac{1}{r} \right) / 4\theta_* \right) \right].$$

$$R = R(r) = \frac{T^*}{1 + (T^*-1)\, U + \frac{\kappa-1}{2} M^2\, T^*\, U(1-U)}.$$

$$P = \text{constant}$$

where

$$\theta_* = \text{"momentum thickness"} = \int_0^\infty U(1 - U)\, dr,$$

$$T^* = \text{temperature ratio} = \frac{T_c}{T_\infty},$$

and

M = jet Mach number = U_c / a_c

T_∞ = ambient temperature

a_c = speed of sound on jet centerline.

APPENDIX B

NONLINEAR INTERACTIONS IN THE JET

The nonlinear forcing terms for the first harmonic, the mean flow distortion and the distortion of the fundamental are given below. First, let

$$F(r) = U - c_0 .$$

$$\nabla_{10}(r) = i\alpha u_{10} + v'_{10} + \frac{1}{r} v_{10} + \frac{i\beta}{r} w_{10} .$$

$$\nabla_{20}(r) = 2i\alpha u_{20} + v'_{20} + \frac{1}{r} v_{20} + \frac{2i\beta}{r} w_{20} .$$

$$\nabla_{01}(r) = i\alpha u_{01} + v'_{01} + \frac{1}{r} v_{01} + \frac{i\beta}{r} w_{01} .$$

$$\nabla_{-10}(r) = i\alpha u_{-10} + v'_{-10} + \frac{1}{r} v_{-10} + \frac{i\beta}{r} w_{-10} .$$

Then

$$F_{20}^{(1)} = -2\rho_{10} \nabla_{10} - v_{10} \rho'_{10} + \rho_{10} v'_{10} + \frac{1}{r} \rho_{10} v_{10} .$$

$$F_{20}^{(2)} = R' u_{10} v_{10} + R u_{10} v'_{10} - U' \rho_{10} v_{10} - R v_{10} \left[u'_{10} - \frac{1}{r} u_{10} \right] .$$

$$F_{20}^{(3)} = v_{10}^2 \left[R' + \frac{1}{r} R \right] + \frac{1}{r} R w_{10}^2 .$$

$$F_{20}^{(4)} = R' v_{10} w_{10} + R v'_{10} w_{10} - R v_{10} w'_{10} .$$

$$F_{20}^{(5)} = -(\kappa + 1) p_{10} \nabla_{10} - p'_{10} v_{10} + p_{10} v'_{10} + \frac{1}{r} p_{10} v_{10} .$$

$$-F_{01}^{(1)} = \rho'_{-10} v_{10} + \rho_{-10} v'_{10} + \rho'_{10} v_{-10} + \rho_{10} v'_{-10} + \frac{1}{r} (\rho_{-10} v_{10} + \rho_{10} v_{-10}) .$$

$$-F_{01}^{(2)} = 2a_0 (\rho_{-10} u_{10} + \rho_{10} u_{-10}) + \left[R' + \frac{R}{r}\right](u_{-10} v_{10} + u_{10} v_{-10})$$
$$+ R (u_{-10} v'_{10} + u_{10} v'_{-10} + v_{-10} u'_{10} + v_{10} u'_{-10})$$
$$+ U' (\rho_{-10} v_{10} + \rho_{10} v_{-10}) .$$

$$-\frac{1}{2} F_{01}^{(3)} = a_0 (\rho_{-10} v_{10} + \rho_{10} v_{-10}) + \left[R + \frac{R}{r}\right] v_{10} v_{-10}$$
$$+ R \left[v_{-10} v'_{10} + v_{10} v'_{-10} - \frac{w_{10} w_{-10}}{r}\right] .$$

$$-F_{01}^{(4)} = 2a_0 (\rho_{-10} w_{10} + \rho_{10} w_{-10}) + \left[R' + \frac{2R}{r}\right](v_{-10} w_{10} + v_{10} w_{-10})$$
$$+ R (v_{-10} w'_{10} + v_{10} w'_{-10} + w_{-10} v'_{10} + w_{10} v'_{-10}) .$$

$$-F_{01}^{(5)} = \kappa p_{-10} \nabla_{10} + \kappa \left[p_{10} v'_{-10} + \frac{p_{10} v_{-10}}{r}\right] + (1 - \kappa) p_{10} \left[i\alpha u_{-10} + \frac{i\beta}{r} w_{-10}\right]$$
$$+ p'_{-10} v_{10} + p'_{10} v_{-10} - i\alpha u_{10} p_{-10} - \frac{i\beta}{r} w_{10} p_{-10} .$$

$$-F_{11}^{(1)} = \rho_{10} \nabla_{01} + \rho_{01} \nabla_{10} + \rho_{20} \nabla_{-10} + \rho_{-10} \nabla_{20} - i\alpha \rho_{-10} u_{20} - \frac{i\beta}{r} \rho_{-10} w_{20}$$
$$+ \rho'_{10} v_{01} + \rho'_{01} v_{10} + \rho'_{-10} v_{20} + \rho'_{20} v_{-10} .$$

$$F_{11}^{(2)} = -(2a_0 + i\alpha F) (\rho_{-10} u_{20} + \rho_{20} u_{-10} + \rho_{01} u_{10} + \rho_{10} u_{01})$$
$$- U' (\rho_{-10} v_{20} + \rho_{20} v_{-10} + \rho_{01} v_{10} + \rho_{10} v_{01})$$
$$- R' (u_{-10} v_{20} + u_{20} v_{-10} + u_{01} v_{10} + u_{10} v_{01})$$
$$- \nabla_{10} (\rho_{-10} u_{10} + R u_{01} + \rho_{10} u_{-10}) - R [u_{10} \nabla_{01} + u_{20} (\nabla_{-10} - i\alpha u_{-10})$$
$$+ u_{-10} \nabla_{20} - \frac{i\beta}{r} u_{-10} w_{20} + v_{10} u'_{01} + v_{01} u'_{10} + v_{-10} u'_{20} + v_{20} u'_{-10}]$$
$$- \rho_{10} u_{10} \nabla_{-10} - \rho_{10} (v_{-10} u'_{10} + v_{10} u'_{-10})$$
$$- v_{10} (u_{-10} \rho'_{10} + \rho_{-10} u'_{10} + u_{10} \rho'_{-10}) - u_{10} v_{-10} \rho'_{10} .$$

$$F_{11}^{(3)} = -(2a_0 + i\alpha F)(\rho_{-10} v_{20} + \rho_{20} v_{-10} + \rho_{01} v_{10} + \rho_{10} v_{01})$$

$$- 2R'(v_{-10} v_{20} + v_{10} v_{01}) - \nabla_{10}(\rho_{-10} v_{10} + R v_{01} + \rho_{10} v_{-10})$$

$$- R\left[v_{10} \nabla_{01} + v_{20}\left(\nabla_{-10} + v'_{-10} + \frac{v_{-10}}{r}\right)\right.$$

$$\left. + i\alpha v_{-10} u_{20} + v_{10} v'_{01} + v_{01} v'_{10} + 2 v_{-10} v'_{20} + \frac{i\beta}{r} v_{-10} w_{20}\right.$$

$$\left. - \frac{2}{r}(w_{01} w_{10} + w_{20} w_{-10})\right] - \rho_{10} v_{10} \nabla_{-10} - \rho_{10}(v_{-10} v'_{10} + v_{10} v'_{-10})$$

$$- v_{10}(2v_{-10} \rho'_{10} + v_{10} \rho'_{-10} + \rho_{-10} v'_{10}) + \frac{w_{10}}{r}(2\rho_{10} w_{-10} + \rho_{-10} w_{10}) .$$

$$F_{11}^{(4)} = -(2a_0 + i\alpha F)(\rho_{-10} w_{20} + \rho_{20} w_{-10} + \rho_{10} w_{01} + \rho_{01} w_{10})$$

$$- R'(v_{-10} w_{20} + v_{20} w_{-10} + v_{10} w_{01} + v_{01} w_{10})$$

$$- \nabla_{10}(\rho_{-10} w_{10} + R w_{01} + \rho_{10} w_{-10}) - R\left[w_{10} \nabla_{01} + w_{20}\left(\nabla_{-10} + \frac{v_{-10}}{r}\right)\right.$$

$$\left. + w_{-10}\left(\nabla_{20} - i\alpha u_{20} - \frac{i\beta}{r} w_{20}\right) + v_{10} w'_{01} + v_{01} w'_{10} + v_{-10} w'_{20}\right.$$

$$\left. + v_{20} w'_{-10} + \frac{1}{r}(v_{10} w_{01} + v_{01} w_{10} + v_{20} w_{-10})\right] - \rho_{10} w_{10} \nabla_{-10}$$

$$- \rho_{10}(v_{-10} w'_{10} + v_{10} w'_{-10}) - v_{10}(\rho_{-10} w'_{10} + w_{-10} \rho'_{10} + w_{10} \rho'_{-10})$$

$$- \frac{w_{10}}{r}(\rho_{-10} v_{10} + \rho_{10} v_{-10}) - \frac{1}{r} \rho_{10} v_{10} w_{-10} - \rho'_{10} v_{-10} w_{10} .$$

$$F_{11}^{(5)} = -\kappa\left(p_{01} \nabla_{10} + p_{-10} \nabla_{20} + p_{10} v'_{01} + \frac{1}{r} p_{10} v_{01} + \frac{1}{r} p_{20} v_{-10} + p_{20} v'_{-10}\right)$$

$$+ (\kappa - 2)\left(i\alpha u_{-10} p_{20} + \frac{i\beta}{r} p_{20} w_{-10}\right) - \frac{i\beta}{r}(w_{01} p_{10} - w_{20} p_{-10})$$

$$- i\alpha(u_{01} p_{10} - u_{20} p_{-10}) - p'_{10} v_{01} - p'_{01} v_{10} - p'_{-10} v_{20} - p'_{20} v_{-10} .$$

REFERENCES

Ahuja, K.K., J. Lepicovsky, and W.H. Brown, "Some Unsolved Questions on Hot-Jet Mixing Control," AIAA Paper 86-1956, 1986.

Ahuja, K.K., J. Lepicovsky, C.K.W. Tam, P.J. Morris, and R.H. Burrin, "Tone-Excited Jet," NASA Contractor Report 3538, 1982.

Arbey, H. and J.E. Ffowcs Williams, "Active Cancellation of Pure Tones in an Excited Jet," J. Fluid Mech., Vol. 149, pp. 445-454, 1984.

Balsa, T.F., "On the Spatial Instability of Piecewise Linear Free Shear Layers," J. Fluid Mech., Vol. 174, pp. 553-563, 1987.

Balsa, T.F., "On the Receptivity of Free Shear Layers to Two-Dimensional External Excitation," J. Fluid Mech., Vol. 187, pp. 155-177, 1988.

Batchelor, G.K., An Introduction to Fluid Dynamics, Cambridge University Press, Cambridge, 1967.

Batchelor, G.K. and A.E. Gill, "Analysis of the Stability of Axisymmetric Jets," J. Fluid Mech., Vol. 14, pp. 529-551, 1962.

Benney, D.J. and R.F. Bergeron, "A New Class of Nonlinear Waves in Parallel Flows," Studies in Applied Math., Vol. 48, pp. 181-204, 1969.

Betchov, R. and W.O. Criminale, Stability of Parallel Flows, Academic Press, New York, 1967.

Betchov, R. and A. Szewczyk, "Stability of a Shear Layer Between Parallel Streams," The Physics of Fluids, Vol. 6, No. 10, pp. 1391-1396, 1963.

Bird, R.B., Stewart, W.E. and Lightfoot, E.N., Transport Phenomena, John Wiley and Sons, New York, 1960.

Browand, F. and Ho, C.-M., "The Mixing Layer: An Example of Quasi Two-Dimensional Turbulence," J. Mec. Theor. Appl., Vol. 2, pp. 99-120, 1983.

Brown, G.L. and A. Roshko, "On Density Effects and Large Structure in Turbulent Mixing Layers," J. Fluid Mech., Vol. 64, pp. 775-816, 1974.

Carrier, G.F., Krook, M. and C.E. Pearson, Functions of a Complex Variable, McGraw-Hill, Inc., New York, 1966.

Chan, Y.Y., "Spatial Waves in Turbulent Jets," The Physics of Fluids, Vol. 17, No. 1, pp. 46-53, 1974.

Corcos, G.M. and F.S. Sherman, "The Mixing Layer: Deterministic Models of a Turbulent Flow. Part 1. Introduction and Two-Dimensional Flow," J. Fluid Mech., Vol. 139, pp. 29-65, 1984.

Crow, S.C., and F.H. Champagne, "Orderly Structure in Jet Turbulence," J. Fluid Mech., Vol. 48, pp. 547-592, 1971.

Drazin, P.G. and W.H. Reid, Hydrodynamic Stability, Cambridge University Press, Cambridge, 1981.

Ffowcs Williams, J.E. and A.J. Kempton, "The Noise from the Large-Scale Structure of a Jet," J. Fluid Mech., Vol. 84, pp. 673-694, 1978.

Freymuth, P., "On Transition in a Separated Laminar Boundary Layer," J. Fluid Mech., Vol. 25, pp. 683-704, 1966.

Gaster, M., "A Theoretical Model of a Wave Packet in the Boundary Layer on a Flat Plate," Proc. Roy. Soc., Vol. A347, pp. 271-289, 1975.

Gaster, M., "On the Generation of Spatially Growing Waves in a Boundary Layer," J. Fluid Mech., Vol. 22, pp. 433-441, 1965.

George, W.D. and J.D. Hellums, "Hydrodynamic Stability in Plane Poiseuille Flow with Finite Amplitude Disturbances," J. Fluid Mech., Vol. 51, pp. 687-704, 1972.

Goldstein, M.E. and Leib, S., "Nonlinear Roll-Up of Externally Excited Free Shear Layers," J. Fluid Mech., Vol. 191, pp. 481-515, 1988.

Herbert, T., "On Pertubation Methods in Nonlinear Stability Theory," J. Fluid Mech., Vol. 126, pp. 167-186, 1983.

Ho, C.-M. and P. Huerre, "Perturbed Free Shear Layers," Ann. Rev. Fluid Mech., Vol. 16, pp. 365-424, 1984.

Huerre, P., "The Nonlinear Stability of a Free Shear Layer in the Viscous Critical Layer Regime," Phil. Trans. Roy. Soc., Vol. A293, pp. 643-672, 1980.

Huerre, P., "On the Landau Constant in Mixing Layers," Proc. Roy. Soc., Vol. A409, pp. 369-381, 1987.

Huerre, P. and P. Monkewitz, "Absolute and Convective Instabilities in Free Shear Layers," J. Fluid Mech., Vol. 159, pp. 151-168, 1985.

Kelly, R.E., "On the Stability of an Inviscid Shear Layer which is Periodic in Space and Time," J. Fluid Mech., Vol. 27, pp. 657-689, 1967.

Ko, N.W.M. and P.O.A.L. Davies, "Some Covariance Measurements in a Subsonic Jet," J. Sound Vib., Vol. 41, pp. 347-358, 1975.

Lees, L. and C.C. Lin, "Investigation of the Stability of the Laminar Boundary Layer in a Compressible Fluid," NACA TN 1115, 1946.

Lepicovsky, J., K.K. Ahuja, W.H. Brown, M. Salikuddin, and B.J. Morris, "Acoustically Excited Heated Jets," NASA Contractor Report 4129, 1988.

Lessen, M., and P.J. Singh, "The Stability of Axisymmetric Free Shear Layers," J. Fluid Mech., Vol. 60, pp. 433-453, 1973.

Lin, C.C., The Theory of Hydrodynamic Stability, Cambridge University Press, Cambridge, 1955.

Maslowe, S.A., "Weakly Nonlinear Stability of a Viscous Free Shear Layer," J. Fluid Mech., Vol. 79, pp. 689-702, 1977.

Metcalfe, R.W., S.A. Orszag, M.E. Brachet, S. Menon and J.J. Riley, "Secondary Instability of a Temporally Growing Mixing Layer," J. Fluid Mech., Vol. 184, pp. 207-243, 1987.

Michalke, A., "Instabilität eins Kompressiblen Ruden Friestrahls unter Berücksichtingung des Einflusses der Strahlgrenzschichtdicke, Z. Flugwiss., Vol. 19, pp. 319-328, 1971. English Translation NASA Tech. Memo. 75190 (1977).

Michalke, A., "On Spatially Growing Disturbances in an Inviscid Shear Layer," J. Fluid Mech., Vol. 23, p. 521-544, 1965.

Michalke, A., "On the Inviscid Instability of the Hyperbolic-Tangent Velocity Profile," J. Fluid Mech., Vol. 19, pp. 543-556, 1964.

Michalke, A., and G. Hermann, "On the Inviscid Instability of a Circular Jet with External Flow," J. Fluid Mech., Vol. 114, pp. 343-359, 1982.

Miksad, R., "Experiments on the Nonlinear Stages of Free Shear-Layer Transition," J. Fluid Mech., Vol. 56, pp. 695-719, 1972.

Mitchell, A.R., Computational Methods in Partial Differential Equations, John Wiley and Sons, New York, 1969.

Miura, A. and T. Sato, "Theory of Vortex Notation and Amplitude Oscillation in an Inviscid Shear Instability," J. Fluid Mech., Vol. 86, pp. 33-47, 1978.

Monkewitz, P.A. and K.D. Sohn, "Absolute Instability in Hot Jets," AIAA Journal, Vol. 26, No. 8, pp. 911-916, 1988.

Monkewitz, P.A. and K.D. Sohn, "Absolute Instability in Hot Jets and Their Control," AIAA Paper 86-1882, 1986.

Morris, P.J., "The Spatial Viscous Instability of Axisymmetric Jets," J. Fluid Mech., Vol. 77, pp. 511-529, 1976.

Ng, L., "The Secondary Instabilities of a Heated Subsonic Jet," Ph.D. Dissertation, Department of Aerospace and Mechanical Engineering, University of Arizona, Tucson, 1989.

Paragiri, R., "The Stability Analysis of Axisymmetric Jets," Master's Report, Department of Aerospace and Mechanical Engineering, University of Arizona, Tucson, 1985.

Petersen, R.A. and M.M. Samet, "On the Preferred Mode of Jet Instability," J. Fluid Mech., Vol. 194, pp. 153-173, 1988.

Peyret, R. and T.D. Taylor, Computational Methods for Fluid Flow, Springer Series in Computational Physics, Springer-Verlag, New York, 1983.

Robinson, J.L., "The Inviscid Nonlinear Instability of Parallel Shear Flows," J. Fluid Mech., Vol. 63, pp. 723-752, 1974.

Schade, H., "Contribution to the Nonlinear Stability Theory of Inviscid Shear Layers," The Physics of Fluids, Vol. 7, pp. 623-628, 1964.

Schlichting, H., Boundary-Layer Theory, 7th Ed., McGraw-Hill Book Company, New York, 1979.

Sen, P.K. and Venkateswarlu, D., "On the Stability of Plane Poiseuille Flow to Finite-Amplitude Disturbances, Considering the Higher-Order Landau Coefficients," J. Fluid Mech., Vol. 133, pp. 179-206, 1983.

Shen, S.F., "Stability of Laminar Flows," (in Theory of Laminary Flows, F.K. Moore, editor), Princeton University Press, 1964.

Sohn, D.K., "Absolute Instability in Hot Jets," Master's Thesis, University of California, Los Angeles, 1986.

Stewartson, K., "The Evolution of the Critical Layer of a Rossby Wave," Geophys. Astrophys. Fluid Dyn., Vol. 9, pp. 185-200, 1978.

Stone, J.R. and D.J. McKinzie, "Acoustic Excitation - A Promising New Means of Controlling Shear Layers," NASA TM-83772, 1984.

Stuart, J.T., "On the Nonlinear Mechanics of Wave Disturbances in Stable and Unstable Parallel Flows," Part 1, J. Fluid Mech., Vol. 9, pp. 353-370, 1960.

Watson, J., "On the Nonlinear Mechanics of Wave Disturbances in Stable and Unstable Parallel Flows," Part 2, J. Fluid Mech., Vol. 9, pp. 371-389, 1960.

Winant, C.D. and F.K. Browand, "Vortex Pairing: The Mechanism of Turbulent Mixing Layer Growth at Moderate Reynolds Number," J. Fluid Mech., Vol. 63, pp. 237-255, 1974.

Wygnanski, I.J. and R.A. Petersen, "Coherent Motion in Excited Free Shear Flows," AIAA Journal, Vol. 25, pp. 201-213, 1987.

Zabusky, N.J. and G.S. Deem, "Dynamical Evolution of Two-Dimensional Unstable Shear Flows," J. Fluid Mech., Vol. 47, pp. 353-379, 1971.